The Northern European Enclosure Dam

A multidisciplinary project on the effects of the NEED

January 29, 2021

Freek Kollaard
Carlijn Meijers
Charlotte van Strien
Irene van der Veer
Laura de Vries

Commissioned by
dr. S. Groeskamp
(NIOZ)

Supervised by
dr. ir. M.M. Rutten
(TU Delft & Delta Futures Lab)
& dr. ir. M. Voorendt
(TU Delft)

TU Delft

Preface

This project is conducted as part of the Master Civil Engineering at the Delft University of Technology. One of the options students have during their masters is to do a multidisciplinary project (MDP), commissioned by an external client. The members of the team have to be from different tracks, hence the multidisciplinary character of the project. Our project team consists of five members from three different tracks: Environmental Engineering, Hydraulic Engineering and Water Management.

This is the final report of our 10-week consultancy and research project. It displays the results of the first study into the effects of the NEED, after the initial study of Groeskamp & Kjellsson (2020). We hope this study will be the initiation of a long series of researches into all aspects of the NEED.

Besides this report a lunch lecture (consisting of a presentation and question round) was given on January 22nd, hosted by the TU Delft Delta Futures Lab. We enjoyed working on this project a lot and are happy to have contributed to gaining more insight in the unique idea of building a dam to protect Europe from sea level rise.

This project has been different than other multidisciplinary projects, but we have learned from it in many ways. This would however not have been possible without the help and flexibility of some people. Therefore we would like to thank Sjoerd Groeskamp for openly and enthusiastically sharing his thoughts and knowledge with us. Also we would like to thank Martine Rutten and Mark Voorendt for their suggestions, help and critical questions. Lastly we thank Caroline Katsman, Jos Timmermans and Joakim Kjellsson for the help in their field of expertise.

Delft
January 29, 2021

Freek Kollaard - 4369572
Carlijn Meijers - 5064783
Charlotte van Strien - 4401093
Irene van der Veer - 4482891
Laura de Vries - 4463749

Abstract

Many low-lying densely populated areas and important economical regions in Europe are threatened by sea level rise. Groeskamp & Kjellsson (2020) suggest an international cooperation to be able to protect these areas if climate change mitigation fails: the construction of the Northern European Enclosure Dam (NEED). In this research first order calculations are used to show the effects the construction of the NEED has inside the enclosed North Sea basin. The topics covered are: monthly water level variations; hydrodynamics (tides, waves and currents); salinity; temperature and lastly sediment transport. At first these topics are treated independently, after which a first step is made with studying their dependencies. Besides the dependencies, the implications of the NEED on the environment, economy and society are explored. The implications are also shown in a case study looking into the Wadden Sea, which is Natural UNESCO World Heritage.

It is found that, with constant pumping, the water level variability stays within a range that is an order of magnitude smaller than the tidal amplitudes that prevail nowadays. The salinity of the top layer drops with an order of magnitude as well, from 35 PSU to 3.5 PSU in 50 years, while the deep, stratified part of the basin stays salt. The surface temperature only changes slightly with a drop of 0.3 °C. The hydrodynamic processes in the enclosed North Sea basin together generate a weak anti-clockwise circulation that replaces the stronger anti-clockwise circulation imposed by the tides that prevailed before the enclosure of the basin. Due to a drop in average flow velocities, the sediment transport in the basin decreases and transforms from tide-dominated to a system where tides and wind are equally important. It is found that all of the above described changes have major implications on environment, economy and society and that much more research is needed to fully understand the changing processes and their effects.

List of symbols

Symbol	Meaning	Value	Unit
P_{atm}	Atmospheric pressure	101392	Pa
c_c	Back radiation cloud cover coefficient for 50°N	0.72	-
c_1	Calibration value	10.42926609	-
c_2	Calibration value	-1.82717842·10^3	-
c_3	Calibration value	-0.07120827·10^6	-
c_4	Calibration value	-0.008774	-
f	Coriolis parameter at 52^{o}N	$1.15 \cdot 10^{-4}$	s^{-1}
$\tau_{dep,cr}$	Critical bed shear stress for deposition	0.2	N/m^2
$\tau_{ero,cr}$	Critical bed shear stress for erosion	0.4	N/m^2
ρ_s	Density sea	1025	kg/m^3
ρ_1	Density layer 1	1003	kg/m^3
ρ_2	Density layer 2	1028	kg/m^3
$\tilde{H}_\infty$	Dimensionless wave height for fully developed waves	0.24	-
C_e	Exchange coefficient between sea surface and atmosphere	0.00143	-
g	Gravitational acceleration	9.81	m/s^2
$C_{p,w}$	Heat capacity of water	3.99·10^3	J/kg/K
$C_{p,a}$	Heat capacity of dry air	1004.64	J/kg/K
ν_h	Horizontal eddy viscosity	10^5	m^2s^{-1}
L	Length scale basin	625	km
N_t	Mean cloud cover	5.6	Okt
σ	Modified value Stefan-Boltzmann constant	1.3134·10^{-9}	$W/m^2/K^4$
T_{ref}	Reference temperature	0	°C
RH	Relative humidity	83	%
c_s	Solar radiation cloud cover coefficient	0.4	-
A	Surface area basin	515625	km^2
k	Thermal conductivity of sea water	0.6	W/(m·K)
Δx	Thickness of the thermocline	20	m
ν_t	Vertical eddy viscosity	10^{-1}	m^2s^{-1}
γ	Wave breaker parameter for significant wave height	0.4	-
W_{10}	Winds speed at 10 m height	8	m/s

Symbol	Meaning	Unit
T_a	Air temperature	K
α	Albedo	-
τ_{bed}	Bed shear stress	N/m^2
ρ_a	Density of air over sea	kg/m^3
h	Depth of the basin	m
T_d	Dew point temperature	K
$\tilde{F}$	Dimensionless fetch	-
$\tilde{H}$	Dimensionless wave height	-
Q	Discharge	m^3/s
F	Fetch	m
Q_{solar}	Incident solar radiation	W/m^2
q_a	Mixing ratio of air	-
q_s	Mixing ratio of air over sea	-
c_{bot}	Near seabed sediment concentration	kg/m^3
P_d	Saturated vapor pressure of air at the sea surface	Pa
T_s	Sea surface temperature	K
w_s	Settling velocity	m/s
τ_s	Shear stress on water by wind	N/m^2
H_{m0}	Significant wave height	m
T	Temperature	°C
ΔT	Temperature difference over the thermocline	K
P_s	Vapor pressure over sea	Pa
z	Vertical dimension	m
u	Water velocity in x-direction	m/s
v	Water velocity in y-direction	m/s

Table of Contents

1 | Introduction

1.1 Problem analysis

Globally, sea levels are rising (e.g. Chen et al., 2017; Church & White, 2006), threatening low-lying deltas and their cities, inhabitants, nature, economies and cultural heritage on enormous scales (e.g. Nicholls & Cazenave, 2010). Many of these low-lying and densely populated areas are located along the coastlines of the North Sea, includin the European capital cities Amsterdam, Copenhagen, London and Oslo. In order to prevent flooding, measures such as dike reinforcements are taken on local and national scale. However, is this individualistic approach still feasible or optimal to protect Europe against the rising water?

Groeskamp & Kjellsson (2020) suggest an international cooperation to protect over 25 million people and important economical regions in northern Europe against sea level rise: the construction of the Northern European Enclose Dam (NEED). This dam turns the North Sea into a massive enclosed basin. The suggested dam consists of three parts (see Figure 1.1), with the first part stretching over 161 kilometers from Brest (France) to the south coast of the United Kingdom. The second and third part run from Scotland via the Orkneys to the Shetland Islands and from there to Bergen (Norway), stretching over 145 and 331 kilometers respectively. The total length of the dam thus equals 637 kilometers.

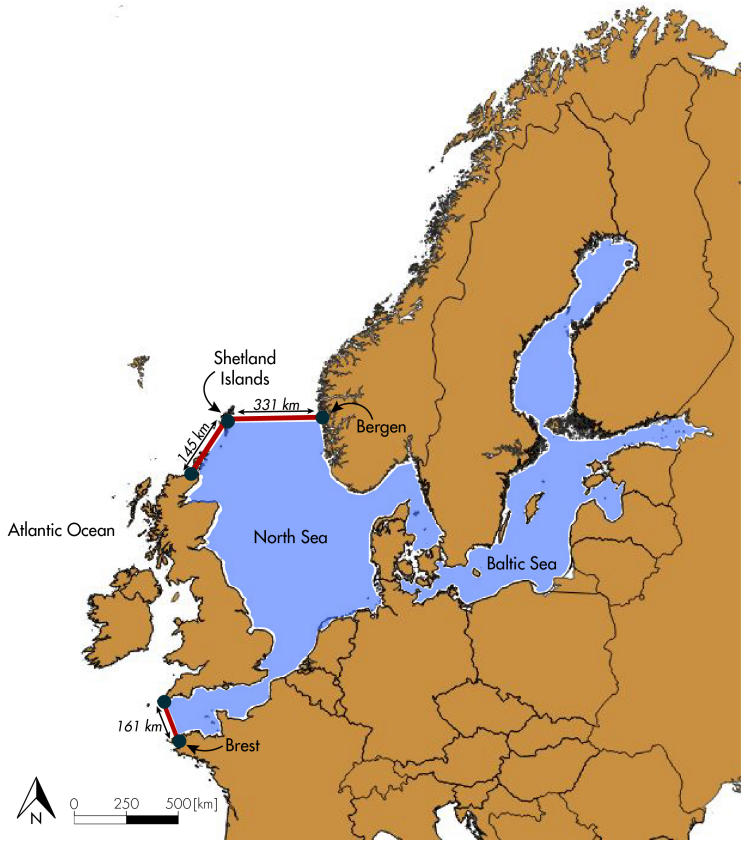

Figure 1.1: The location of the NEED (in red) and the enclosed basin consisting of the North Sea and the Baltic Sea (in blue), as proposed by Groeskamp & Kjellsson (2020).

This proposal is of enormous impact and may seem unrealistic at first sight. However, in their paper, Groeskamp and Kjellsson prove with a preliminary study that the NEED might be a realistic option (technically and economically) when comparing it to alternatives such as country-by-country efforts or massive migration. The study can be seen as a first step in thinking big and out-of-the-box when it comes to protection against sea level rise. Also, it is a serious warning: drastic measures alike the NEED might become necessary if nothing is done in time to mitigate the effects of climate change.

Yet, after the preliminary study, there is still a lack of (detailed) knowledge about the impact of the NEED. Examples of these knowledge gaps are the impact on shipping, currents, sedimentation, marine species, tourism, precipitation and many more aspects. These examples also show that when evaluating the impact of the NEED, many stakeholders need to be considered.

1.2 Research question

This research, commissioned by Sjoerd Groeskamp (oceanographer at NIOZ), aims to gain additional insights in the effects of the NEED on the North Sea basin. The goal of this research is to perform an analysis on the changing hydrodynamics inside the North Sea basin. The research may show positive as well as negative aspects of the NEED. Alterations in currents, salinity, temperature and sediment transport will be investigated. Also a case study is conducted, zooming in on the effects the NEED will have on the Wadden Sea, which is UNESCO World Heritage.

The main research question is formulated as follows:

How do average water levels, hydrodynamics, salinity, temperature and sediment transport change in space and time within the North Sea basin due to the construction of the NEED and what are the effects?

The research is divided further into the following sub-questions. Question b until f compare the current situation to the situation with the NEED.

a) What is the effect of the NEED on the average water level variations inside the North Sea basin?
b) How do the hydrodynamics in the North Sea basin change?
c) How does the salinity in the North Sea basin change?
d) How does the temperature in the North Sea basin change?
e) How do the sediment transport and availability in the North Sea basin change?
f) How do the changing temperature and salinity influence the hydrodynamics?
g) What are the possible implications of the results on the environment, economy and society?

Evidently, the consequences of the dam will extend beyond the aspects covered by the research questions, however the scope of this research is limited to be able to contribute in-depth to the understanding of the effects of the NEED. The possible changes outside the North Sea basin are not considered. Furthermore, implications of the dam concerning its construction, politics, economy or climate are outside the scope of this research.

In the study, the considered conditions are those that prevail in the North Sea basin nowadays. It is assumed that external parameters, such as the discharge of rivers and climatic conditions (for example solar radiation, wind and rainfall), and the distribution of those parameters in space and time do not change. In practice, these parameters may change in the future due to, amongst other things, climate change. This is only considered in Chapter 3.

1.3 Approach

This study uses literature and first order calculations to gain more insight in the processes inside the North Sea basin after the construction of the NEED. A highly simplified North Sea basin will be used, in order to reduce complexity for the first order approximations. Literature is used to study the current dynamics in the North Sea. With the outcomes from the literature study, the first order approximations are executed for the changes in five domains within the enclosed basin: water level variations, hydrodynamics, salinity, temperature and sediment transport. Only average changes over the whole North Sea basin are studied and spatial variations are not considered. The different domains are treated independently at first, in order to reduce complexity. Only from Chapter 8 onward, different aspects of the interactions between the domains and the implications imposed by their changes are covered.

1.3.a Report outline

To start off, Chapter 2 presents the concept used to obtain the simplified North Sea basin the research will be working with. In this chapter, some of the main characteristics of the North Sea basin are presented as well. With these simplifications in mind, the different domains are presented in Chapter 3 until 7. In general, these chapters are structured as follows.

First of all the situation before the construction of the NEED, indicated as the "current situation", is presented. This is studied using literature. After this, the theory for the calculations regarding the future situation, thus after the construction of the NEED, is given. This theory provides the formulas and background needed to understand the steps taken to arrive at the results. These are presented in the next section. Subsequently the sensitivity of the obtained results is analysed. Here also the most crucial parameters are evaluated. This is useful, as it provides insights in the reliability and stability of the obtained results. Last of all, an interpretation of the presented findings is given for the domain under consideration.

Chapter 8 combines the results that were obtained within the different individual domains in a dependency analysis, adopting the structure of a theoretical background followed by the results. In order to connect the results with the societal aspect of the NEED, the Wadden Sea is used as a case study. This UNESCO World Heritage is analysed in Chapter 9, with an integrated approach using literature and the results from the different domains. After this, Chapter 10 discusses the implications the NEED has on the environment, economy and society. Chapter 11 provides an overall discussion of the results obtained by the research after which in Chapter 12 and 13 final conclusions are drawn and recommendations are presented respectively.

2 | Conceptualisation of the North Sea

In this chapter the conceptualisation of the enclosed North Sea basin is introduced. This is done by first explaining how the enclosed area is simplified to a rectangular basin (a bucket). Then it is shown how the interactions between the bucket and its surroundings are reduced to fluxes. Next, multiple characteristic formulas and numbers are presented. The final concept forms a basis for the calculations and analyses in further chapters.

2.1 The North Sea basin as a bucket

For this study it is assumed that the NEED can be built technically and will be built on the location as proposed by Groeskamp & Kjellsson (2020). Also, it is assumed that the dam will both horizontally and vertically block any exchange between the North Sea basin and the Atlantic Ocean, concerning water-, heat-, sediment- and salt transport. The enclosed area that is studied in this research will be called "the North Sea basin" and is depicted in Figure 2.1a. As can be seen from the figure, the North Sea basin is defined without the English Channel and the Kattegat. This is done for simplicity as their characteristics are expected to differ from those of the main part of the basin. They experience different flow patterns, friction forces and resonance. Using Figure 2.1a, the North Sea basin is schematised as a rectangular shaped basin of 625 km by 825 km. The depths of the basin are defined based on the depth contour map that can be found in Appendix A.1. It consists of a southern part that covers one third of the basin length with a depth of 40 m and a northern part that covers two thirds of the basin with a depth of 100 m. Figure 2.1b shows this conceptualisation.

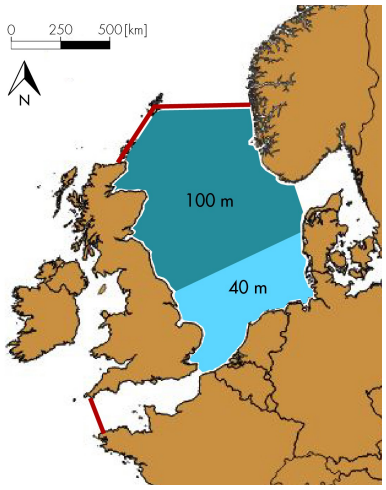

(a)

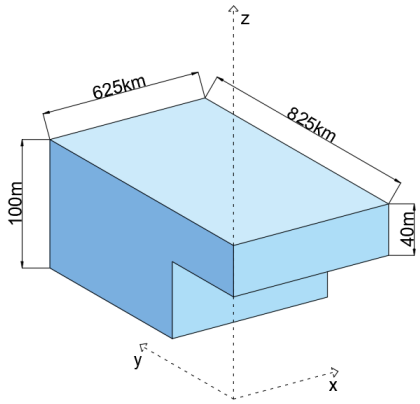

(b)

Figure 2.1: a) The study area for this research with simplified depths. b) The simplified rectangular basin with its dimensions.

2.2 Interactions between the North Sea basin and its surroundings

The water volume, salinity, temperature and sediment volume in the North Sea basin are influenced by external sources in the atmosphere, land and other water bodies. The connections with these sources are simplified and combined into several fluxes into and out of the basin. For example, the interaction with the Baltic Sea regarding all the domains is also simplified as in- and outgoing fluxes. It can be thought of as a big river flux that causes an exchange of water, sediment, salinity and heat.

An illustration of the simplified water mass fluxes that are used as a starting point for calculations throughout the study is given in Figure 2.2. It can be seen that the North Sea knows three main sources of water: precipitation, rivers and the Baltic Sea. It is a water supplier for evaporation and the Atlantic Ocean. The latter receives the sum of the other fluxes (29200 m^3/s) in order to close the water balance. After closure

of the North Sea basin, this flux should be replaced by the pumps in the dam. It is assumed that the pumps extract water from the surface layer, and that they pump at a constant rate over the year in order to reduce energy use and complexity. Chapter 3 elaborates more on the water balance and the relating water levels.

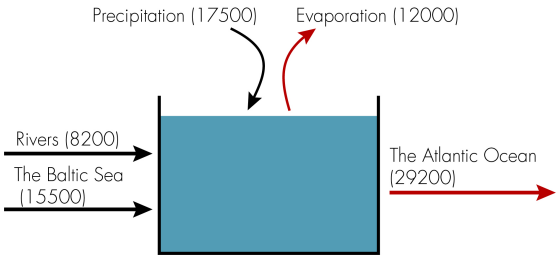

Figure 2.2: The water balance for the current North Sea basin. The units of the fluxes are in m^3/s (Quante & Colijn, 2016; Groeskamp & Kjellsson, 2020).

2.3 Characteristics formulas

In this section a number of variables are calculated that form the basis of other formulas and concepts throughout this research. The following formulas will be explained: The Coriolis parameter, the Ekman boundary layer, the Rossby number and the density formulation.

The first variable is the Coriolis parameter f, which defines the frequency of the earths rotation at a specific latitude. This is an important parameter as the rotation of the earth can have a big influence on the large volume of water in the North Sea basin. It is defined as follows:

$$f = 2\Omega \sin \psi \tag{2.1}$$

Ω is the rotational frequency of the Earth and is equal to $7.27 \cdot 10^{-5}$ rad^{-1}. ψ is the latitudinal coordinate of the North Sea basin and is taken at 52°N. Therefore the Coriolis parameter is equal to $1.15 \cdot 10^{-4}$ s^{-1}.

The Ekman boundary depth provides an estimate of the depth of the frictional boundary layer induced by wind. In this research this is defined as the depth where the wind will mix the water throughout the column. This means that the Ekman boundary layer defines the depth where the salinity and temperature will be in a mixed state. The state of stratification is a necessary variable to be able to determine properties of salinity and temperature. The depth of the Ekman boundary layer δ is defined as follows (Pietrzak, 2019a):

$$\delta = \sqrt{\frac{2\nu_t}{f}} \tag{2.2}$$

In this equation, $\nu_t = 10^{-1}$ m^2/s is the vertical eddy viscosity (Pietrzak, 2019a). This gives an Ekman boundary layer depth of 41.7 m.

In order to make hydrodynamic computations in the following chapters, the horizontal momentum equation (see Appendix A.1) will often be used. This equation is simplified based on the circumstances in the North Sea basin by deciding which terms can be neglected. A good indicator for which terms dominate is the Rossby number. For a small Rossby number, Coriolis is dominant over nonlinear advection terms and the momentum equation reduces to a balance of Coriolis and wind friction. The Rossby number is defined by:

$$Ro = \frac{u}{fL} \tag{2.3}$$

Where $L = 625$ km (length scale of the short side of the basin), we find that $Ro < 0.1$ for $u < 7$ m/s. This is much larger than the expected flow velocities. Hence, we can say that, for velocities until the order of 7 m/s, the Rossby number is small and nonlinear advection terms are negligible.

To be able to calculate the density of seawater, all of the thermodynamic properties of seawater should be taken into account. The TEOS-10 equation of state (Sarraf, n.d.) is therefore used throughout this research. It includes the values of salinity, temperature and pressure to calculate the density of the seawater.

3 | Water level variations

The water level in the North Sea basin is maintained by a series of pumps that are placed in the NEED. However, given the assumption of a constant pumping volume over the year and a fluctuation of the in- and outgoing fluxes, the water levels will vary. In this chapter, these water level variations are calculated, thereby answering the question what the effect of the NEED is on the average water level variations inside the North Sea basin. This is done for three situations: the current water balance with NEED, a future water balance with climate change taken into account, and an extremely wet weather scenario. Finally, it is evaluated whether free fall pumping is possible and, if not, how much energy pumping requires. In this analysis local variations due to for example tides and wind setup are not taken into account. Also, unlike the other chapters, this section does not compare its results to the current situation as average water level variations do not occur due to the existing connection to the ocean.

3.1 Theoretical background

Five fluxes are considered in the water balance of the North Sea basin: rivers (R), precipitation (P), Baltic Sea (B), evaporation (E) and pumps (P). Of these fluxes, the first three are directed into the North Sea basin and the latter two are outgoing fluxes, as can be seen in Figure 2.2 in Section 2.2. The pumping capacity that is needed to maintain a constant water level, follows from the sum of the first four fluxes. This is equal to the flux to the Atlantic Ocean.

3.1.a Water balance with NEED

For the current situation, the following methods have been used to retrieve monthly values for the four fluxes.

- The Rivers flux (R) is found using discharge data of the biggest rivers that flow into the North Sea. These are, from high to low discharge: the Rhine, Meuse, Elbe, Glomma, Gota Alv and Weser. An overview of their monthly discharges can be found in Figure B.1 in Appendix B. The average monthly fluctuations of the big rivers are then applied to the approximated average discharge of the remaining smaller rivers. The sum of all river discharges is used as the river flux (R) in the water balance.
- The precipitation and evaporation fluxes (P and E) into and out of the North Sea basin are found by scaling the yearly values of Groeskamp & Kjellsson (2020) with the monthly variations as found in the precipitation (Copernicus Climate Change Service (C3S), 2017) and evaporation (Saha et al., 2011) data obtained with the Google Earth Engine. The years 2010-2019 are used to obtain the average precipitation and evaporation values for the North Sea basin.
- The monthly influx from the Baltic Sea (B) is assumed to be the surplus of its local water balance (consisting of precipitation, evaporation and river discharge). This is on average 15500 m^3/s (Quante & Colijn, 2016). Monthly precipitation and evaporation data are retrieved from Rutgersson et al. (2002). The monthly river discharges are based on the discharge variability of the two largest rivers flowing into the Baltic Sea. These two largest rivers represent one fourth of the river influx into the Baltic sea as well as the two major discharge regimes and thus are assumed to be representative. An overview of the fluxes forming the discharge from the Baltic Sea is show in Figure B.3 in Appendix B.

The fluxes as described form a water balance with monthly mean fluxes (in m^3/s). The balance is used to determine the required monthly pumping rate:

$$P_{monthly} = R + B + P - E \tag{3.1}$$

Of this monthly flux, a yearly mean is calculated to find the constant pumping rate (P_{const}). The difference between the constant pumping rate and the monthly required pumping is the pumping deficit (Δ_{pumps}):

$$\Delta_{pumps} = P_{const} - P_{monthly} \tag{3.2}$$

Assuming that the water levels change equally over the entire basin, the monthly water level variations in the North Sea basin (η) are determined. This is done using Δ_{pumps}, the area of the basin A ($5.16 \cdot 10^{11}$ m^2) and a factor to convert from m^3/s to cm/month:

$$\eta = \Delta_{\text{pumps}} \ / \ \text{A} \cdot 3600 \cdot 24 \cdot \text{days in month} \cdot 100 \tag{3.3}$$

With the calculated water level variations it can be determined whether using a constant pumping rate gives a feasible situation, or if variable pumping should be chosen to reduce water level variations.

3.1.b Water balance with NEED and climate change

The water balance as calculated in the previous subsection takes into account the current situation. However, the climate is expected to change in the future. In this section the projected flows due to climate change are considered, using the RCP8.5 scenario in 2100. All of the fluxes will change by a scaling factor. By multiplying the current fluxes with these factors, an estimate can be made for the future situation. The scaling factors are determined as follows and are presented in Table 3.1.

- Precipitation rates will rise. Annually this will be 5 to 20% for the North Sea area, whilst in summer the precipitation remains the same (European Environment Agency, 2017). Based on this information, a monthly scaling factor can be determined that causes no increase in summer, but a (maximum) annual increase of 20%.
- The evaporation rates will rise due to higher temperatures in summer. For the scaling of evaporation, the same method as for precipitation is used and the factors can be found in Table 3.1 as well. These factors are a very rough estimate based on the research of Laîné et al. (2014).
- River discharges will increase in winter and early spring by 20 to 30% due to higher amounts of melt water and rain. In summer the flows will decrease by about 30% due to more evaporation and an increased water use (European Environment Agency, 2016; Buishand et al., 2004).
- The change in flux from the Baltic sea is a result of the change in all three other fluxes on a local scale. However, as precipitation and evaporation in the Baltic Sea almost cancel each other out, the rivers regime is leading for the regime in Baltic Sea flux. The change in this flux is therefore taken equal to the change in the rivers flux.

Table 3.1: Monthly scaling factors for evaporation (E), precipitation (P), Baltic Sea (B) and river discharge (R) from the current flux to the flux in 2100 under RPC8.5 climate change circumstances.

	Jan	**Feb**	**Mar**	**Apr**	**May**	**Jun**	**Jul**	**Aug**	**Sept**	**Okt**	**Nov**	**Dec**	**Avg**
E	1.0	1.0	1.1	1.1	1.2	1.3	1.4	1.3	1.2	1.1	1.1	1.0	1.15
P	1.4	1.3	1.3	1.2	1.1	1.0	1.0	1.1	1.2	1.2	1.3	1.3	1.20
B	1.1	1.2	1.3	1.2	1.0	0.9	0.8	0.7	0.8	0.9	1.0	1.1	1.00
R	1.1	1.2	1.3	1.2	1.0	0.9	0.8	0.7	0.8	0.9	1.0	1.1	1.00

3.1.c Extremely wet events

The approach in subsections 3.1.a and 3.1.b only considers monthly variability in water fluxes. Nevertheless, events with extremely high precipitation, river- and Baltic discharge and very low evaporation can occur. Such a situation will become more likely in the future (KNMI, 2020) and should therefore be evaluated to see how water levels respond to these circumstances. This is done by analysing extreme discharges into the North Sea during one week, as this is expected to be normative: each of the terms in equation 3.1 are considered for an extreme event and combined.

- Precipitation rates are increased to 117 mm/week. This is the rate during eight days with a return period of 50 years over a surface area of 1656 km^2 in the Netherlands (Beersma et al., 2019). It is assumed that this value is applicable for the entire North Sea basin.
- Evaporation is for simplicity set to 0 mm/week.
- The discharge from the Baltic Sea is 20500 m^3/s, as it can vary yearly between 10500 and 20500 m^3/s (Quante & Colijn, 2016).

- The river discharge is assumed to be four times the average discharge, based on the discharge peaks of the major rivers connected to the North Sea (Buishand et al., 2004).

These rates are combined into a water balance, assuming that the pumping capacity remains constant (estimated under subsection 3.1.a). The water level rise due to the extreme discharge is subsequently computed with the same approach as described in subsection 3.1.a.

3.1.d Pumps

In order to evaluate whether free fall pumping is possible and how much energy is required for the pumps in the dam, the following steps have been made. First, it is assumed that discharge under free fall can occur if the water level in the basin is higher than the water level on the Atlantic side of the dam. Moreover, it is assumed that the water level in the basin is maintained at its current level. The average water level in- and outside of enclosed basin is thus initially equal. This means that discharging under free fall could occur during low tide in the Atlantic Ocean. The amplitudes of the tides inside the basin are assumed to be dampened by the NEED (see Section 4.3). On the outside of the dam however, the tidal ranges are on average about 1.5 m (Accad & Pekeris, 1978). Free fall discharging is possible until the sea levels has risen by more than the tidal range.

Secondly it is computed how much energy is required for the pumping stations. It is assumed that the pumping stations have to lift water over a head of 5 meters (accounting for sea level rise), which requires 0.014 kW per 1 m^3/h. By multiplying this with the computed pumping discharge from previous sections, the energy required is obtained.

3.2 Results

This results section shows the water balance with NEED and with the climate change scenario RCP8.5, and eventually what water level variations this brings along. Moreover, it presents by how much the water levels can rise during extremely wet weather conditions. Lastly, an evaluation of opportunities for free fall discharging and the pumping energy required is given.

3.2.a Water balance with NEED

Using the water balance and fluxes as described in Section 3.1.a, the solid lines with dots as presented in Figure 3.1 are found. From the figure it becomes clear that in summer more water is pumped than needed in those months. In winter this is the other way around as more water comes in than is pumped out.

With the resulting pumping deficit the water level variations for this situation are found. They are presented in Figure 3.2. This figure shows that the monthly averaged water level variability stays within a range of 16.2 cm.

3.2.b Water balance with NEED and climate change

With the scaling factors as presented in Table 3.1, ranges for the fluxes are found. These are presented in Figure 3.1 as the coloured areas between the two lines. It can be seen that the constant pumping rate slightly increases from 29200 to 30747 m^3/s, while the pumping deficit more than doubles. Due to the larger pumping deficit, the variability in water levels will become larger. This becomes clear from Figure 3.2: the maximum water level in spring triples and the minimum water level in autumn doubles. The averaged water level variability increases to 37.6 cm.

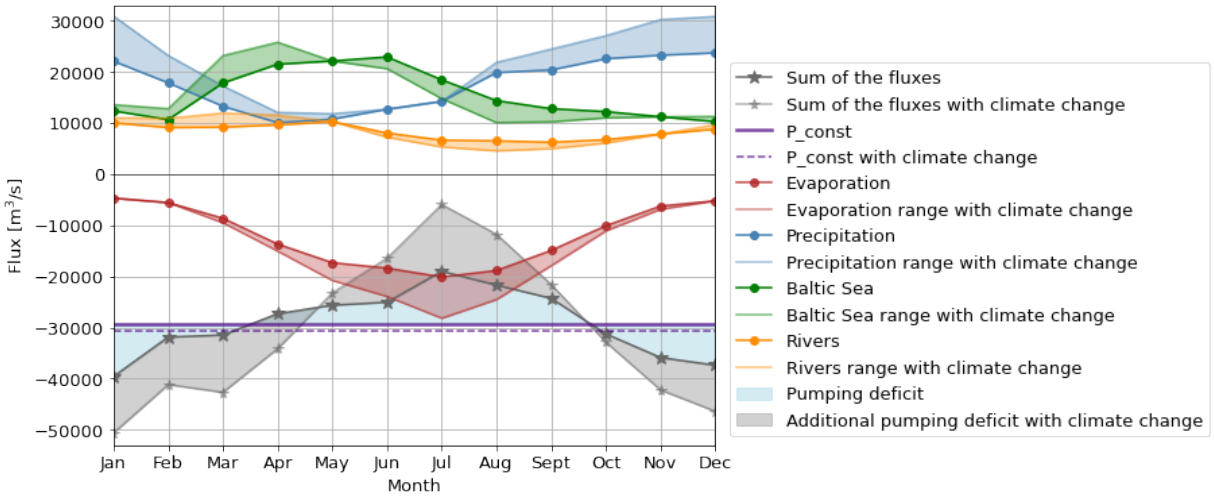

Figure 3.1: Monthly average water fluxes into (positive) and out of (negative) the North Sea basin in m^3/s and their ranges for a future situation with climate change (RCP8.5 in 2100). The "Sum of the fluxes" is the same as $\text{Pumps}_{\text{monthly}}$ in equation 3.1. The exact corresponding values of the current situation can be found in Figure B.2 in Appendix B. The applied scaling factors are presented in Table 3.1.

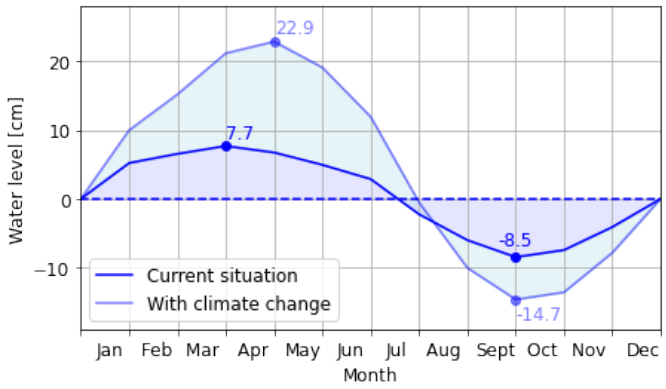

Figure 3.2: Monthly water level variation in cm for a yearly averaged pumping rate for the current situation and a situation with climate change (RCP8.5).

3.2.c Extremely wet events

The extreme situation as described, leads to a net surplus into the North Sea basin of $8 \cdot 10^{10}$ m^3 during the week. The high flux is dominated by the high rate of precipitation ($6 \cdot 10^{10}$ m^3 in the week). This results in a sea level rise of approximately 15 cm during that week. It should be noted that the situation as evaluated occurs rarely. After all, all the fluxes should be extreme at the same time and act on the entire basin. Also, the size of the basin dampens the response of the water level rise.

3.2.d Pumps

The NEED project is designed for a 5-11 m sea level rise in 2500 of which 1-2 m has occurred by 2100 (Groeskamp & Kjellsson, 2020). Given the tidal amplitudes of 1.2-1.5 m, this means that discharging under free fall becomes impossible after 2100. As can be seen from the previous results, the pumping stations in the NEED have to pump a lot of water in order to close the water balance: 29200 m^3/s, which can be compared to the volume of twelve olympic swimming pools per second. This results in a required amount of power of more than 1.4 GW. On a yearly basis, this is comparable to the yearly electricity consumption of almost 4.5 million Dutch households (CBS, 2019).

3.3 Interpretation of results

By choosing a constant pumping rate, the pumps do not have to be over-dimensioned, which reduces costs. This choice goes however hand-in-hand with water level variations over the year as in some months there will be pumped more than flows into the basin, while in other months there will be a pumping deficit. The results show that in the current situation the monthly averaged water level variability stays within a range of 16.2 cm. This is negligibly small compared to the tides without the NEED, or the heights waves may reach, as these are both in the order of meters.

For the future situation with climate change, uncertainty has to be taken into account as for example the choice of a more gentle RCP scenario narrows the ranges in Figure 3.1. Also the scaling factors for evaporation are rough estimates, while they highly influence the needed pumping rates. Still, with the high-end climate change perspective an average yearly water level variation of 37.6 cm is found, which is more substantial when looking at for example local water defences, but still small compared to waves and former tides.

When looking at extreme wet circumstances in the time span of about a week, a water level rise in the order of 15 cm is found. Like the other variations this is in a range that seems acceptable. All together, a constant pumping rate thus seems a valid choice.

It should be noted that the calculated water level changes mark a maximum, as the connections to the Baltic Sea and the English Channel will in practice increase the basin area (A) and thus reduce the water level variations. On the other hand, a combination of seasonal high water (highest water levels in spring) and an extreme week could occur. An additional rise by wind set-up and waves can substantially contribute to a risky high water situation.

4 | Hydrodynamics

This chapter answers the research question on how the hydrodynamics in the North Sea change due to the construction of the NEED. Changes in waves, tide and currents are described. Currents are driven by several factors: tide, discharge through the basin, wind and water level differences. These currents will first be addressed separately and then combined into a complete circulation pattern in the North Sea.

Orders of magnitude of the currents by their main drivers are estimated to find which factors contribute most to the circulation in the basin. To get an idea of the general behaviour of the basin after closure, the mean circulation is most interesting. Therefore, the currents will be computed for average weather and hydrodynamic conditions. Wind set-up and waves are computed for extreme conditions as well, since extreme conditions can be determining for coastal safety in these cases.

4.1 Current situation

The predominant circulation before the construction of the NEED in the basin is anticlockwise. Atlantic water enters at the north of the basin and flows southward, meeting incoming ocean waters at the English Channel. The waters mix with fresher water from the continent and brakish water from the Baltic Sea (Winter & Johannessen, 2005). In the mixing of Atlantic water with freshwater, density-driven flows play a major role (Quante & Colijn, 2016). The water flows back northwards to the Atlantic Ocean, closely following the Norwegian coast. This flow is also called the Norwegian Coastal Current (NCC) (Winter & Johannessen, 2005). At the same time, underneath the NCC, more salty Atlantic water is entering the North Sea basin (see Figure 4.1 for an overview of the fow pattern).

Figure 4.1: Overview of the circulation pattern in the North Sea basin without the NEED (Quante & Colijn, 2016).

The dominating wind directions in the area are southwest and west. The strongest winds are found in autumn and winter (Winter & Johannessen, 2005). These southwesterly and westerly winds drive an anticlockwise circulation. Occasionally, in the case of easterly winds (which occur sometimes during the summer months), this circulation reverses (Quante & Colijn, 2016). The flow responds to the wind forcing on a weekly timescale. Therefore, a great variability in the wind-driven flows can be observed, as they change with the wind strength and direction. Only the flow in the deeper Norwegian Trench has a long response time to the wind patterns and is therefore more steady (Winter & Johannessen, 2005).

At this moment, tidal currents dominate any other flow in the North Sea. They move the entire water column and therefore give rise to a strong mixing (Quante & Colijn, 2016). The velocities of the tidal currents vary strongly in time and space. In shallow coastal areas, velocities of 0.5 m/s up to 1 m/s at spring tide are reached. In the deeper areas, tidal velocities are in the order of 0.2 to 0.5 m/s (Waypoint Amsterdam, 2020). The tides in the North Sea show strong nonlinearities and an asymmetric tidal curve due to the shallow water depth. This gives rise to significant residual currents (up to 0.3 m/s) which support the anticlockwise circulation in the North Sea (Sündermann & Pohlmann, 2011).

4.2 Waves

The NEED has the potential to reduce wave heights in the North Sea by blocking incoming waves from the Atlantic. It is assessed how the presence of the NEED alters the wave height in the North Sea.

4.2.a Theoretical background

The fetch that is needed for waves to fully develop is found for two scenarios: average and extreme wind speeds. The average wind speed is 8 m/s and the year-round dominating direction is southwest (Appendix D, (KNMI, 2013)). For extreme wind speeds 35 m/s is taken, having a 100 year return period. This data was retrieved from the Meteomast IJmuiden (MMIJ), located 75 km off the coast between the Netherlands and the UK (shown in Figure 4.2b). Data from the MMIJ is assumed to be representative for the whole North Sea.

If the waves are able to fully develop within the North Sea basin itself, the wave climate will not change due to the NEED. Fully developed waves reach a dimensionless wave height of $\tilde{H}_\infty = 0.24$ (Holthuijsen, 2007). The dimensionless wave height ($\tilde{H}$) and dimensionless fetch ($\tilde{F}$) are defined as (Holthuijsen, 2007):

$$\tilde{H} = \frac{gH_{m0}}{W^2} \tag{4.1}$$

$$\tilde{F} = \frac{gF}{W^2} \tag{4.2}$$

Where H_{m0} is the significant wave height in meters, F is the length of the fetch in meters and W is the wind speed in m/s. To check whether waves are fully developed for the given wind speed and fetch the following equation is used, where $\tilde{H}_\infty$ is the dimensionless wave height for fully developed waves (Holthuijsen, 2007).

$$\tilde{H} = \tilde{H}_\infty \left(\tanh\left(4.41 \cdot 10^{-4} \tilde{F}^{0.79}\right)\right)^{0.572} \tag{4.3}$$

However, even if the waves are not fully developed, the wave climate could still be identical to the wave climate before NEED if the waves are depth-limited. Depth limitation occurs at:

$$H_{m0,lim} = \gamma h \tag{4.4}$$

Where γ is the dimensionless breaker index, relating the water depth (h) to the maximum possible significant wave height ($H_{m0,lim}$), both in meters. When dealing with significant wave heights, $\gamma = 0.4$ (Holthuijsen, 2007). Therefore, it holds that the expected wave height found in equation 4.3 is limited to a maximum of $H_{m0,lim}$, both with and without NEED.

These results hold for wind waves only. The NEED does block a significant part of the swell waves entering the North Sea. The reduction in swell wave height and the contribution of swell to the total wave climate has not been studied here.

4.2.b Results

Using the equations 4.1, 4.2 and 4.3, wave heights with the NEED are determined and compared to wave heights in a fully developed wave field. Four scenarios are considered: average and extreme winds over the long and short side of the basin. The results are given in Table 4.1.

Table 4.1: Computed significant wave heights with the NEED (H_{m0}) versus significant wave heights in a fully developed wave field (H_∞) for four scenarios.

Wind speed [m/s]	Side [km]	H_{m0} [m]	H_∞ [m]
8	625	1.56 m	1.56 m
8	825	1.56 m	1.56 m
35	625	16.5 m	30.0 m
35	825	18.5 m	30.0 m

Table 4.1 shows that for average wind speeds, fully developed wave fields occur within the North Sea basin. Thus, for average wind speeds, NEED does not alter the wave climate. For extreme wind speeds, a fully developed wave field of 30 m high cannot be reached within the basin itself.

The depth-limited wave height is used to compute the maximum waves that can occur in the basin (equation 4.4). This results in $H_{m0,lim}$= 40 m in the deep part and $H_{m0,lim}$=16 m in the shallow part. This means that in the shallow part of the basin, waves are limited to a wave height of 16 m and thus there is no difference in wave climate with and without NEED. In the deep part of the basin, waves without NEED can reach larger wave heights than with NEED. However, the practical impact of this will be small because in coastal areas, the waves will be depth limited. Moreover, this extreme wave climate occurs rarely. Thus, it can be said that on average, the wave climate for wind waves will not significantly change.

4.3 Tide

After closure, the North Sea basin is the largest completely enclosed water basin in the world. Currently, the tides are the most significant driver of currents in the North Sea. Closing off the North Sea will take away the connection to the ocean tide, which is currently the most important driver of currents in the North Sea.

4.3.a Theoretical background

After closure of the NEED, a separate tide is generated inside the basin due to solar and lunar gravitational forcing. The amplitude of this new tide will be much smaller due to the limited water mass. To estimate the new tidal range, a comparison is made with tides in three other (semi) closed off seas with comparable sizes: the Caspian Sea, the Black Sea and the Baltic Sea. The Caspian Sea is the only sea to be fully closed off from ocean forcing. However, for the other two seas the influence of external forcing is small (Medvedev et al., 2016).

The amplitude of the tide can be affected strongly by the occurrence of resonance for one of the tidal constituents. Each constituent has a different wavelength. Whether resonance will occur or not depends on the ratio between the wavelength of the tidal constituents L and the length of the basin L_b. For a closed basin, resonance occurs for the following L_b/L ratios: 1/2, 1, 3/2, etc. Thus, the wavelengths of the two major semi-diurnal (M_2 and S_2) and diurnal (K_1 and O_1) tidal constituents are computed and compared to the length of the basin.

The periods of given constituents can be found in Appendix C.3. The wavelengths are determined using Equation 4.5 linking the wavelength L to the wave propagation speed c and the wave period T (Bosboom & Stive, 2015):

$$L = c \cdot T \tag{4.5}$$

The wave propagation speed is found using the shallow water approximation (Equation 4.6), which holds in the North Sea for a tidal wave due to the large wavelength (Bosboom & Stive, 2015). An average depth h of 80 m used.

$$c = \sqrt{gh} \tag{4.6}$$

Finally, the flow velocity induced by the tides can be computed using (Bosboom & Stive, 2015). This flow velocity contributes to the total current regime in the basin and will be determined for the tidal constituent that is assumed to be governing.

$$u = \frac{gak}{\omega} sin(\omega t - kx) \rightarrow \hat{u} = \frac{gak}{\omega} \tag{4.7}$$

Where $\hat{u}$ is the maximum velocity induced by the tides in m/s, a is the tidal amplitude in m, ω is the angular frequency in rad^{-1} and k the wave number in m^{-}1. ω and k are respectively defined as:

$$\omega = \frac{2\pi}{T} \tag{4.8}$$

$$k = \frac{2\pi}{L} \tag{4.9}$$

4.3.b Results

Table 4.2 shows that the Baltic, Caspian and Black Sea have maximum tidal ranges in the order of 20 cm (Medvedev et al., 2016). The North Sea basin is expected to obtain a comparable maximum tidal height after closing.

Table 4.2: Tidal heights for three (semi)-closed off seas with areas comparable to the North Sea and the expected order of magnitude for the North Sea.

	Caspian Sea	Black Sea	Baltic Sea	North Sea (Expected)
Area	370.000 km^2	435.000 km^2	375.000 km^2	515.000 km^2
Tidal range	21 cm	18 cm	24 cm	$\mathcal{O}$(20 cm)

To assess whether resonance occurs, the wavelength of each tidal constituent is computed using equation 4.5 (see Appendix C.3 for the elaboration). Table 4.3 shows the values of L_b / L for the short and long side of the basin. For M_2 and S_2, L_b / $L \approx \frac{1}{2}$ for the short side. Resonance could thus occur for these constituents over the short side of the basin.

Table 4.3: Values of L_b / L for the short side (L_b = 625 km) and long side (L_b = 825 km) of the basin

Tidal constituent	L_b / L long side	L_b / L short side
K_1	0.34	0.26
O_1	0.32	0.24
M_2	0.66	0.50
S_2	0.68	0.52

Finally, the flow velocities induced by the tides are computed. The M_2-constituent is assumed to be governing, as M_2 is in normal situations dominant over the other constituents and resonance for M_2 is expected. The computation can be found in Appendix C.3. This gives a maximum tidal velocity of 0.035 m/s. It is expected that the tidal wave will move through the basin in a counterclockwise circle, as it does nowadays. This results in counterclockwise velocities during flood and clockwise flow during ebb.

4.4 Discharge-driven currents

After the construction of the NEED, the rivers, Baltic Sea and precipitation bring a water discharge into the basin that needs to be pumped out at the dam. This discharge will induce a current from the rivers and the Kattegat towards the dam.

4.4.a Theoretical background

The mean velocity contributing to the circulation in the basin (Figure 4.2a) is computed as follows:

$$u = Q/A \tag{4.10}$$

Where Q is the discharge through the pumps in m^3/s as computed in Chapter 3. A the cross-sectional area in m^2 over which the flow is spread out. Assuming the pumps are distributed equally over the dam, width of the cross-section is equal to the length of the northern dam, which is 476 km. The height of the cross-section is 10 m, since the flow will probably be concentrated near the surface as both river outflow and pumping take place close to the surface.

4.4.b Results

The theory on discharge driven currents gives a flow velocity of $4.6 \cdot 10^{-3}$ m/s (as computed in Appendix C.1). This flow is directed from the rivers and Kattegat towards the Northern dam (Figure 4.2a).

4.5 Wind-driven currents

Surface shear stresses induced by wind cause currents. These currents can be computed using the horizontal momentum equation (Pietrzak, 2019a) (see Appendix C.2).

4.5.a Theoretical background

In Section 2.3, it is shown that the Rossby number is small and thus the momentum equation reduces to a balance of Coriolis and wind friction. Therefore, the currents due to wind can be computed using the Ekman velocity. The influence of Coriolis causes the current to deviate 45° to the right of the actual wind direction (on the Northern hemisphere). The velocity vector decreases with depth and describes a spiralling motion to the right, the Ekman Spiral. The equations from Pietrzak (2019a) will be used to derive the wind-driven currents from the surface shear stress.

The surface shear stress due to wind τ_s is given by:

$$\tau_s = 1.4 \cdot 10^{-3} \rho_{air} W^2 \tag{4.11}$$

The density of air (ρ_{air}) is 1.24 kg/m^3 (as computed using equation 6.9) in Chapter 6 and W is the wind speed in m/s.

The wind-driven velocity vector at the surface is given by:

$$V_0 = \frac{\tau_{s,y}}{\rho\sqrt{\nu_t f}} \tag{4.12}$$

Where V_0 is the surface velocity in m/s, ρ is the water density in m^3/s and for the vertical eddy viscosity, $\nu_t = 10^{-1}$ m^2/s is taken (Pietrzak, 2019a).

The velocity over depth in both u (in x-direction) and v (in y-direction) direction is then given by:

$$\begin{aligned} u_E &= V_0 e^{z/\delta} \cos\left(\frac{z}{\delta} + \frac{\pi}{4}\right) \\ v_E &= V_0 e^{z/\delta} \sin\left(\frac{z}{\delta} + \frac{\pi}{4}\right) \end{aligned} \tag{4.13}$$

The δ in this equation is the depth of the Ekman Boundary layer, as computed in Section 2.3 and z is the vertical coordinate.

4.5.b Results

The shear stress due to wind on the water surface is found to be 0.11 N/m^2. This gives a wind-driven velocity at the surface of $V_0 = 0.023$ m/s (Appendix C.2), directed 45° to the right of the wind direction (see Figure 4.2b). This velocity reduces over the depth: the average depth-integrated velocity is 0.014 m/s. This depth-averaged velocity is directed 90° to the right of the wind direction.

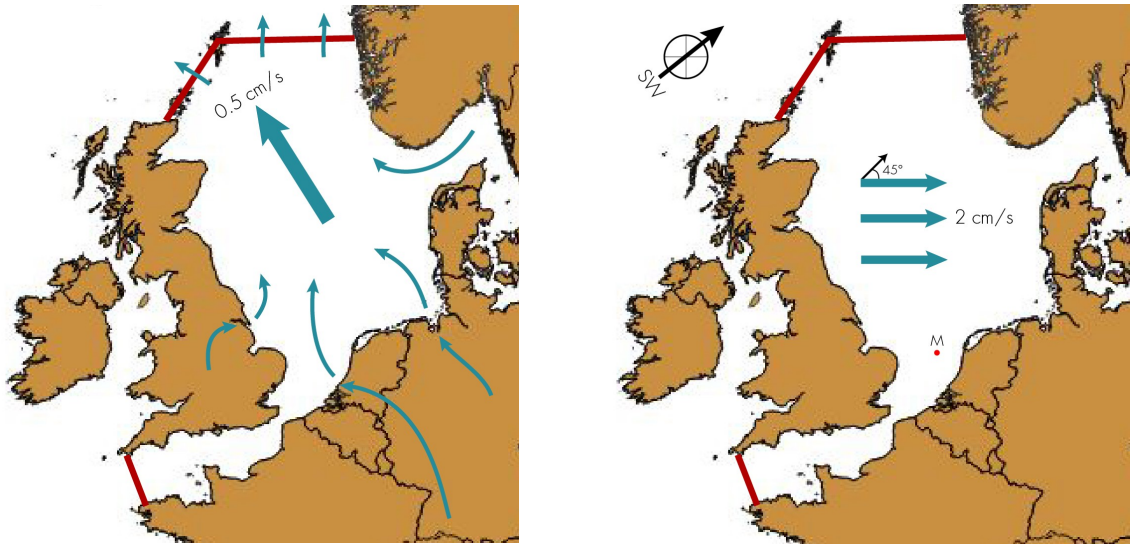

(a) (b)

Figure 4.2: a) Discharge-driven currents: The big arrow shows discharge-driven currents currents through the Northern Dam, coming from the rivers and the Baltic Sea. b) Wind-driven currents: The blue arrows show the wind-driven currents for a southwesterly wind. For the wind direction and wind speed, year-round average values are taken, to get an idea of the mean circulation patterns. The red dot with the letter 'M' indicates the location of Meteomast IJmuiden, from where the wind data was obtained.

4.6 Wind set-up

Besides the effect of currents, wind over the North Sea basin will cause a water level set-up. This set-up is relevant for two reasons. Firstly, a tilt in the water level will induce pressure differences and thus barotropic currents. Secondly, storm surges increase the water level at the coast. Hence, set-up values are computed for two scenarios. Wind set-up values for average wind speeds (8 m/s, as defined in Section) are used to find the barotropic currents that contribute to the mean circulation. Set-up due to extreme wind speeds (35 m/s) are used to assess the impact of NEED on coastal safety.

4.6.a Theoretical background

The set-up is computed for a southwesterly wind, which is the dominant wind direction as well as a northwesterly wind, where there is the longest fetch, and thus higher possible piling up of the water (Figure 4.3b).

The tilt in water level can be computed using the following equation (Zitman, 2019):

$$\frac{dh}{dx} = 3.5 \cdot 10^{-6} \frac{W^2}{gh} \tag{4.14}$$

In this formula, dh/dx is the slope in water level induced by the wind. This slope is given by the wind speed W over the local water depth h. In deeper water, the slope is less steep for equal wind conditions. Therefore, the shallower part of the basin will have a higher wind surge. The actual set-up at the coast dh can be computed using the length of the fetch dx and mass conservation, assuming the basin to be fully closed so the total volume of water is constant.

4.6.b Results

The values of the wind set-up are computed using equation 4.14. The results are shown in Figure 4.3a and 4.3b. Table 4.4 shows the water level slope.

Table 4.4: The water level slope dh/dx with NEED as computed from equation 4.14, due to the setup created by different wind speeds. These slopes are used to find barotropic currents in the next section.

	Average wind [8 m/s]	Storm [35 m/s]
Deep [100 m]	$2.3 \cdot 10^{-7}$ m/m	$4.4 \cdot 10^{-6}$ m/m
Shallow [40 m]	$5.7 \cdot 10^{-7}$ m/m	$1.1 \cdot 10^{-5}$ m/m

4.7 Barotropic currents

The tilt in water level induced by the wind causes a pressure gradient in the basin, leading to barotropic currents.

4.7.a Theoretical background

Since the Rossby number is small, geostrophic flows apply. The velocity is found by balancing the Coriolis term and the pressure gradient. This gives:

$$v = \frac{g}{f} \frac{dh}{dx} \tag{4.15}$$

Where dh/dx is the water level slope and f the Coriolis parameter. The geostrophic velocity is computed for the average scenario (8 m/s wind from the Southwest), for both the water level slope in the deep and the shallow part of the basin (as presented in Table 4.4).

4.7.b Results

In the deep part (dark blue part in Figure 4.3a and 4.3b), the geostrophic velocity is equal to 0.02 m/s. In the shallow part, the geostrophic velocity is 0.05 m/s. Due to the Coriolis term, the barotropic currents are directed perpendicular to the pressure gradient. The barotropic currents are shown in Figure 4.3c

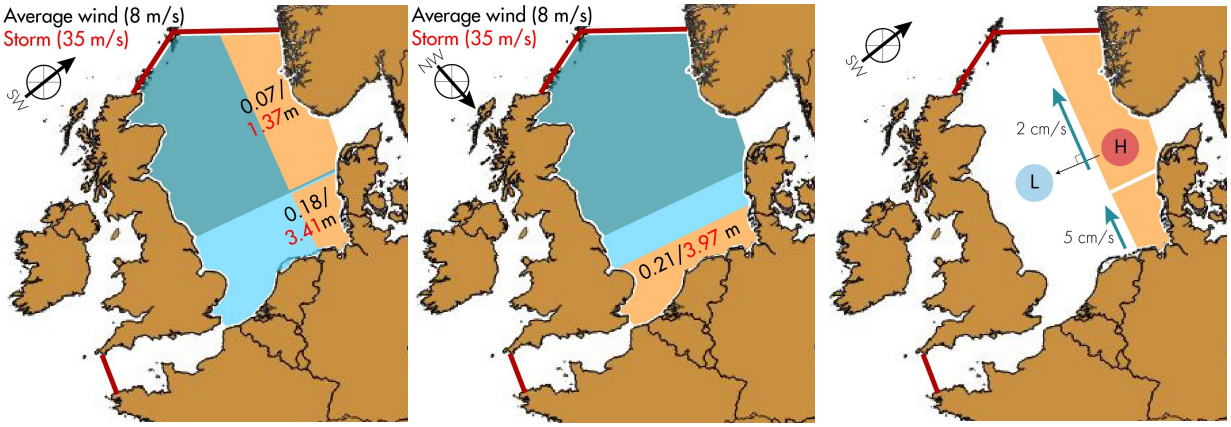

(a) (b) (c)

Figure 4.3: a) The area where wind set-up occurs for southwesterly wind is highlighted in orange. The shades of blue indicate the different depths (and thus different set-ups). The set-up heights for average wind speeds are given in black, for extreme wind speeds in red. b) The area where the wind set-up occurs for northwesterly winds highlighted in orange. This wind direction does not occur as often but the fetch is longer, leading to larger wind surges. The set-up heights for average wind speeds are given in black, for extreme wind speeds in red. c) The barotropic currents, due to a wind set-up resulting from an average southwesterly wind. For the wind direction and wind speed, year-round average values are taken, to get an idea of the mean circulation patterns.

4.8 Sensitivity analysis

Most of the parameters used to compute the results in this chapter can vary within certain ranges. Therefore, it is important to assess the sensitivity of the results to the input parameters. Table 4.5 shows the results of varying the input parameters within certain bounds. An explanation of the applied ranges can be found in Appendix C.4.

From the table, it can be concluded that the wave height H_{m0} strongly depends on the wind speed. Also the water level set-up, which is relevant for coastal protection, is heavily impacted by the wind speed.

Concerning the flows, the table shows that factors such as the air density, the water density, the Coriolis parameter and the pumping discharge only have a small influence on the flow velocities. Several factors can be distinguished that have a strong impact on the currents. First of all, an increase of only 2 m/s in the wind speed can almost double the flow velocity. Moreover, the tidal range, which could only be estimated by comparison to other (semi)-enclosed seas and is therefore rather uncertain, has an enormous influence. Therefore, accurately predicting the tidal range in the North Sea is of importance. Lastly, the cross-sectional discharge area A impacts the discharge-driven currents. It should be kept in mind that locally, flow velocities can be higher, especially in the vicinity of the pumps.

Overall, it can be concluded that a lot of the hydrodynamic variables (wind-driven currents, wind set-up, barotropic velocity and waves) show a strong dependency on the wind velocity. Hence, it is important to have a reliable estimate of wind velocities.

Table 4.5: Sensitivity of the computed wave heights, set-up and velocities by their input parameters

Varied parameter			Impacted parameter		
Parameter	Lower bound	Upper bound	Parameter	Lower bound	Upper bound
$W_{extreme}$	30 m/s	40 m/s	H_{m0}	15.3 m	21.6 m
			Set-up	2.9 m	5.18 m
$W_{average}$	7 m/s	9 m/s	H_{m0}	1.2 m	2.0 m
			u_{wind}	1.7 cm/s	2.7 cm/s
			$u_{barotropic}$	1.4 cm/s	2.3 cm/s
ρ_{air}	1.22 kg/m^3	1.26 kg/m^3	u_{wind}	2.2 cm/s	2.3 cm/s
ρ	1000 kg/m^3	1025 kg/m^3	u_{wind}	2.3 cm/s	2.2 cm/s
f	$1.13 \cdot 10^{-4}$	$1.26 \cdot 10^{-4}$	$u_{barotropic}$	2.0 cm/s	1.8 cm/s
			u_{wind}	0.23 cm/s	0.21 cm/s
Q	29200 m^3/s	30747 m^3/s	$u_{discharge}$	0.5 cm/s	0.6 cm/s
A	2380000 m^2	9520000 m^2	$u_{discharge}$	0.96 cm/s	0.24 cm/s
Tidal range	5 cm	40 cm	u_{tide}	0.88 cm/s	7.0 cm/s

4.9 Interpretation of the results

The barotropic- , wind-driven- and tidal flows are all in the order of centimeters per second. The discharge driven currents are an order of magnitude smaller and will thus not have a significant influence. Therefore, the flows due to tide, wind and barotropic flows together dominate the mean circulation in the basin. The eastward directed wind-dominated current and the northward barotropic flow could together drive an anticlockwise circulation as shown in Figure 4.4. Flood currents also drive an anticlockwise circulation, while during ebb, the flow might reverse or come to a standstill, depending on how the tidal flow interacts with the other currents.

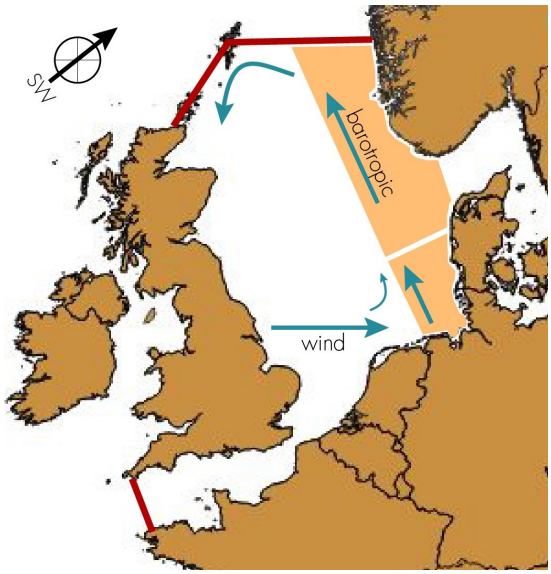

Figure 4.4: The total average circulation based on the year-round dominating wind conditions, found by superimposing the three dominant flow drivers: tide, wind-driven currents and barotropic currents due to wind set-up.

The found anticlockwise wind-driven circulation in the basin corresponds to nowadays mean circulation patterns for Southwesterly winds. Yet, the wind-driven flow patterns in the North Sea can fluctuate on a weekly timescale due to the variety in atmospheric forcing. Therefore, it must be noted that the found circulation is the average pattern, based on the year-round mean wind circumstances, but the flow is strongly variable and will rarely be in exactly this state.

Concerning the tide, the North Sea has been compared to several other inland seas with similar areas. However, the other characteristics of those seas, for example the depth should also be compared. The Black Sea has depths ranging up to 2 kilometers, which could cause the tide to behave differently. Resonance is expected for the M_2 and S_2 component over the short side of the basin. This means that the tidal character will most likely be semi-diurnal. However, local effects will probably play a much stronger role. In the compared seas, tidal heights differ strongly on a local scale. For example, in the Caspian Sea, tidal heights are significantly larger in the Southern Part. In the Baltic Sea, the maximum tidal height from Table 4.2 is concentrated in a small gulf, due to local resonance effects. Hence, it is impossible to predict the exact character of the tidal wave after NEED using only first-order hand calculations. It is recommended to use a model for further prediction of the tidal elevations in the North Sea basin.

Moreover, the different drivers for currents have been investigated independently and the final flow pattern has been found by superposition of the different currents. However, the different currents could influence each other, which has not been taken into account in this study.

The wave conditions have been computed so far for average and extreme wind conditions. In the case of average wind conditions, the wave field was fully developed, for extreme wind conditions not. It would be interesting to find the 'tipping point'; the wind speed where the wave field is just fully developed and the return period of that wind speed. Moreover, the fetch has been computed on the scale of the total North Sea basin. Close to the dam, for example in southern Norway or northern England or Scotland, the wave climate will be reduced compared to a situation without the NEED, especially for northerly winds.

5 | Salinity

When the NEED is build, the salty oceanic water will not be able to reach the North Sea basin anymore. Naturally, this has an impact on the salinity of the basin. Therefore, this chapter discusses how the salinity in the North Sea basin changes due to the NEED.

5.1 Current situation

The salinity in the North Sea is influenced by the influx of oceanic water PSU (Practical Salinity Unit) > 35 (OSPAR, 2000) and the influx of freshwater PSU $= 0$. The water supply from the Atlantic Ocean exceeds the sum of all freshwater sources by two orders of magnitude. Therefore the North Sea currently has a relatively high salinity, with seasonal variability due to the precipitation and continental discharge (Sündermann & Pohlmann, 2011).

The North Sea salinity distribution can be divided into two regions. In the southern shallow water region, the salinity values are in the range of 30 to 35 PSU in both the summer and in the winter. In the northern deep water region, the salinity values range from 27 to 35 PSU in the summer and from 31 to 35 PSU in the winter (Otto et al., 1990). The lower values in these ranges are due to the proximity of freshwater influxes.

An important factor when looking at salinity is the stratification in the ocean. In the northern region the depth is large and there is a fresh water influx to the upper layer from; the Baltic Sea, the continental coastal water and Norwegian coastal water. The deep water in this region is not mixed with the surface water as the tidal flow is small. This results in a year-round stable stratification in the northern region (OSPAR, 2000). The southern region has a shallow depth and the tidal flow is large. This induces a year-round mixed water region. In Figure 5.1 the exact distribution and transition zones can be observed.

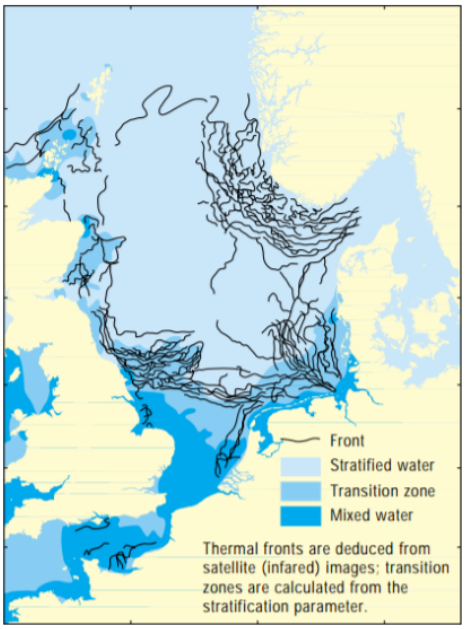

Figure 5.1: Transition zones between mixed and stratified water in the North Sea (OSPAR, 2000).

5.2 Theoretical background

The current state of the North Sea as seen in Figure 5.1 will change according to new boundary conditions, due to the build of the NEED. This results in a basin with a new equilibrium state, which will be derived in this subsection. Then the effects and interactions due the new salinity distribution will be examined based on characteristic formulas.

5.2.a The equilibrium state

In this subsection the equilibrium state will first be derived. This derivation is based on the initial state and is then compared to the Baltic Sea, which has similar properties as the equilibrium state.

The initial state of the basin has been evaluated in Section 5.1, and is visualised in Figure 5.2a. The southern region up until the Doggerbank (at 54 °N) is assumed to be in a mixed state and the northern region is assumed to be stably stratified. When the NEED will be built, the saltwater influx will stop and only the freshwater influxes remain. Eventually a new equilibrium state will be reached, which will be the basis of this chapter.

To be able to derive the new equilibrium state of the salinity in the basin, three currents are considered: Discharge-driven currents, wind-driven currents and tidal currents. These are the currents that are studied in Chapter 4 and considered the main drivers of the salinity distribution. Therefore these will have the largest impact on the stratification in the basin. The implication of the discharge-driven current on the salinity will be that the fresh water influx spreads horizontally through the whole basin. The wind-driven currents imply that the water influxes mix instantaneously with the present surface water layer. This assumption is made based on the theory of the Ekman boundary layer depth (approximately 40m). The tidal currents amplify the discharge-driven and wind-driven currents, but do not have a direct impact on the salinity, therefore this current is not taken into account. Lastly, the barotropic current is an effect of the wind-driven current and also does not have any direct implications on the salinity and is therefore not taken into account.

From these estimations an equilibrium state is sketched, shown in Figure 5.2b. The equilibrium state should be compared to a similar basin or lake to verify if this is a realistic estimate. In this research the Baltic Sea is used as reference case. The Baltic Sea has a small tidal component, which results in an influx of salt water into a relatively freshwater sea (on average 7 PSU (Leppäranta & Myrberg, 2009)). This results in a distribution as seen in Figure E.1 in the appendix, where there is a mixed layer on top, with a more salty stratified layer at the bottom. This is a representative profile for the Baltic Sea, and is similar to Figure 5.2b.

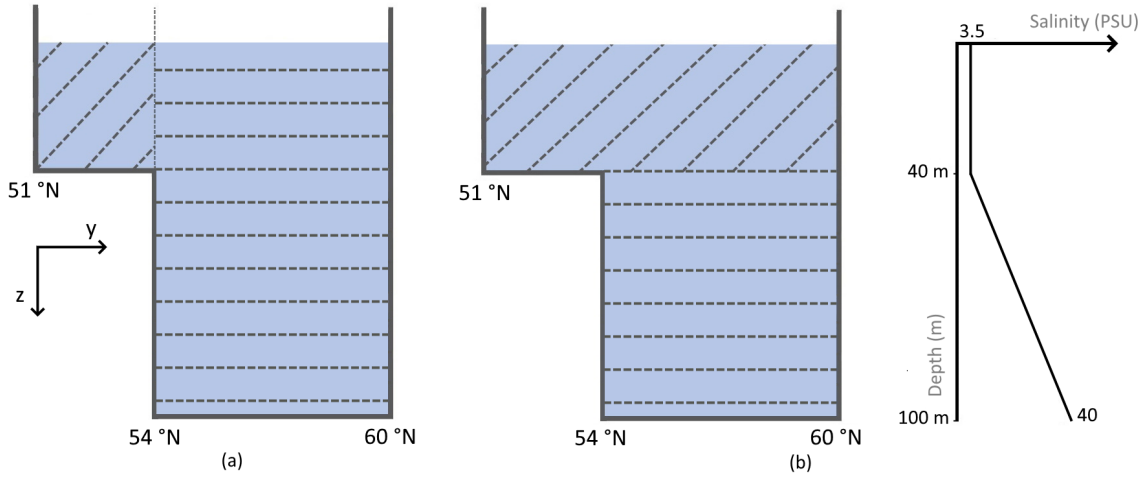

Figure 5.2: An average intersection of the North Sea basin, from South to North. The sloping lines define the mixed state and the horizontal lines the stratified state. a) The initial state based on salinity of the North Sea basin. b) The equilibrium state, with the salinity over the depth plotted.

A difference between the situations in the Baltic Sea and the North Sea is that the halocline is not observed in Figure 5.2b. It is assumed there is no halocline in the North Sea basin, as it is hard to determine if a mixed layer at the interface of these layers will be able to form, given the limited information on the vertical salinity distribution and flow velocities.

Calculating the exact salinity values for the equilibrium state will be difficult, as salinity has complex behaviour which cannot be estimated in a first order approximation. However, to be able to continue researching possible effects of the salinity change, approximate salinity values are necessary for these layers. Therefore, the salinity values will be estimated by comparing it to the values of the Baltic Sea.

The upper mixed layer will have a constant value that is 3.5 PSU and the lower stratified layer will range from 3.5 PSU to 40 PSU. For now, a linear salinity increase in the deep layer is assumed, as this is also the case for the Baltic Sea.

5.2.b Effects and interactions

In the following subsection the equilibrium state will be further quantified and analysed. This will be done based on numerous characteristic formulas.

First is discussed how long it takes before the equilibrium state is reached. The relevant interaction for this measurement is the amount of water that needs to be pumped out from the basin. The water is pumped out from the surface of the basin, therefore the freshening will only take place in the mixed layer. The freshening timescale can be calculated using the equivalent salt flux (R. X. Huang, 1993; Nurser & Griffies, 2019) and the assumption that the amount of water discharge D (m^3/s) is pumped out with a salinity S (PSU). Therefore the time it takes to change the salinity in a volume V (m^3) is:

$$\Delta t = \frac{V}{D} \log\left(\frac{S_{new}}{S_{old}}\right) \tag{5.1}$$

The Ekman spiral depth will be assessed next. This value indicates until what depth the wind can drive a flow. At the Ekman spiral depth the flow will be 25 times smaller than the surface velocity and will be directed in the opposite direction of the wind direction (Pietrzak, 2019a). The formula is as follows:

$$D_E = \pi\sqrt{\frac{2v_t}{f}} \tag{5.2}$$

The Ekman spiral depth is used to indicate what the flow velocities are at the bottom of the basin. This velocity can be used to calculate the renewal time at the bottom of the stratified layer. The renewal time is the time it takes to completely replace the water at a given location. This can be done by taking the length L (m) of the basin and divide it by the flow velocity U (m/s) at the bottom of the basin, where wind induced flow is the smallest. This yields the renewal time T (s):

$$T = \frac{L}{U} \tag{5.3}$$

Next, the geostrophic balance is analysed by looking at the Ekman number and Rossby radius. The Ekman number (E_x) indicates whether friction or Coriolis is dominant.

$$E_x = \frac{v_h}{fL^2} \tag{5.4}$$

When the Ekman number is smaller than one, friction can be neglected, this means the Coriolis force is in equilibrium with the pressure gradient. This is called the geostrophic balance. If the Ekman number is larger than one, the friction needs to be taken into account.

The external and internal Rossby radius (R_d and R_i respectively) of deformation give an indication on what scale the geostrophic balance becomes important.

$$R_d = \frac{\sqrt{gh_1}}{f} \tag{5.5}$$

$$R_i = \frac{\sqrt{g'h_2}}{f} \text{ where } g' = \frac{\rho_2 - \rho_1}{\rho_s} g \tag{5.6}$$

Here g' (m/s^2) is the reduced gravity term and is used for particles that are immersed under water. The average densities (ρ_1 and ρ_2) of each layer are calculated with the TEOS-10 equation of state. ρ_s is assumed as 1025 kg/m^3 as this is the average density of seawater and H (m) is the depth of the relevant layer. If the radii are smaller than the area of the basin and the flow is in geostrophic balance, gyres will be able to form. A gyre can either cause upwelling or downwelling.

The wind set-up, as explained in Section 4.7, has an effect on the internal interactions in the basin. The basin in its equilibrium state is defined as a two-layer flow with at the top a mixed layer and below that

a stratified layer. It is assumed that the wind has blown long enough that the flow has reached a steady state and is in geostrophic balance. The additional weight on one side of the basin due to the wind set-up will cause an increase in the surface slope in the direction of the wind. At the interface of the two layers the slope will decrease in the direction of the wind (Pietrzak, 2019b). This difference in slope can be calculated by relating the external slope to the density adjusted internal slope:

$$\frac{\partial h_1 + h_2}{\partial x} = -\frac{\rho_2 - \rho_1}{\rho_1}\frac{\partial h_2}{\partial x} \tag{5.7}$$

Where $\partial x = 625$ km and the subscripts indicate what layer it refers to. Subscript 1 indicates the top layer and subscript 2 the bottom layer.

5.3 Results

The equilibrium of the basin is now well defined within its boundaries in subsection 5.2.a. Therefore in this Section the effects and interactions of the salinity in the equilibrium state can be calculated and quantified.

The discharge D that needs to be pumped out of the basin follows from the water balance in Section 2.2. The salinity reduction from 35 PSU to 3.5 PSU will take approximately 50 years, the supporting calculations can be found in Appendix E.2.

The Ekman spiral depth is 131 m. From this depth it follows that the renewal time at the Ekman depth is approximately 20 years, see Appendix E.2 for the complete calculation.

The Ekman number is 0.00223, which means that Coriolis dominates highly over friction and therefore the flow is in geostrophic balance.

The internal and external Rossby radius of deformation are respectively 33 km and 172 km. These values are significantly smaller than the basin and as the flow is in geostrophic balance, gyres will be able to form. The complete calculation can be found in Appendix E.2.

The mean temperature for the whole basin after building NEED will be 9.2 °C, this is derived in Section 6.3. The average salinity in the upper layer is 3.5 PSU and the average pressure in this layer is 20 dbar (at 20 m depth in the middle of the upper layer). The average salinity in the lower layer is 35 PSU and the average pressure in this layer is 70 dbar (at 70 m depth in the middle of the bottom layer). The following average densities are found:

$$\rho_1 = 1003 \text{ kg/m}^3 \qquad \rho_2 = 1028 \text{ kg/m}^3$$

The internal slope is calculated for both an average wind and a storm. During a storm the internal slope has a value of $\partial h_2 = 110$ m and therefore results in a downwards tilt of 55 meters at Norway and an upwards tilt of 55 meters at Scotland. This extreme situation is sketched in Figure 5.3. For the average wind the internal slope has a value of $\partial h_2 = 5.8$ m and therefore results in a downwards tilt of 2.9 m at Norway and an upwards tilt of 2.9 m at Norway. Both calculations can be found in Appendix E.2.

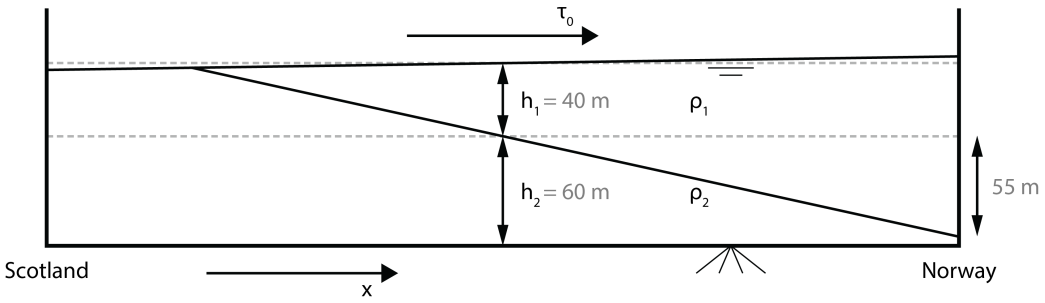

Figure 5.3: A storm from the west induces a wind set-up at the Norwegian coast. Due to the increase in surface slope, the internal slope will decrease in the other direction. Adapted figure from Pietrzak (2019b)

5.4 Sensitivity analysis

In Section 5.2 it is assumed that the salinity in the top layer decreases by a factor 10, from 35 PSU to 3.5 PSU. However, this is a scenario that was based on a comparison with the Baltic Sea, where salinity values of 0 PSU are not present. It could be possible that the North Sea basin will reach a salinity value of nearly 0 PSU as it will only exchange salt water through sluices. Multiple scenario's like this can be compiled, with different salinity values and also different stratification configurations. With these scenarios completely different results could be obtained. In Chapter 8 the sensitivity of the salinity is explained in more detail in relation to the density.

The value for the vertical eddy viscosity, used in Equations 2.2 and 5.4, is the standard value for an open ocean. This value is smaller in a shallow basin and near the coast, however the exact value is difficult to derive. This means that the Ekman boundary layer will also decrease, which will cause the mixing layer to be smaller. For a decrease of one order of magnitude, the Ekman boundary layer will decrease by an exponential relation and would result in a depth of 13 m. The same holds for the Ekman spiral depth, which will also decrease by an exponential rate to 41 m.

The value for the average density of the seawater ρ_s is assumed as the initial seawater density that was in open contact with the ocean. When the basin is closed off and starts to desalinate, this value will decrease throughout the years. Again this sensitivity is related to Chapter 8 as the density will change due to the change in salinity.

5.5 Interpretation of the results

As mentioned in Section 5.3, gyres will be able to form inside the basin. Resulting from Chapter 4, an anti-clockwise (cyclonic) flow is observed in the North Sea basin. This means that the Coriolis force will push the water from the gyre outwards, which will be replaced by water from deeper parts of the basin (called upwelling), as seen in Figure 5.4. Upwelling causes the salty stratified layer to mix with the upper mixed layer. This can cause the freshening time of the basin to be longer, as the top layer becomes saltier due to the gyres.

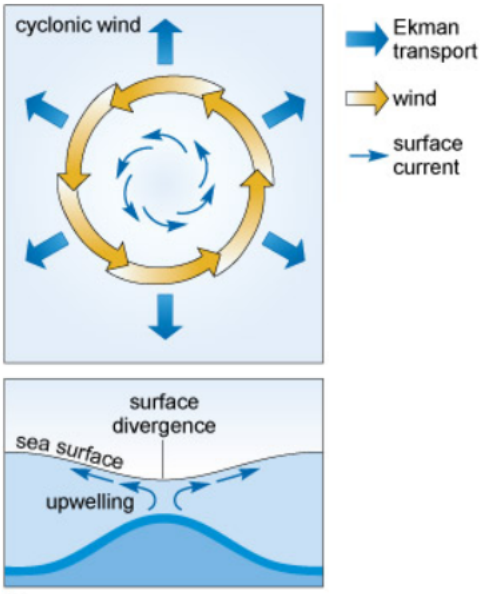

Figure 5.4: The effect an anti-clockwise wind on the surface on the North Sea basin. (Brandon, n.d.)

The internal slope (as seen in Figure 5.3) has been determined based on a two-layer system where both layers have a uniform density. However, this is a strong simplification. In reality, the bottom layer is stratified and the salinity only increases gradually. As a result, a sharp halocline is not present. Moreover, because the internal slope can be very large during storm events, mixing between the two layers is likely to happen.

6 | Temperature

The NEED also influences the temperature of the basin. This chapter takes a look at the change of temperature within the basin. The current situation is taken as starting point and both the average change as well as the monthly change in temperature due to the dam are presented.

6.1 Current situation

The temperature of the North Sea experiences a strong annual cycle, but the intensity of this cycle depends on the location. The amplitude of the yearly cycle and the mean, minimum and maximum sea surface temperature of the North Sea are shown in Figure 6.1. This figure shows that the minimum temperature is around 0 °C and that the maximum temperature is around 21 °C. Moreover, the strongest temperature variations are along the coasts of the Netherlands and Denmark and in the Skagerrak.

The areas in the Southern part of the North Sea have a well mixed temperature profile throughout the year. This corresponds with the shallow part of the simplified basin. The rest of the North Sea has a stratified temperature profile (OSPAR, 2000). The areas with a stratified temperature profile have a maximum thermocline at the end of the summer, which can have a slope of up to 0.7 °C/m (Lee, 1980). The vertical temperature distribution depends on the location and the water depth.

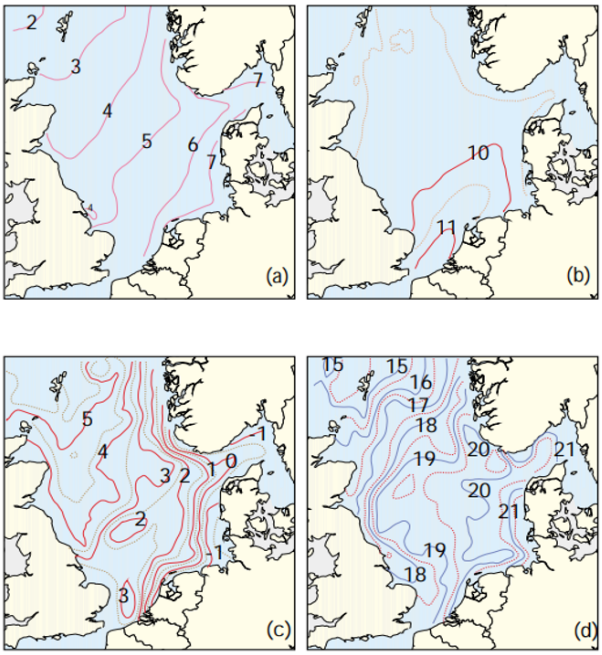

Figure 6.1: Sea surface temperature in °C. (a) Amplitude of the yearly cycle. (b) Mean temperature (c) Minimum temperature. (d) Maximum temperature. (OSPAR, 2000)

The North Sea exchanges heat with the Atlantic ocean via advection and with the atmosphere via radiation. It gains heat through the inflow of water from the North Atlantic and the English Channel and loses heat in exchange with the Baltic Sea (Becker, 1981). The values of the various fluxes are shown in Figure 6.2. In interaction with the atmosphere, it gains heat by solar radiation (Q_{sw}) and loses heat due to longwave radiation (Q_{lw}), the latent heat flux (Q_{lh}) and the sensible heat flux (Q_{sh}) (Lane, 1989).

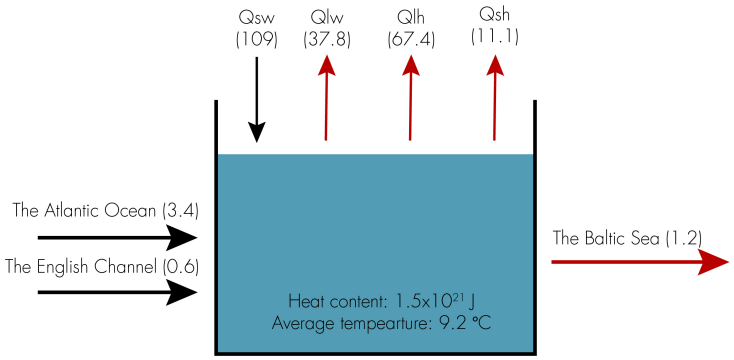

Figure 6.2: Average heat balance of the North Sea with fluxes in W/m^2 (Becker, 1981; Lane, 1989; Quante & Colijn, 2016)

The heat fluxes depend on the air temperature, sea surface temperature, dew point temperature, atmospheric pressure, wind speed and cloud cover (Becker, 1981). The most substantial exchange of heat (90%) takes place at the ocean-atmosphere boundary (Figure 6.2). The advective processes are in the order of 10% of the total change of the heat content of the ocean throughout the year (Schrum & Backhaus, 1999). Moreover, the North Sea gains heat by advective transport, but loses heat due to the atmospheric heat fluxes. However, there are local variations. Until the 1980s, the sea surface temperature and the heat content of the North Sea showed no positive or negative trend. However, the last 20 years (from 1987 onwards) a positive trend is visible for both parameters. The increase in sea surface temperature is 0.8 °C over the last 20 years and average heat content, the increase is $2.0{\cdot}10^5$ J/m^3/year (Meyer et al., 2011). This is much less than the seasonal variation of the heat content, which is about $5.0{\cdot}10^{20}$ J and stayed approximately constant over the last 20 years (Quante & Colijn, 2016).

6.2 Theoretical background

This section gives an overview of how the initial heat content and temperature profile are obtained and how the heat fluxes are calculated, Also, it shows the procedure which is followed to calculate the heat content and temperature when the NEED is built.

6.2.a Initial Heat Content and Temperature

To obtain the initial temperature profile, the dataset of Cummings & Smedstad (2013) is used. This data gives the average daily temperature of the sea water T_s for different depths at different locations. The years 2010-2020 are selected to obtain the temperature of for every 10 m depth, starting at the sea surface and finishing at a depth of 100 m, the maximum depth of the simplified basin. The mean of these temperature data gives the mean temperature for every depth for the whole North Sea. The temperature data is converted to heat content (HC) with equation 6.1 in order to be able to calculate the change due to the heat fluxes (Hjøllo et al., 2009). With equation 6.2 it is possible to convert the calculated heat content to temperature.

$$HC = \rho_s \cdot C_{p,w} \cdot z \cdot A \cdot (T - T_{ref}) \tag{6.1}$$

$$T = \frac{HC}{\rho_s \cdot C_{p,w} \cdot z \cdot A} + T_{ref} \tag{6.2}$$

Where ρ_s is the density of the sea water equal to 1025 kg/m^3, $C_{p,w}$ the heat capacity of water with a value of $3.99{\cdot}10^3$ J/kg/m, z the depth in m, A the surface area of the basin in m^2, T the sea water temperature at a certain depth in °C given by the dataset and T_{ref} the reference temperature, chosen to be 0 °C.

The result gives a temperature profile of the sea water and the heat content of the basin of the last 10 years. The average of these values is used as the initial condition for when the dam is built. Based on this result, the North Sea basin is divided into three layers: a surface layer (layer 1), a thermocline layer (layer 2) and a deep layer (layer 3), as shown in Figure 6.3a. The surface layer and the thermocline layer form the upper part of the basin, as given in the conceptualisation in Figure 2.1b.

6.2.b Heat Balance

The influx of relatively warm ocean water will not reach the North Sea basin anymore after the construction of the NEED. The fluxes that remain in the heat balance of the North Sea basin are: Q_{sw}, Q_{lw}, Q_{lh}, Q_{sh} and Q_{bs} (the Baltic Sea). The resulting heat balance is given in equation 6.3. The equations to calculate the terms in this balance are presented in this section and based on Lane (1989).

$$Q_{net} = Q_{sw} - Q_{lw} - Q_{lh} - Q_{sh} - Q_{bs} \tag{6.3}$$

To calculate the shortwave radiation, equation 6.4 is used.

$$Q_{sw} = Q_{solar}\left(1 - \frac{1}{8}N_t \cdot c_s - 0.38 \cdot \frac{1}{64} \cdot N_t^2\right)(1-\alpha) \tag{6.4}$$

Where Q_{solar} is the incident solar radiation in W/m^2 and α the sea surface albedo coefficient, both varying per month. N_t refers to the mean cloud cover and equals 5.6 Okt and c_s is the solar radiation cloud cover coefficient equal to 0.4, both obtained for 50°(Lane, 1989). Since the solar radiation does not depend on the temperature of the sea, it is assumed that this flux does not change after the construction of the NEED.

The infrared back radiation Q_{lw} is calculated using equation 6.5.

$$Q_{lw} = 0.96\sigma T_a^4(11.7 - 0.0023P_d)(1 - \frac{1}{8}N_t c_c) + 3.84\sigma T_a^3(T_s - T_a) \tag{6.5}$$

Where σ is the modified value of the Stefan-Boltzmann constant in W/m^2/K^4, equal to $1.3134{\cdot}10^{-9}$. The back radiation cloud cover coefficient is given by c_c for 50°N from Lane (1989) and has a value of 0.72. T_a is the air temperature in K, determined using the dataset Copernicus Climate Change Service (C3S) (2017). This dataset gives the average air temperature per day at a height of 2 m. T_s is equal to the temperature of the sea surface in K. P_d, the saturated vapor pressure of air at the sea surface in Pa, is determined with equation 6.6.

$$P_d = 10^{\left(c_1 + \frac{c_2}{T_d} + \frac{c_3}{T_d^2}\right)} \tag{6.6}$$

Where c_1, c_2 and c_3 are calibration constants obtained from Lane (1989) and T_d refers to the dew point temperature in K, determined with equation 6.7.

$$T_d = T_a - \frac{100 - \mathrm{RH}}{5} \tag{6.7}$$

Where RH the relative humidity in %, taken as a constant equal to 83%.

Equation 6.8 gives the latent heat flux. Equation 6.9 gives ρ_a (density of air over sea in kg/m^3), equation 6.10 gives q_s (mixing ratio of air over sea) and equation 6.11 gives q_a (mixing ratio of air). P_s, representing the vapor pressure over sea in Pa, is given by equation 6.12.

$$Q_{lh} = (2500970.8 - 2365.09T_a)\rho_a W(q_s - q_a)C_e \tag{6.8}$$

$$\rho_a = \frac{P_{atm}}{287.04T_a(1 + 0.61q_a)} \tag{6.9}$$

$$q_s = 0.662\frac{P_s}{P_{atm} - P_s} \tag{6.10}$$

$$q_a = 0.662\frac{P_d}{P_{atm} - P_d} \tag{6.11}$$

$$P_s = 10^{\left(c_1 + \frac{c_2}{T_s} + \frac{c_3}{T_s^2} + c_4\right)} \tag{6.12}$$

Where W is the wind speed in m/s and has a value of 8. C_e, equal to 0.00143, is the exchange coefficient between sea surface and atmosphere. P_{atm} is the atmospheric pressure and equal to 101392 Pa and c_4 a calibration constant given by Lane (1989).

The last atmospheric flux is the sensible heat flux, given by equation 6.13.

$$Q_{sh} = -(T_a - T_s)\rho_a W C_{p,a} C_e \tag{6.13}$$

Where $C_{p,a}$ represents the heat capacity of dry air equal to 1004.64 J/kg/K.

The value of Q_{bs} is taken as a constant throughout the year and equals 1.2 W/m^2 (Becker, 1981). This value is assumed to stay the same after the construction of the NEED.

The atmospheric fluxes only depend on the sea surface temperature. Therefore, the heat balance is only applied to the surface layer. The depth of this layer depends on the initial temperature profile. However, since there is exchange of heat between the surface and deep layer over the thermocline layer, the heat balance of the surface layer needs to be expanded with a diffusion term (Q_{dif}) given by Fourier's law in equation 6.14.

$$Q_{dif} = k\frac{\Delta T}{\Delta x} \tag{6.14}$$

Where k is the thermal conductivity of sea water equal to 0.6 W/(m·K) (Sharqawy et al., 2010), ΔT the difference in temperature between the surface layer and deep layer in K and Δx the thickness of the thermocline in m. Since Q_{dif} has a value in the order of 10^{-1} it is neglected in further research because it is one or two orders of magnitude smaller than the other heat fluxes. Thus, the heat balance given in equation 6.3 is applied to the surface layer only. The change of the heat content of the whole basin in treated proportional to the change in the surface layer. The change of the heat content of the other layers is not taken into account. In reality the temperature of these layers will change due to the NEED.

6.2.c Heat content and Temperature with NEED

With the formulas for the heat balance and the initial temperature profile being known, it is possible to determine what happens to the surface layer of the North Sea basin after the construction of the NEED, following the described procedure below.

First, the initial heat content of the surface layer is determined based on the average temperature of this layer. With this initial value, the change of the average heat content is determined, using time steps of one day. Therefore, the average values of the following parameters are determined based on the provided data and given equations: Q_{net}, HC_1, HC_2, HC_3, T_a, ρ_a, T_d, Q_{solar} and α. These values represent the initial condition of the surface layer of the basin just after construction of the NEED. The change of the heat content is determined as follows. First, to the previous HC_1, the Q_{net} is added. This Q_{net} is converted from W to J/day. The next step is to calculate the corresponding temperature of the upper layer based on the new HC_1 with equation 6.2. The temperature of the upper layer is used to determine the fluxes Q_{sw}, Q_{lw}, Q_{lh} and Q_{sh} with equations 6.4, 6.5, 6.8 and 6.13, respectively and converted to J/day. The last step is to calculate the new Q_{net}, with equation 6.3. With this value, it is possible to determine the new heat flux.

The new heat content of the surface layer is added to the heat content of layer 2 and 3 to get the heat content of the basin. With this heat content, the average temperature of the basin is determined. The temperature of the upper layer is used to determine the fluxes Q_{sw}, Q_{lw}, Q_{lh} and Q_{sh} with equations 6.4, 6.5, 6.8 and 6.13, respectively. All these fluxes are converted to J/day. The last step is to calculate the new Q_{net}, with equation 6.3. With this value, it is possible to determine the new heat flux. For the monthly change in heat content, the same procedure is followed.

With the calculated heat content in the surface layer, the new heat content of the basin can be calculated by adding the unchanged heat content of layer 2 and layer 3. This gives also the new temperature of the whole basin.

6.3 Results

This section gives the initial temperature profile. It also provides the initial heat balance and the change of the temperature after construction of the NEED, both on a yearly and monthly basis.

6.3.a Initial Heat Content and Temperature

The mean temperature profile is given in Figure 6.3a. The figure also presents the three different layers and the correspoding mean temperatures. The mean temperature are 10.5 °C, 9.8 °C and 8.5 °C for layers 1, 2 and 3, respectively. The mean temperature of the basin is 9.2 °C.

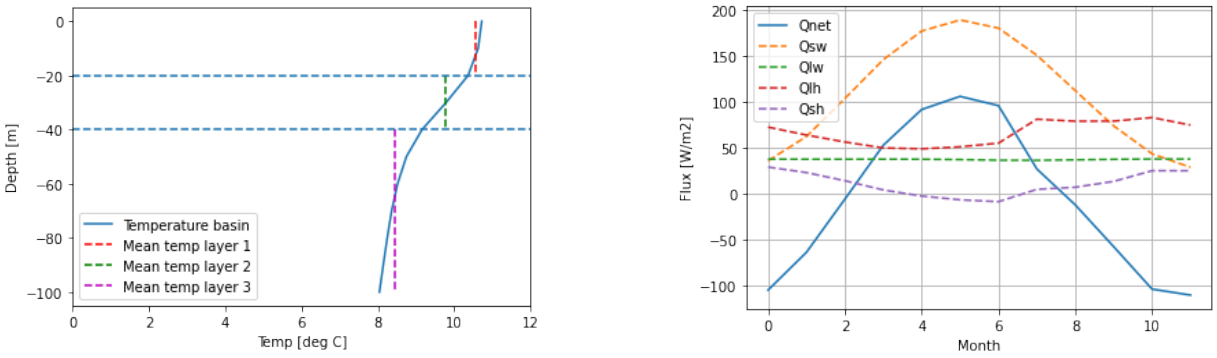

(a) (b)

Figure 6.3: a) Vertical initial temperature profile North Sea with average temperature of the surface layer and basin. b) Initial heat fluxes of the North Sea in exchange with the atmosphere per month, where Q_{net} is the net radiation, Q_{sw} the shortwave radiation, Q_{lw} the longwave radiation, Q_{lh} the latent heat flux and Q_{sh} the sensible heat flux.

6.3.b Heat Balance

Based on the obtained sea temperature and air temperature data, the monthly values of the fluxes in exchange with the atmosphere before the NEED are calculated. The result is given in Figure 6.3b.

6.3.c Heat Content and Temperature with NEED

With the initial condition being known, it is possible to determine what happens after the construction of the NEED. The average decrease of the heat content is $1.2{\cdot}10^{19}$ J. The corresponding decrease in the temperature for both the surface layer and basin is shown in Figure 6.4a. The temperature decrease of the surface layer is 0.3 °C, with a final temperature of 10.2 °C. For the basin, the temperature decrease is equal to 0.1 °C, which results in a final temperature of 9.1 °C. The new equilibrium is reached after 200 days.

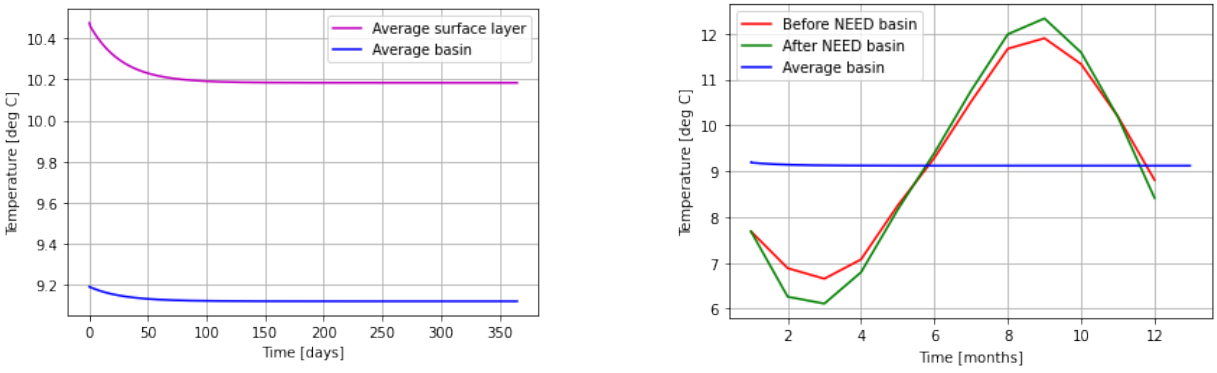

(a) (b)

Figure 6.4: a) Change of the temperature after the construction of the NEED using yearly averages, given both for the surface layer and the whole basin. b) Change of the temperature after the construction of the NEED, using monthly averages. The result presented, shows the temperature of the entire basin.

The result using monthly averages in temperature is given in Figure 6.4b. From this figure, it is clear that the amplitude of the temperature increases after the construction of the NEED. Concerning the entire basin, the difference between the minimum value of the initial temperature and new temperature is 0.5 °C. The difference in the maximum value is 0.4 °C. The average annual change is small compared to the yearly variation and happens within the first year.

6.4 Sensitivity analysis

For the change in the monthly values of the temperature, the month January is selected as the starting month. However, it might be possible that a different starting month gives a different outcome. To test if this is the case, every month is used as a starting month. This results in a slightly different outcome in maximum and minimum temperature of the basin in the first year. In the following years, there is no significant difference. The average annual condition of the North Sea basin is also used as a starting position and gives roughly the same outcomes as any other month. The average condition might be the best option, since it will take some years to build the NEED.

The value of T_{ref} in equations 6.1 and 6.2 is chosen to be 0 °C. There is a difficulty with this choice. If the temperature of the North Sea is below zero, the heat content becomes negative which is physically impossible. The average temperature of the North Sea basin is not below 0, but when looking at smaller scale, temperatures can drop below 0. Attention should be paid to the location and spatial scale of the study when using the parameter T_{ref}.

The result of the final temperature of both the basin and the surface layer depend on the values obtained for the air temperature and sea surface temperature. Or, more specifically stated, to the difference between the air temperature and sea surface temperature, which is on average equal to 0.7 °C. To test how sensitive the outcome is to this difference, the value is both increased and decreased. The results of this change to the final temperature of the entire basin are shown in Figure 6.5a. From this figure, it is clear that if the difference increases with 1.0 °C, the temperature of the basin increases instead of decreases. The difference of the minimum and maximum temperature of the basin on a monthly basis is given in Figures 6.5b and 6.5c, respectively.

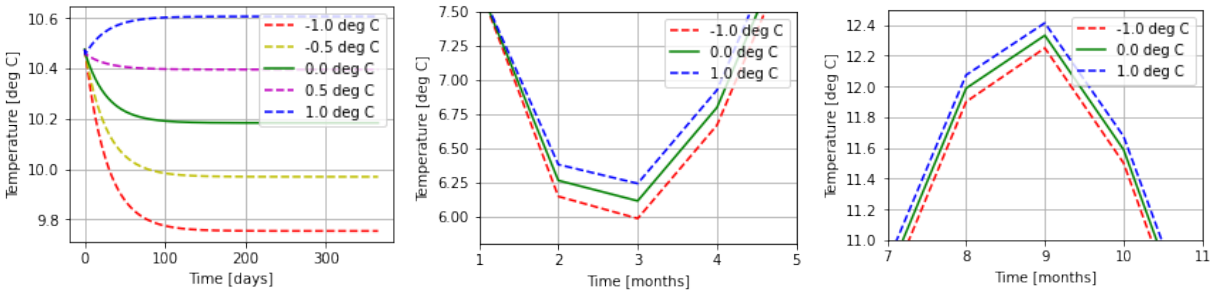

(a) (b) (c)

Figure 6.5: Sensitivity of the temperature of the basin to the difference in air and sea surface temperature in a) On average, b) On a monthly basis when the temperature of the sea is at a minimum and c) On a monthly basis when the temperature of the sea is at a maximum.

Next, the influence of the depth of the sea surface layer is investigated. Therefore, the depth of the surface layer (layer 1) is varied between 10 and 40 m. The thermocline layer (layer 2) thus changes from 30 to 0 m. The deep layer stays constant. The results of the temperature of the basin before and after NEED and of the temperature of the surface layer are shown in Table 6.1. From this table, it is clear that the final temperature of the basin depends on the depth of the surface layer. The final temperature of the surface layer does not depend on the depth.

Table 6.1: Temperature change of the basin (T_{basin} and surface layer (T_{srf}) depending on the depth of the surface layer.

	T_{basin} [°C]		T_{srf} [°C]	
Depth [m]	Initial	Final	Initial	Final
10	9.3	9.2	10.6	10.2
20	9.2	9.1	10.6	10.2
30	9.1	9.0	10.5	10.2
40	8.9	8.9	10.3	10.2

The sensitivity of the result to the choice of the values of the parameters Q_{bs}, W, C_c, N_t, RH, c_c and c_s is tested as well. The final temperature of the surface layer and basin after the NEED with a perturbation of 10% in the value for a parameter is given in Table 6.2. This table also gives the fluxes that are affected by a change in the value of the parameter. For the case where the relative humidity increases with 10%, the temperature of the North Sea basin does not decrease but increase. From the table it can be seen that the final temperature is most sensitive to the value of the relative humidity. The value for the Baltic Sea seems to have the least influence on the final temperature of the basin and surface layer.

Table 6.2: Final surface layer temperature (T_{srf}) and basin temperature (T_{basin}) if parameters either decrease or increase with 10%.

		T_{basin} [°C]		T_{srf} [°C]	
Depth [m]	Perturbed flux	-10%	+10%	-10%	+10%
Q_{bs}	Q_{bs}	9.1	8.1	10.2	10.2
W	Q_{sh} & Q_{lh}	9.2	9.1	10.4	10.0
C_e	Q_{sh} & Q_{lh}	9.2	9.1	10.4	10.0
N_t	Q_{sw} & Q_{lw}	9.2	9.0	10.4	9.9
RH	Q_{sh} & Q_{lh} & Q_{lw}	8.9	9.3	9.4	11.0
c_c	Q_{lw}	9.1	9.1	10.1	10.3
c_s	Q_{sw}	9.2	9.1	10.4	10.0

6.5 Interpretation of the results

The temperature of the North Sea basin decreases slightly and its amplitude increases when the NEED is built. This might have several implications. The first one is the possibility that more ice forms in the North Sea basin due to the lower temperature of the sea in winter. Moreover, the fact that the salinity of the surface layer decreases, as presented in Section 5.3, strengthens this tendency. The second implication is related to ecology. It is possible that some species are not able to cope with these increased fluctuations. The last mentioned implication is that the change in temperature can also have an influence on the weather in some coastal regions.

7 | Sediment transport

Sediment in the North Sea plays an important role in the transportation and absorption of contaminants, plankton primary production, marine ecosystems, coastal protection, mining and dredging of navigation channels (Dobrynin et al., 2011). This chapter answers the question on how the sediment availability, transport and distribution in the North Sea basin change due to the construction of the NEED. To illustrate the implications of these changes Section 7.4 applies the results to three small-scale locations: the Rhine ROFI, the Wash and the Southern Bight.

7.1 The current situation

The sediment transport in the North Sea is mainly driven by tidal currents. This results in a counterclockwise circulation of sediment along the coasts with most deposition taking place where the flow direction reverses: in the Kattegat and along the Dutch and German coasts, similar to the circulation pattern as shown in Figure 4.1 in Section 4. Sediment in suspension is mainly brought in via the English Channel and from the northern coast of the UK, whereas sediments brought in via the main rivers deposit quickly close to the river mouths.

7.1.a Sediment budget

The North Sea knows a history of sediment infilling, which means that the basin receives more sediment than it supplies to external locations. During the Quaternary period (starting 2.6 million years ago), this led to more than one kilometer of sea bed rise (Ottesen et al., 2014). Taking a closer look into the current supply, a sediment budget can be set up that consists of eleven in- and outgoing fluxes. It should be noted that the boundary of the budget is the transition layer between seawater and seabed. This means that sediment in suspension is part of the sediment storage and sediment at the seabed is not part of this storage. As can be seen from Figure 7.1, most sediment enters the North Sea via the English Channel and via rivers, followed by sediment dumping into the basin from dredging activities in harbors and river mouths, bed erosion and coastal erosion (predominantly cliff erosion at the English coast). Supply via the Baltic Sea, atmospheric deposition and primary production are small. The major sediment outflux is provided by depositional processes, mainly taking place in estuaries. Interaction with the Atlantic Ocean also functions as a small net outflux, likewise dumping on land for beach nourishment. In Appendix F.1, the literature and assumptions used to retrieve the magnitudes of the fluxes are given.

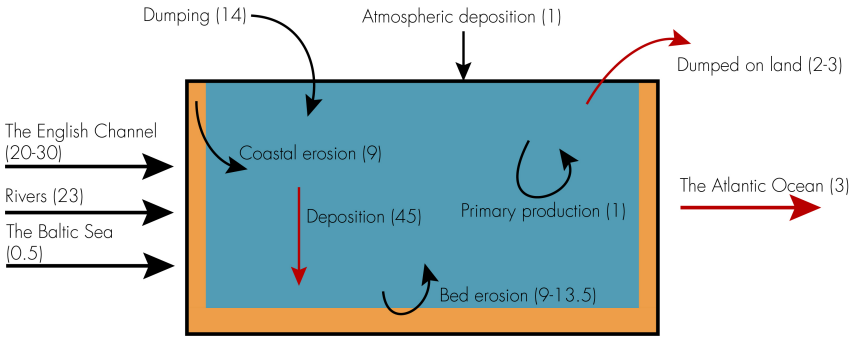

Figure 7.1: Current sediment budget of the North Sea basin in fluxes. The numbers in brackets indicate the average annual flux in Mtons/year for the entire basin.

7.1.b Horizontal and vertical sediment distribution

Sediment can be found in two conditions: as suspended particulate matter (SPM) throughout the water column and as bed load on the seabed, which consists on average of coarser particles. SPM is transported by currents and deposits when the flow velocity drops below a certain threshold. A typical time scale for SPM transport through the North Sea from Normandy in France to Denmark is about 1 year (Gerritsen et al., 2000). In Appendix F.2, maps of the distribution of sediment in suspension and at the seabed can be found. The maps show that at some locations, both suspended sediment and fine seabed material

concentrations are high. This can be explained as follows: the influence of vertical mixing by waves is bigger at shallow than at deep water locations, entraining more sediment from the seabed and resulting in higher SPM concentrations. The SPM concentrations in the North Sea are thus highest at shallow locations where much turbulence is induced by fluvial discharge, by tidal forcing, or close to eroding cliffs (Pietrzak et al., 2011). At the seabed, fine sediments (which are most prone to resuspension) are mostly found along the 40 meter depth contour (Dobrynin et al., 2011; Holt & James, 1999), with the German Bight and the English river mouths being depositional hotspots (Dobrynin et al., 2011). From the maps in Appendix F.2 it can also be seen that there is a seasonal variability in sediment transportation and distribution. During summer, calm weather with low wind speeds and wave heights prevails, resulting in stratification and deposition. During winter, stronger winds induce mixing of the water column and bring in more sediment by rivers and by cliff-, coastal- and bed erosion at shallow locations (Quante & Colijn, 2016; Dobrynin et al., 2011).

7.2 Theoretical background

Sedimental processes are complex and often interrelated. Therefore, large-scale studies on (fine) sediment transportation vertically as well as horizontally are based on many simplifications and use various empirical relations (Gerritsen et al., 2000; Puls et al., 1995). This results in a wide range of outcomes. The analysis on the change of sediment transport in the North Sea basin after the construction of the NEED is therefore executed with the use of a conceptual framework set up for this research. The framework is based on literature and generic sediment transport- and deposition relations, and is inspired by the framework on fine sediment distribution by Hendriks et al. (2020). It helps to provide a rough quantitative insight into the sedimentary changes due to the NEED by separating the fundamental processes of sediment transport (later mentioned as pillars).

The framework is first applied to the entire enclosed North Sea basin to have an overview of the major changes. Eventually, to gain a better understanding of the morphological and ecological implications of the changes, in Section 7.4 three regions in the North Sea are used as case studies: the Rhine ROFI, the Wash and the southern part of the Southern Bight (see Appendix F.4 for the topographical locations). These regions are chosen because of their characteristic or problematic sediment transport and/or storage. It is assumed that the changes that take place in the entire basin can also be used for the changes on a smaller scale.

The basis of the conceptual framework are the fundamental processes of sediment transportation. These are limited by various factors and parameters, such as: sources of sediment supply, flow velocity, sediment grain size, bed shear stress velocity, settling velocities, stratification of the water column and availability of fines at the seabed (Dobrynin et al., 2011; Gayer et al., 2006; Gerritsen et al., 2000; Otto et al., 1990; Quante & Colijn, 2016). The major processes as described by Gerritsen et al. (2000) and Dobrynin et al. (2011), combined with the limiting factors, are restructured into a conceptual framework that consists of four pillars affecting the sediment dynamics and distribution in a basin: (1) source, (2) flow velocity, (3) tidal presence and dominance, and (4) vertical transportation and distribution of suspended sediment. The pillars however do not act completely independent and therefore the interaction between them should also be taken into account. This is illustrated in Figure 7.2 and further explained in the upcoming subsections. When using the framework, it is assumed that no sediment is taken out of the basin by the pumps in the dam, that anthropogenic activities affecting the sediment budget do not change over time, that river sediment supply does not change and that the influence of precipitation on sediment transport can be neglected.

7.2.a Source

Sediment is supplied by various sources in the form of suspended sediment or bed load, as described in 7.1.a. Concerning SPM, the seabed is an important source (Quante & Colijn, 2016), as resuspension can only occur if there is enough fine sediment present in the upper seabed layer (Dobrynin et al., 2011). The change in sediment sources due to the construction of NEED is estimated by comparing the sediment budget with and without the NEED. The new sediment budget is set up by checking whether fluxes are cutoff, increase or decrease. Only the biggest fluxes from Figure 7.1 are considered (the English Channel, rivers, the Atlantic Ocean, dumping, coastal erosion, deposition and bed erosion), as it is assumed that the small fluxes do not significantly alter.

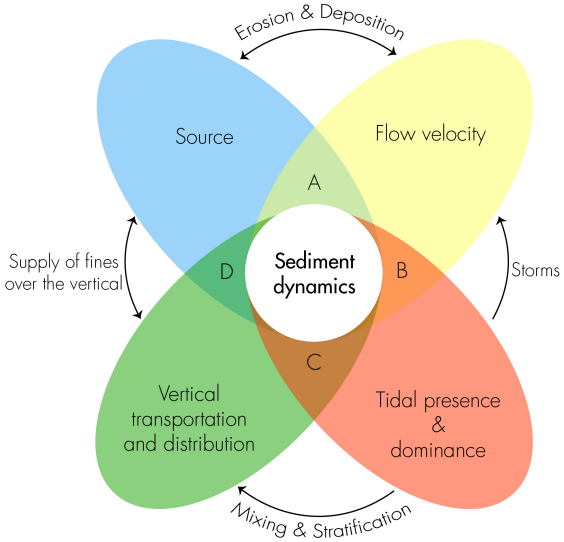

Figure 7.2: The conceptual framework that is used for describing the changes in sediment transport due to the construction of the NEED. The framework consists of four pillars (the colored leaves) that are interrelated (shown with A, B, C and D).

7.2.b Flow velocity

Flow velocities in the North Sea basin are altered by the NEED (see Chapter 4), and consequently change the ratio of deposition, sediment transportation and erosion. Firstly, this ratio is determined by using the Hjulström curve: an empirical relation between deposition, flow velocity and sediment grain size. The curve is shown in Appendix F.3. Secondly, sediment transportation is further analysed by following the approach of Dobrynin et al. (2011). However, the exact shear stress velocities are not computed as this is highly location dependent. The equations are thus used for the relations between shear stress velocities and flow velocities. This can be used to analyse by how much the bed stresses change with the altering flow velocities. The method of Dobrynin et al. (2011) shows that the bed shear stress velocity V* can be analysed using equation 7.1, with ρ the water density in kg/m^3 and τ the shear stress in N/m^2. The mean bed shear stress consists of two components (see equation 7.2): the stress induced by currents that is linearly related to the squared flow velocity U (equation 7.3) and the stress induced by winds (equation 7.4). C_D is the friction coefficient that is dependent on the median grain size (0.0025 m), U_w is the wave velocity in m/s and f_w the friction factor. During this analysis, it is assumed that τ_{wave} does not change due to the NEED (see Section 4.6).

$$V* = \sqrt{\frac{\tau}{\rho}} \tag{7.1}$$

$$\tau_{mean} = \tau_{cur} \cdot [1 + 1.2(\frac{\tau_{wave}}{\tau_{cur} + \tau_{wave}})^2] \tag{7.2}$$

$$\tau_{cur} = \rho \cdot C_D \cdot U^2 \tag{7.3}$$

$$\tau_{wave} = 0.5 \cdot \rho \cdot f_w \cdot (U_w)^2 \tag{7.4}$$

Last of all, a spatial analysis on the change in resuspension is executed. This is done by combining the retrieved changes in shear stress velocities and the current spatial bed shear data of NOAH (2006), shown in Appendix F.3. The maps show the spatial bed shear stress distribution, induced by waves and by tides separately. In order to initiate sediment transport via resuspension, the bottom shear stress velocity should exceed the critical shear stress velocity (0.2 N/m^2 (Gayer et al., 2006)). The new bed shear stresses are compared to these thresholds in order to see whether resuspension takes place.

7.2.c Tidal presence and dominance

Sediment dynamics can be dominated by tides or by storms, varying per location in the North Sea basin (Quante & Colijn, 2016). If the tidal effect is dominant, the variability of sediment transport is bounded to hourly fluctuations that are relatively constant on the long-term, whereas storm dominant processes react directly to the magnitude of the storm. The latter is less predictable and is bounded by the seasons: the storm period in the North Sea runs approximately from October until April. A qualitative analysis is executed by using the changes in tides and wave climate from Sections 4.6 and 4.3.

7.2.d Vertical transportation and distribution of suspended sediment

Stratification of the water column results in a vertical distribution with less SPM at the surface and more SPM at the deepest layer of the water column. Suspended matter becomes trapped below the pycnocline (Quante & Colijn, 2016). Mixing however, lifts sediments from close to the seabed to higher levels, which is counteracted by the process of settling. The exchange of sediment with the seabed (the boundary of the model) is analysed by using the deposition formula of Krone (1962) (Dobrynin et al., 2011; Puls et al., 1995):

$$M_{dep} = w_s \cdot c_{bot} \cdot \left(1 - \frac{\tau_{bed}}{\tau_{dep,cr}}\right) \tag{7.5}$$

Where M_{dep} is the SPM mass deposited per unit time and unit bottom area (kg/s/m^2), w_s the settling velocity, c_{bot} the near-bottom SPM concentration in kg/m^3, τ_{bed} the bed shear stress velocity and $\tau_{dep,cr}$ the critical bed shear stress that should not be exceeded in order for deposition to occur (0.2 N/m^2 (Gayer et al., 2006)). Settling velocities are retrieved from Puls et al. (1999). Next, the erosion is analysed using the method of Gerritsen et al. (2000):

$$M_{ero} = E_0 \cdot \left(\frac{\tau_{bed}}{\tau_{ero,cr}} - 1\right) \tag{7.6}$$

Where M_{ero} is the sediment mass eroded per unit time and unit bottom area and $\tau_{ero,cr}$ the critical bottom shear stress (0.4 N/m^2) and E_0 the erosion rate (0.1 kg/m^2/s). For simplicity of the analysis, it is assumed that the parameters w_s, c_{bot} (equation 7.5) and E_0 (equation 7.6) are not altered by the NEED.

7.2.e Interactions

The interactions between the pillars of the conceptual framework are depicted with capital letters and arrows in Figure 7.2, and can be explained as follows.

A Bed erosion and resuspension are sediment supplying sources, whereas deposition extracts sediment from the system. The fines that sink to the seabed become available for resuspension again.

B Storms increase the flow velocity during a limited period. However, it can have big impact on the exceedance of resuspension and erosion thresholds. During calm periods, tidal currents are at most locations too weak to exceed the thresholds by themselves.

C Storms and tides lead to mixing of the water column. Storm induced waves have highest impact at the surface and are restricted to a maximum depth of influence, whereas tidal currents affect the entire water column (Otto et al., 1990).

D Stratification brings sediment to lower water levels, what decreases the settling distance and thus enhances deposition and the supply fines at the bottom. Mixing results in the availability of SPM over the entire water column.

7.3 Results

Application of the conceptual framework to the North Sea basin with NEED results in the following outcomes. A summary is shown in Figure 7.3.

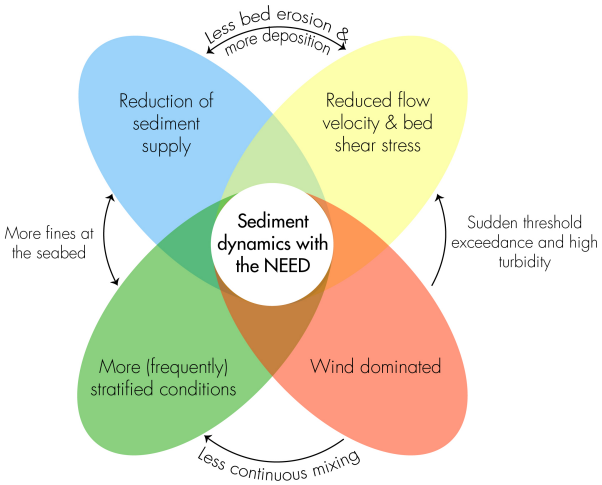

Figure 7.3: Qualitative results of the conceptual framework applied to the North Sea basin with NEED.

7.3.a Source

Enclosing the North Sea basin results in a new sediment budget, as fluxes to and from the ocean are cut off and flow velocity decreases. An overview of the largest fluxes that are evaluated is given in Figure 7.4 and more extensively in Appendix F.1. It can be seen that the minimum net incoming sediment mass rate of 30 Mton/yr in current circumstances would decrease to maximum 12 Mton/yr by enclosing the North Sea basin. The remaining main fluxes are deposition, river supply, dumping and bed- and coastal erosion. Due to the high decrease in flow velocity (see Section 4) sediment supply by bed erosion is decreased, whereas deposition rates are increased (see Subsection 7.3.d). Using the assumption that the waves (see Section 4.6) and anthropogenic activities do not change, the other fluxes do not alter. As sediment cannot leave the basin anymore via the Atlantic Ocean, the sediment will mostly end up at the bottom of the deeper waters (in the centre of the basin, due to the circulation). The deposited fines in shallower water become available for resuspension during storms.

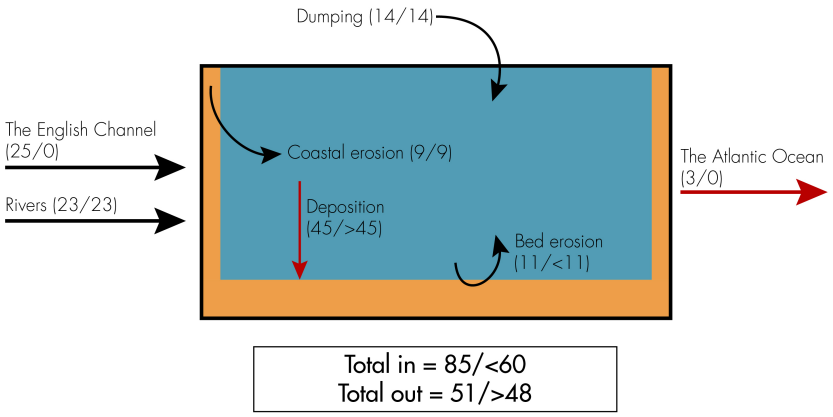

Figure 7.4: Sediment budget of the North Sea Basin in fluxes. The numbers in brackets indicate the average annual flux in Mtons/year. The number before the slash refers to the current situation and after the slash refers to the situation with NEED. The total in- and outfluxes are the sum of the fluxes, including the small fluxes that are shown in Figure 7.1. These are assumed to not significantly change due to the NEED.

7.3.b Flow velocity

The average flow velocity reduces approximately by a factor 14 from 50 cm/s to 3.5 cm/s after construction of the NEED (see Chapter 4). Using the Hjulström curve (Appendix F.3), it can be seen that almost no sand can be in suspension anymore under these conditions. Taking into account that velocities at low depths decrease even more, also part of the suspended silt and clay in the lower water layers of the North Sea will deposit. Deposition rates along the British coast will be high, as this is currently the location with the highest suspended sand concentration (NOAH, 2006).

Using equations 7.1 to 7.4, it can be stated that the bed shear stress reduces as a consequence of the reduced flow speed. Wave magnitudes do not change (see Section 4.6) and thus neither does the wave induced bed shear stress. Using the linear relation between current induced bed shear stress and squared flow velocity (see equation 7.3) results in a reduction of the current induced bed shear stress of a factor 200. Besides, it is assumed that the median grain size does not change and that the wave shear stress and current shear stress do not differ much in magnitude nowadays (except for deeper parts, where already rarely resuspension takes place (NOAH, 2006)). With those conditions, equation 7.2 shows that a decrease in flow velocity by a factor 14 eventually results in a reduction in mean bed shear stress and average shear stress velocity by respectively more than 100 and 10 times.

Combining this information, the resuspension threshold and the bed shear stress map of NOAH (2006) (see Appendix F.3) gives insight in the new distribution of resuspension. Resuspension in the North Sea occurs most often at locations where shear stress induced by tides prevails (Neil & Scourse, 2010; NOAH, 2006). If the current induced shear stress is reduced by a factor 200, regions of resuspension by only ocean currents do not exist anymore. Adding up the regions of average resuspension due to waves, results in the locations of resuspension that are shown in Figure 7.5.

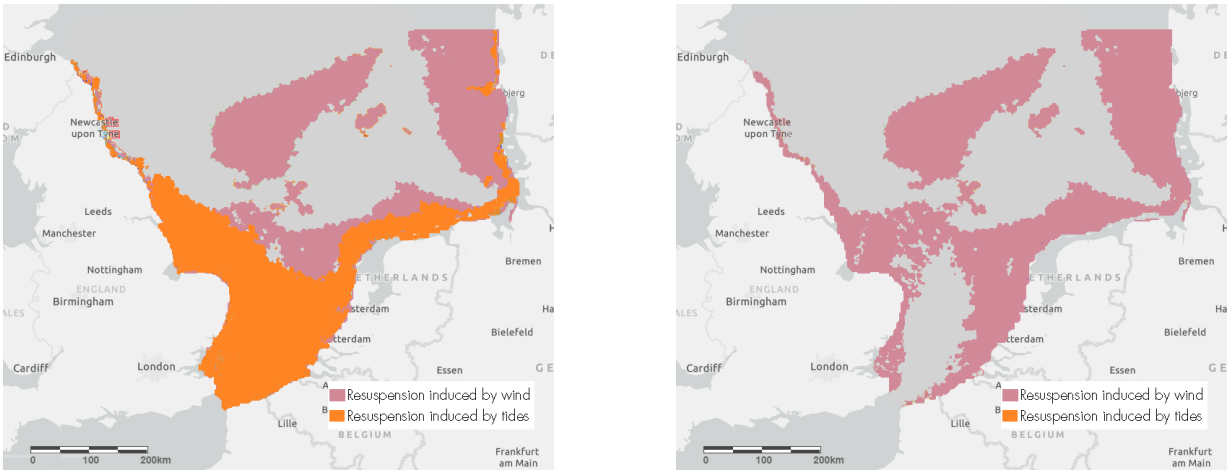

(a) (b)

Figure 7.5: Maps with average resuspension locations in the North Sea in the current situation (a) and in the situation with NEED (b). The orange color depicts the resuspension induced by tides and the pink color depicts the resuspension induced by waves. It can be seen that in the situation with NEED, no resuspension by tides occur.

7.3.c Tidal presence and dominance

The tidal currents will be reduced to values comparable to wind currents for average wind (see Section 4.3). Therefore, the sedimentary processes will be dominated by storm events. The seasonal difference in resuspension and SPM between calm and stormy periods is therefore enhanced. As more fine sediment is available at the seabed (see Section 7.3.a), a lasting storm can extend the time of resuspension which was previously limited by the amount of fines (this for example occurs at the Dogger Bank (Dobrynin et al., 2011)). A storm after a relatively calm period can thus suddenly turn the clear sea into a highly turbid state.

7.3.d Vertical transportation and distribution of suspended sediment

The reduction of tides limits vertical mixing of the water column. This leads to vertical stratification with little suspended sediment at the surface. Suspended sediment stays at lower water levels where it deposits more easily. Using the Krone formula (see equations 7.5 and 7.6), it can be calculated that throughout the basin a decrease in flow velocity by a factor 14 results in:
(1) an initial increase of deposition rate of approximately $w_s \cdot c_{bot} \cdot \frac{\tau_{bed}}{\tau_{dep,cr}}$;
(2) an initial decrease in erosion rate of approximately $E_0 \cdot \frac{\tau_{bed}}{\tau_{ero,cr}}$.

It should be noted that the changes only hold if τ_{bed} still exceeds (for erosion) or stays below (for deposition) the critical thresholds. The exact changes vary per location as it depends on the concentrations, bed shear stresses and the sediment grain size. An example for the Rhine ROFI is given in Appendix F.4.

7.4 Case studies

Applying the results of the framework (see Figure 7.3) on a smaller scale provides better insight into the implications of the alterations. Therefore three locations are studied: the Rhine ROFI, for its coastal protection, The Wash, for its ecology, and the southern part of the Southern Bight, for its morphology. The focus of this subsection is on the changes in characteristic sediment transport based on the generic changes in the enclosed North Sea basin.

7.4.a The Rhine ROFI

The Rhine Region of Freshwater Influence (ROFI) extends 20-40 km from the coast and is around 100 km long (Simpson et al., 1993). The freshwater influx of the Rhine into the North Sea forms a buoyant current that establishes stratified conditions during ebb tide and plays an important role in the transportation and supply of sediment (de Boer et al., 2009). Moreover, the interplay between tides and wind induced flow leads to an interesting balance between alongshore and cross-shore sediment transportation. Flood tide and storms cause vertical mixing, bringing sediment onshore, which leads to northward alongshore transport. During ebb, stratified conditions lead to a clockwise circulation at the surface and an counterclockwise circulation at the bottom transporting sediment offshore (de Boer et al., 2006). Both waves and tides are thus important factors in the dynamics of the Rhine ROFI (Quante & Colijn, 2016) and they both cause relatively high bed shear stresses (NOAH, 2006). The median tidal bed shear stress is higher offshore, whereas the impact of waves on the bed shear is higher close-shore (Hendriks et al., 2020). These high bed shear stresses make the region a permanent resuspension zone (Dobrynin et al., 2011) with high sediment transport rates and a high annual deviation in SPM (Pietrzak et al., 2011).

With the construction of the NEED and the reduction of tides, the ROFI will become storm dominated, experiencing the highest shear stresses close to the shore (Hendriks et al., 2020). The storm conditions will not change and are leading for coastal protection, as this has the most impact close-shore. However, as stratified conditions will occur more often, the cross-shore sediment export will be enhanced. This requires more caution concerning coastal protection. Analysis on the erosion and deposition rates shows that the erosion rates drop to zero with the reduced flow velocity and deposition is initiated at a small rate (see Appendix F.4). This means that the region is not a permanent resuspension zone anymore. However, concerning coastal protection it is beneficial that more fines are available for resuspension at the seabed during storms, reducing erosion more close-shore. Currently, the seabed consists mainly of sand, which requires higher flow velocities to initiate erosion (Hendriks et al., 2020).

7.4.b The Wash

The Wash is an embayment on the East coast of England that consists of a complex system of salt marshes, shoals and sand banks. This attracts a wide range of shellfish and birds. Also, the region is known for its high accretion rate: it experiences a net influx of 6-8 Mton sediment per year, mainly originating from offshore locations, from cliff erosion at Holderness and from rivers such as the Great Ouse (Ke et al., 1996). A map of the topography and places of accretion and accumulation is given in Appendix F.4. Tidal currents in the embayment are the main driver for flow and transport (mainly during flood tide), as wind induced waves dissipate on the sand banks before reaching the southeastern coasts (Pye, 1995).

With the reduction of tides, external sediment supply, flow circulation and erosion become limited. The biggest change in resuspension will be located in the northwestern part of the bay, where the bed shear

stress induced by tides is currently highest (Ke et al., 1996). It is likely that more deposition will take place at the entrance because of the reduced flow velocity. These effects play an important role for the flora and fauna in the area. The oscillation in water marks by tides will reduce, resulting in 2 consequences: parts of the intertidal mudflats will stay dry for longer periods and the refreshing of the water reduces (which is comparable to the situation in the Wadden Sea, described in Section 9). This has negative impact on the reefs that thrive on the intertidal properties of the area, but also on the water quality in general. On the other hand, eastward flow induced by winds keeps eroding the north- and west side of the mudflats and accreting on the east side. New pieces of land provide room for new species to grow that do not long for constant water level oscillation. However, the plants can store sediment easily in the slow flowing water, lifting the mudbanks and disconnecting them from the water. These "dry" mudflats are more vulnerable to storms, giving opportunities for rejuvenation on its turn.

7.4.c The Southern Bight

The southern part of the Southern Bight is the most prominent area for interaction between tide and topography in the North Sea (Otto et al., 1990). The characteristic linear sand ridges located in the Southern Bight are a result of the tidal effect that shapes the banks with an counterclockwise offset (shown in Appendix F.4). The tidal forcing through the English Channel transports the sediment that is source of the sand banks, as the fine content in the seabed itself is too low for significant supply. Moreover, bed shear stress is predominantly induced by tides and hardly by waves (see Figure 7.5). The highest shear is located along the southeastern English coast, close to the Thames river mouth.

For the analysis with the NEED, the flow in the Southern Bight induced by the pumps in the southern dam is not considered. Due to the NEED, the area loses its major sediment source and sediment supply from the Thames becomes dominant. This is also the location with the biggest reduction in shear stress and thus relatively high deposition rates occur. This makes the Deep Water Channel, a pass through for bottom water just off the coast, prone to high deposition rates. The loss of sediment sources and the essential effect of ebb and flood, stagnate the process of the sand ridge formation. The high reduction in flow speed will flatten the banks by deposition in the depressions. Moreover, eastward storms would erode the ridges at their ends, migrating them eastwards and losing their characteristic shape orientation. This on its turn changes the flow patterns in the area, as this is currently influenced by the banks (Otto et al., 1990).

7.5 Sensitivity analysis

The method that is used for the analysis on sediment transport in this study, depends highly on the outcomes of the study on hydrodynamics in Chapter 4. After all, sediment is transported by water and resuspension is limited by the flow velocity. However, sediment settlement is also dependent on temperature and salinity. Cooling and freshening of the basin increases the settling velocity by limiting the ions available for attachment (Winkler et al., 2012). This exact effect is unknown and is therefore neglected in this study.

Moreover, the results of the study depend on the initial conditions concerning SPM concentrations, seabed sediment grain size and the distribution of fines at the seabed. The SPM concentration determines how much sediment can deposit, whereas the latter influences how much sediment can be taken into resuspension. If the seabed consists of mostly fine sediment, the threshold value for resuspension is lowered and relatively more erosion can take place. The interrelations are also included by the values of w_s, c_{bot}, C_D and E_0 that are considered constant in this study, but in fact depend on these initial conditions as well.

Lastly, the results can differ per location. The parameters used in this study are all spatially determined by depth, SPM concentrations and sediment grain size. For example at deep water locations, the effect of storms on the seabed is limited, whereas at shallow locations the waves do reach the bottom. Caution should therefore be paid when averaging the parameters for the entire basin.

7.6 Interpretation of the results

The results show that the NEED alters the sediment transport highly. Firstly, there is a decrease in net sediment influx from 30 Mton/yr to 12 Mton/yr. This results eventually in a decelerating effect on the rising seabed. Also, as sediment cannot leave the basin anymore via the Atlantic Ocean, this sediment will mostly end up at the bottom of the deeper waters (in the centre of the basin, due to the circulation). At shallow coastal locations with high SPM concentrations however, the increased rate of deposition can cause local hotspots for deposition and might require more dredging.

Secondly, storms will dominate the amount and timing of resuspension. During calm periods, the water will quickly turn into clear conditions as resuspension cannot occur and sediment deposits quickly. However, during a storm the water turns suddenly into a turbid state, as the deposited fines at the bottom are swept up easily. Although the turbid state would not last much longer than the storm itself due to quick settlement, this has big implications for aquatic life.

Lastly, the results mainly show insight into the initial response of sediment transport to the NEED. On the longer term however, particles have settled and are gradually transported and stored in the seabed after consumption by macrobenthos (Puls et al., 1999). This results in a courser seabed and leaves behind a smaller SPM concentration that consists of the smallest particles. That in its turn decreases the settling velocity w_s and the concentration at the bottom c_{bot} and would eventually lead to a smaller deposition rate. On the other hand, the decrease in grain size of the depositing sediments causes a fining of the seabed on the long term. This would result in relatively more erosion for a moderate storm with NEED.

8 | Dependency between salinity, temperature and currents

In previous sections, the changes in hydrodynamics, salinity and temperature due to the NEED have been treated as separate domains. However, these domains do influence each other. This chapter answers the research question on how the changing temperature and salinity affect the hydrodynamics by investigating the density driven flows.

8.1 Theoretical background

Temperature, salinity and hydrodynamics interact with each other as shown in Figure 8.1a. This section looks into the influence of salinity and temperature on density, which is determined by these two factors. Density differences give rise to density driven flows and are thus part of the hydrodynamics. Since the temperature and salinity change, the density driven flows might change as well.

However, the obtained values for the change in temperature and salinity are the result from a study in 1D. Therefore, only average values for the whole North Sea have been computed and spatial variations are not taken into account. In reality, the change in temperature and salinity will most likely not be uniform within the basin. For example, temperature differences between North and South might increase and freshening might be stronger in coastal areas. Therefore, it is valuable to investigate how the density-driven flows change due to those variations.

The flows for the cross-section given in Figure 8.1b are determined. This 1D cross-section, with 112 data points in North-South direction, ranges from 51°N to 60°N at 2.5°E.

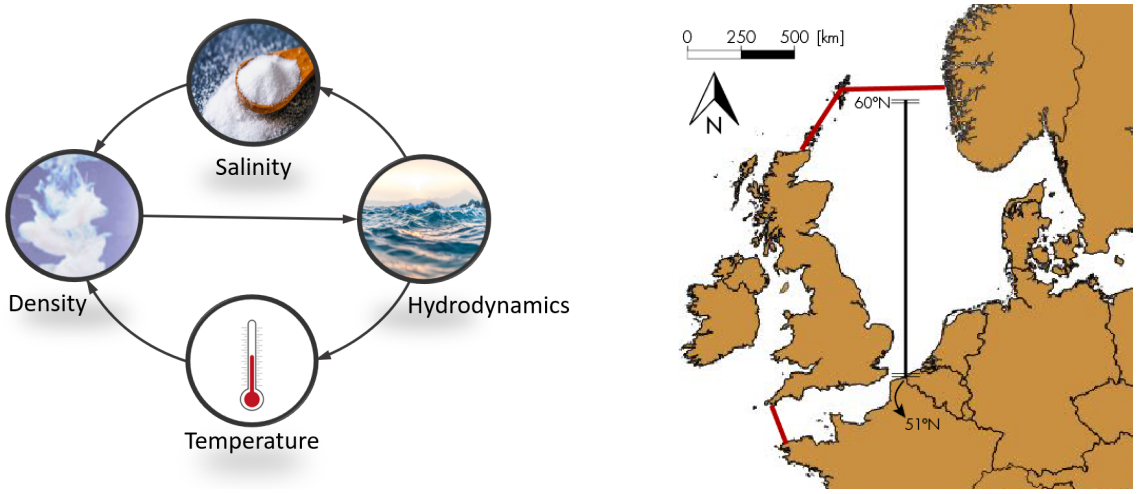

(a) (b)

Figure 8.1: a) Graphical overview of the interactions. b) 1D cross section to investigate the interactions.

The density driven flows that prevail nowadays are calculated and used as the initial situation. Data for temperature and salinity at the surface for the years 2015-2020 is retrieved from dataset Cummings & Smedstad (2013). Moreover, the flows in the case with the NEED are calculated as well. Therefore, the salinity and temperature change with the values obtained in Chapters 5 and 6, respectively. From temperature this means a decrease of 0.3 °C and for salinity a reduction with a factor 10.

Two aspects will be investigated to account for the possible variations in temperature and salinity. Firstly, it will be studied how sensitive the density is to changes in either temperature or salinity. Does a variation in one of the factors give a stronger density change? For this, both temperature and salinity are first increased by a factor 1.2 and then decreased by a factor 0.8 to see the resulting change in density driven flows.

Secondly, the effect will be studied in case the change in density due to the NEED is not uniform within the basin. This is done by applying a gradient in the distribution of temperature and salinity. To get an idea of how this would affect the density driven currents, three scenarios are investigated:

1. In the first scenario, the change in temperature and salinity with respect to the initial situation is larger in the North than in the South. This is done using a linear function for both temperature and salinity.

2. In the second scenario, the change in temperature and salinity is larger in the South than in the North

3. In the third scenario, the change of salinity is smaller in the middle of the North Sea, while the coastal regions experience a high reduction in the salinity. This is established with a polynomial function, with a decrease of salinity with a factor 20 at the coasts and almost 0 in the middle of the basin.

For the different situations and scenarios presented, the following procedure is executed to calculate the density driven flows. With the values for temperature and salinity for each data point, different for each situation or scenario, the TEOS-10 method (described in Section 2.3) gives the values for the annual average density of the sea water for each data point. The density differences between the data points are used to compute the density driven flows between the locations, using the thermal heat equation (Pietrzak, 2019a). This is done at 10 m depth because directly at the surface, there are no pressure differences and thus no density-driven currents.

$$\frac{du}{dz} = \frac{g}{f\rho_0}\frac{d\rho}{dy} \tag{8.1}$$

This equation describes the increase of flow velocity over depth du/dz. f is the Coriolis parameter and for ρ_0, the mean density in kg/m^3 in the respective situation is chosen. $d\rho/dy$ is the density gradient. A positive density gradient in North-South direction leads to a flow from West to East due to a balance of Coriolis and the internal pressure gradient.

8.2 Results

The values of the density in the situation with and without the NEED are given in Figure 8.2a. In general, the density increases from the South to the North. This leads to an eastward flow (positive values in the graph) due to Coriolis. Figure 8.2b shows that the velocities due to density differences are very small and decrease even further after building the NEED: they are in the order of millimeters per second.

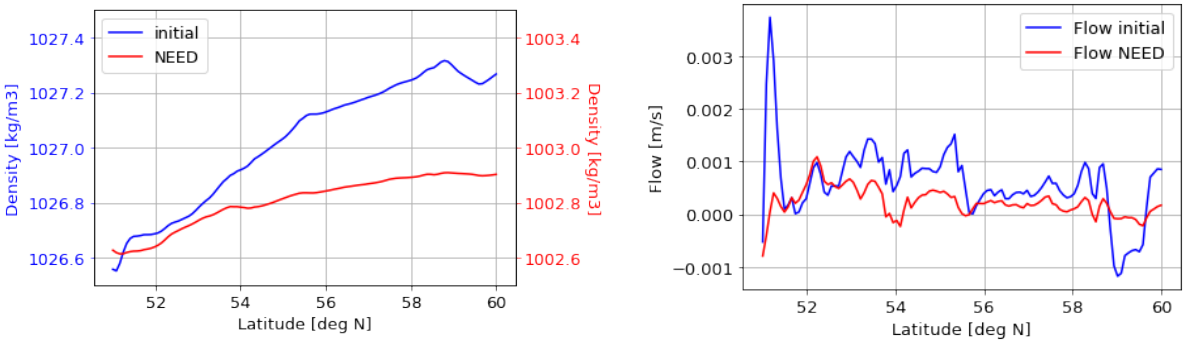

(a) (b)

Figure 8.2: Results before and after the NEED, where the situation after the NEED uses a temperature reduction of 0.3 °C and a reduction in salinity with a factor 10, using data points on the cross-section depicted in Figure 8.1b a) Absolute density values. b) Density driven flows at 10 m depth.

Figure 8.3 shows the result of the density driven flow due to a change in salinity and temperature with factors 0.8 and 1.2 respectively compared to the initial situation. It shows that, if temperature and salinity are changed by equal amounts, the influence of the temperature on the density is larger. This is shown

by the orange and green line which deviate more from the initial situation than the lines representing the change in salinity (red and purple).

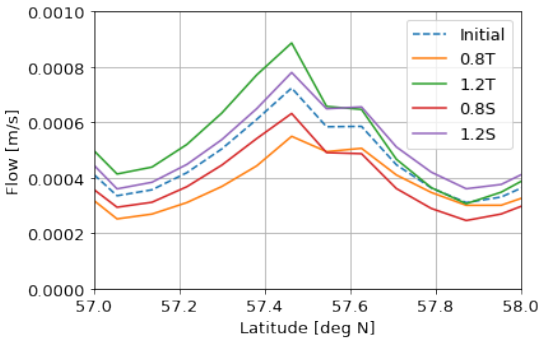

Figure 8.3: Change of density driven flows compared to the initial situation without NEED when temperature and salinity are multiplied with a factor of 0.8 and 1.2. The contributions are shown for each case separately.

Next, the three scenarios for the spatial distribution of salinity and temperature over the North Sea are considered. The results for scenarios 1 and 2 are shown in Figure 8.4a. It shows clearly that a gradient in temperature and salinity over the North Sea increases the density driven flows.

The results for scenario 3 are shown in Figure 8.4b. This figure shows that the density driven flows are largest in the middle of the basin, where there is a large difference in the densities. Moreover, there is a more or less sudden transition from a flow going from one direction to another direction.

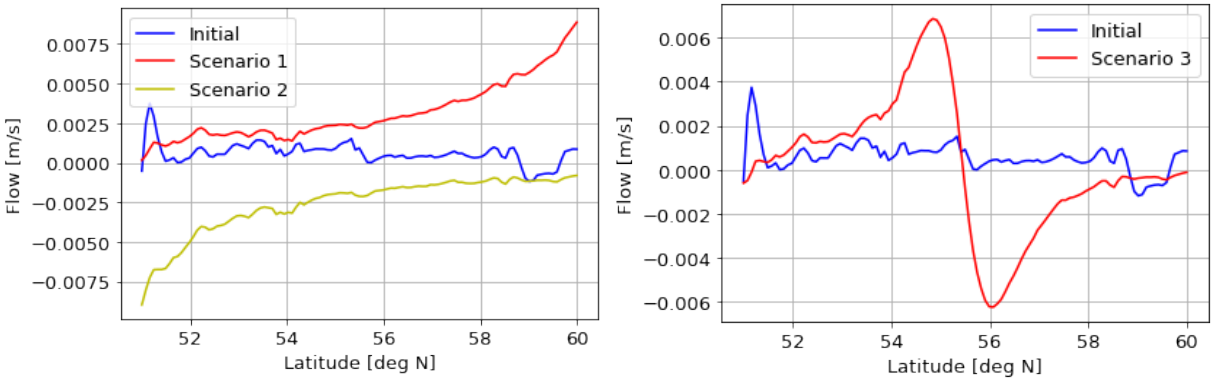

(a) (b)

Figure 8.4: a) Density driven flows if a gradient is applied to S and T. Scenario 1 refers to a larger change in the South with respect to the initial situation and Scenario 2 to a larger change in the North. b) Density driven flows if the change in salinity is largest near the coasts and smallest in the center of the basin.

8.3 Interpretation of the results

The density driven flows show a reduction when comparing the situation before and after NEED and using the changes in temperature and salinity as computed in the previous chapters (Figure 8.2a). The density reduction that is seen here is mainly due to the decrease in salinity with a factor 10. The temperature only decreases by 0.3°C and therefore has a less strong influence. The results in Figure 8.3 suggest that with equal change, a change in temperature would have more effect on the density.

Figure 8.4b shows a rather sudden transition of the flow direction. In reality, this will not occur due to a more even mixing of the water. Still, this figure does give useful insight in what might happen with the density driven flows if the salinity values of the water vary within the basin.

9 | Case study: The Wadden Sea

In its attempt to protect large parts of Europe from rising sea levels, the NEED will also enclose the entire Wadden Sea. Since 2009 the Wadden Sea (as shown in Figure 9.1) has been appointed the status of *Natural UNESCO World Heritage*, with an extension since 2014 (UNESCO World Heritage Center, n.d.), giving the area the same status as the Great Barrier Reef and the Grand Canyon.

This chapter illustrates some of the implications of the NEED and compares these to the effects of sea level rise, which is the situation that will arise if no action is taken. Thereby it contributes to answering the question what the possible implications of the NEED are on environment, economy and society. In the first section the current situation of the Wadden Sea is considered. In the subsequent sections the potential effects of sea level rise and the NEED on the Wadden Sea are described. Lastly, these changes are compared.

Figure 9.1: Area of the Wadden Sea World Heritage - Reprinted from "One Wadden Sea. One World Heritage." by the Common Wadden Sea Secretariat, 2019 (https://www.waddensea-worldheritage.org/one-wadden-sea-one-global-heritage)

9.1 Current situation of the Wadden Sea

The UNESCO World Heritage Center (n.d.) describes the Wadden Sea as a mostly undisturbed, temperate, flat coastal transition wetland between land, sea and fresh water. It has a unique combination of habitats such as small tidal channels, sea-grass meadows, sandbars, mudflats, salt marshes and dunes, that are home to a lively ecosystem (Common Wadden Sea Secretariat, 2019). The Wadden Sea ecosystem sustains wildlife populations well beyond its borders and around 2300 species of flora and fauna are hosted in the salt marshes of the Wadden Sea whilst marine and brackish areas host a further 2700 species (UNESCO World Heritage Center, n.d.). Moreover, the area is considered as one of the most important areas for migratory birds in the world, providing locations for staging, moulting, breeding and wintering (Tentij et al., 2009).

The flow of water and air as well as biological processes cause an ever-changing morphology (topography as well as bathymetry) of the islands, channels and tidal flats (Wang et al., 2012). Together with the composition of the bottom, the morphology is of great importance for the ecological system. For example, mud content has a big impact on flora and fauna since it is a carrier of many important nutrients. Flora and fauna on the other hand change erosion and water movement by generating eco-morphological landscapes such as mussel beds (Wang et al., 2018).

Aside from the biomorphology, hydrodynamics highly influence the sediment transport in the Wadden Sea, forced by the effects of tides, wind, waves and density-driven flow patterns (Wang et al., 2012). Under the influence of relative sea level rise and man-induced coastal interventions such as the closure of the Zuiderzee, the Wadden Sea acts as an important sediment sink of the North Sea coastal system (Wang et al., 2012).

The supply of fresh water and sediment by river runoffs is limited in the entire Wadden Sea. Only around the river mouth of the German Elbe (fresh) river runoffs interfere on a large scale with the merely salt environments, bringing sediment along as well (Kerner, 2007; Hickel, 1980). In the Dutch part of the Wadden Sea discharges from the Lake IJssel are the dominant fresh water flux. Even though this discharge is minor compared to the tidal fluxes, density gradients due to salinity and temperature might play an important role in the sediment exchanges through the inlets (Elias et al., 2005; Burchard et al., 2008).

At the moment, man-induced key threats for the Wadden Sea ecosystem are formed by maritime traffic, fishery activities, the development and maintenance of harbours (dredging and construction works) and industrial facilities in the area (e.g. wind farms, oil and gas rigs and tourism development) (UNESCO World Heritage Center, n.d.). Also climate change and the subsequent sea level rise is a key threat (e.g. Reise et al. (2010); Wang et al. (2018)).

9.2 Effects of sea level rise on the Wadden Sea

Currently, the average sedimentation rates in the Wadden Sea are 2.5 to 4.7 mm/year, dependent on the exact location (Elias et al., 2012). This rate is higher than the average relative sea level rise of 2 mm/year in Wadden Sea area (Elias et al., 2012). The sea bed is thus rising faster than the water levels. This difference between sea level rise and sedimentation rates is the result of a large sediment deficit in the Wadden Sea after the reclamation or closure of the Zuiderzee, Lauwerszee, German lower Elbe, Meldorfer Bucht and Nordsrander Bucht (Van Maren et al., 2016; Wang et al., 2012; Elias et al., 2012). At the same time relative sea levels are rising in an accelerating process (e.g. Meehl et al., 2007), increasing the sediment deficit.

If the accumulation rates of sediment on the tidal flats cannot keep up with the rate of the sea level rise, these tidal flats will start to submerge (Hofstede, 2015; Wang et al., 2012). This effect is also known as *drowning of the Wadden Sea*. Some studies about the effect of accelerated sea level rise find that coastal wetlands like the Wadden Sea are highly threatened by sea level rise and may drown (e.g. Van Wijnen & Bakker, 2001; Hughes, 2004). Others find that the sedimentation may be able to keep up with the rate of sea level rise (e.g. Morris et al., 2002; Madsen et al., 2007). Wang et al. (2018) recently performed an elaborate research on this topic. They found a range of critical sea level rise rates for the tidal basins in the Dutch part of the Wadden Sea, ranging from 6.3 mm/year to over 30 mm/year, dependent on the location and its characteristics. When comparing this to relative sea level rise projections, it can be found that submergence will happen at some locations in the Wadden Sea for the higher-end emission scenarios, mostly at the Vlie basin (inlet between Vlieland and Terschelling) where the relative sea level rise exceeds sedimentation with 5.6 mm/year. Table G.1 and G.2 in Appendix G show the critical sea level rise values and relative sea level rise projections for the six locations of the research of Wang et al. (2018).

Drowning of the typical Wadden Sea shoals and mudflats has negative consequences for nature conservation as they are of great importance for the ecological system (Hofstede, 2015; Wang et al., 2012). Also from a coastal flood risk management perspective drowning of the flats has a negative impact since waves will be able to develop further, imposing the flood defence structures to higher water levels (Hofstede, 2015). Of course these changes are part of a gradual process, in which for example coastal nourishments may (partially) mitigate the arising changes and consequences (e.g. Wang et al., 2012).

9.3 Effects of the NEED on the Wadden Sea

To get to know the effect the NEED will have on the Wadden Sea Unesco World Heritage, the external factors (boundary conditions) that will change are defined. This is done based on the results of this research as described in Chapters 4 - 7. The changing factors are described first, starting with the most influential one. Then the effects are elaborated on.

Changes in the Wadden Sea due to the NEED:

- **Tidal range**: The tidal range will go from the current tidal range of 1.5 to 4 metres (Reise et al., 2010) to about 20 centimetres (see Section 4.3).
- **Sediment availability**: Decrease in sediment availability and transport in the North Sea basin and a shift towards finer suspended sediments at the top of the bed layer (see Chapter 7).
- **Currents and circulation**: The velocity of the currents and circulation in the North Sea basin will be approximately 25 times smaller than without the NEED (see Chapter 4).
- **Salinity**: The upper layer of the North Sea basin, in which interaction with the Wadden Sea takes place, becomes about ten times fresher (see Chapter 5).
- **Wind set-up, Waves & Water temperature**: These factors will be comparable to the current situation. Temperature only drops by about 0.3 degrees Celsius in the upper layer (see Chapter 6). Wave heights are comparable to the situation without the NEED (see Section 4.6) and the wind set-up is similar in average situations and just a little less in storm situations.

With a tidal range of only $\pm$ 10% of the initial tidal range, the water level differences decrease drastically. The small remainder of the tidal range, together with waves and a fluctuating wind set-up, will give the banks a fraction of the tidal character they used to have. The tidal flats will now be either submerged or above water level, which will cause the area to start to behave and look more like a beach environment. Since the tidal flats are essential to support the Wadden Sea ecosystem, this will have big consequences for the system.

Besides the lack of tidal range to maintain the flats, the lack of tidal motion will let currents come to a standstill. Only a fraction of the tidal currents will remain. This, supported by the decrease of currents in the North Sea basin itself, gives the water motions less power to maintain the channel structure that is typical for the Wadden area. On its turn this causes erosion rates to drop and sediment transport to decrease drastically. Waves and wind will start to play a more important role in erosion and sediment transport (Grunnet et al., 2005; Elias et al., 2012; Vermeersen et al., 2018). This will eventually lead to a Wadden Sea that is flattened out: the banks will lower and the channels will become less deep. Together with the changing characteristic of the tidal flats, this will change a large part of the abiotic system of the Wadden Sea area, which, on its turn, has inevitable consequences for the biotic system.

The decreased water exchange between the North Sea basin and the Wadden Sea will limit the transport of salt water into the Wadden area, whilst the fresh water inflow from rain and the Lake IJssel still prevails. This makes the Wadden Sea brackish in many places. The decreased water exchange also causes that the slight drop in temperature of the North Sea basin will not be felt in the Wadden Sea. The water temperature in the Wadden Sea might even rise since, in general, the inflow of water from the North Sea into the Wadden Sea is cold. This exchange is now limited.

9.4 Comparison of effects

In this chapter it was found that the situation with the NEED changes the conditions that make the Wadden Sea so unique, thereby endangering the stability of the ecosystems in the area. The situation subject to sea level rise imposes the risk to drown tidal flats. This threatens the Wadden Sea ecosystem as well. Also relative sea level rise imposes higher flood risks on the coastal communities since the drowning of the tidal flats and beaches makes it possible for waves to develop to a larger extent. Together with the sea level rise this exposes the water defences to more extreme water levels.

A major difference between the two situations is the time scale of change. The changes due to the NEED might be imposed very quick (although a gradual building strategy might be implemented as well), whereas the changes due to sea level rise take place relatively gradual. The latter gives the (eco)system time to adapt.

10 | Implications of the NEED

This chapter looks into the possible implications of the results found in Chapter 3 until 9 on environment, economy and society and thereby answers the last sub-question.

To study this, it has been explored what sectors are dependent on the current characteristics of the North Sea, with a focus on the domains that have been studied in this research. These sectors have then been categorized into environment, economy and society and are restructured into three causal diagrams. These diagrams are presented in the following sections. It should be noted that this chapter only gives a brief overview of the impacts the results of this research might have, it does not cover all possible effects and impacts.

10.1 Environment

Due to the NEED, the temperature and the salinity in the North Sea basin decrease. This has an impact on different elements, as shown in Figure 10.1. The change in temperature, together with the freshening of the basin, has an influence on the ice formation, which might be enhanced in winter. Moreover, the temperature influences evaporation, precipitation and clouds. These elements interact with each other and influence the albedo, which is an important feedback for temperature (Winton, 2006).

The salinity influences the vegetation, marine life and birds (Gunter, 1961). Moreover, the CO_2 uptake by the North Sea basin might reduce due to limited mixing. This results in more saturation of the surface layer with CO_2 (Takahashi et al., 2002), influencing marine life. The coastal landscape is changed due to the NEED as well, for example because of the changing sediment transport patterns which alter the the tidal flats and beaches. A detailed example is described in Chapter 9. Salt intrusion, impacted by the changing salinity due to the NEED, affects the vegetation, and thus the coastal landscape, as well.

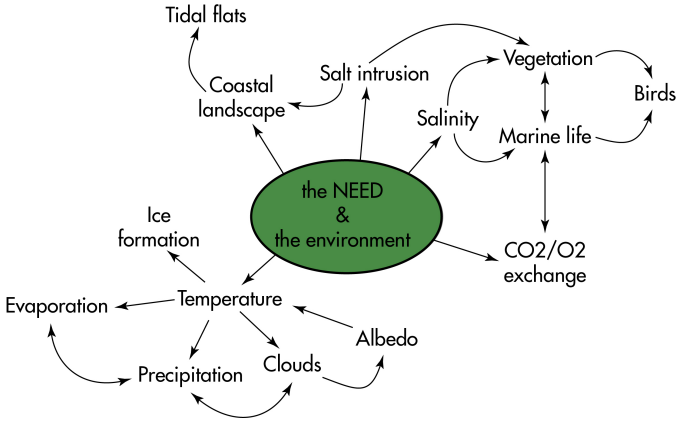

Figure 10.1: Causal diagram of the implications of the NEED for the environment.

10.2 Economy

The NEED might offer economic benefits, however, it can also affect this sector negatively. Figure 10.2a gives an overview of the possible impacts on economy. The dam offers opportunities in the sense that the NEED can become a landmark and therefore attract tourists. It also provides safety to many economically important areas, like the densely populated Dutch Randstad, which are threatened by sea level rise. Besides this, the NEED offers an opportunity to gain knowledge about something that never happened on this scale before: closing off an entire sea. This knowledge can be used in other places where enclosing a sea might offer a solution to sea level rise as well. Moreover, it provides new insights into the studied domains and processes.

On the other hand, fishery, shipping and ports might not be very pleased with the NEED. Due to the desalinization of the sea, the fish population changes at best and diminishes at worst. This means an

economical shock for the many fishermen who earn their living with fishing in the North Sea. Also, the NEED hinders the free passage of vessels to ports located in the North Sea basin, like Antwerp, Hamburg and Rotterdam. Almost all of Europe's most important ports are located within the enclosed area and currently the English Channel is one of the busiest shipping passages. It will be a huge challenge to let all ships through the NEED without too much hindrance.

The last element discussed here is use and generation of energy. Energy is needed to pump water out of the basin, if discharge under free fall is limited (see Section 3.1.d). On the other hand, when discharging under free fall is possible there is an opportunity to generate energy using turbines. Another option to generate energy is by making use of developed difference in salinity between the in- and outside of the dam. With the use of membranes and the separation of positively and negatively charged ions, a battery-like situation can be created that continuously produces energy. This has already been tested at the Afsluitdijk, that deals with a comparable difference in salinity (REDstack, 2020).

Also, the North Sea basin is a good location for wind farms (Ministerie van Algemene Zaken, 2020). Enclosing the North Sea basin can make this an even more favourable spot due to, for example, a less corrosive environment. Various offshore wind parks in the North Sea are planned to be realized in the coming years. These turbines are designed with a power of approximately 10 MW (Rijksoverheid, 2020). This would mean that 280 turbines are needed to cover the entire power of the pumping stations over an area of approximately 1100 km^2. Lastly, options such as generation of energy by waves or tides can be explored.

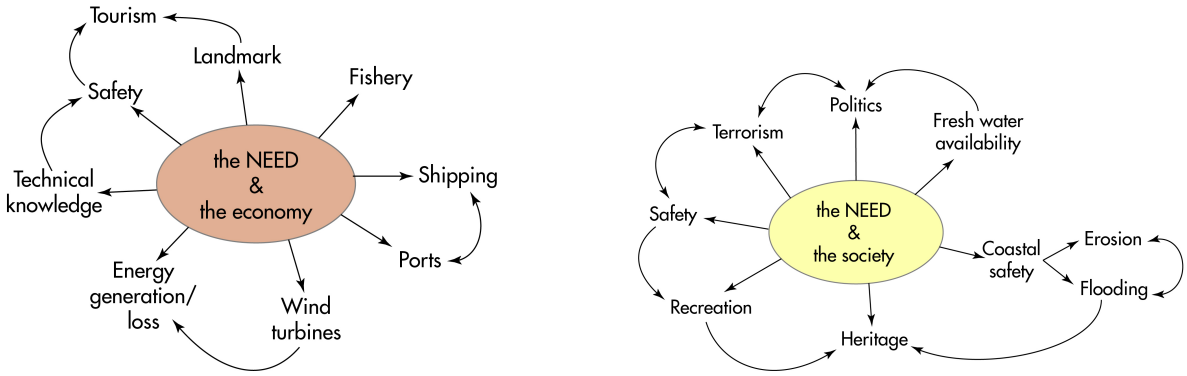

Figure 10.2: Causal diagram of the implications of the NEED a) for the economy and b) for society.

10.3 Society

The impact of the dam on society is given in Figure 10.2b. The NEED provides safety for many people and their living environments from the rising sea level. Besides this, it also offers an opportunity for recreation and protects heritage located onshore. Due to the fact that the basin changes from a salty to a more brackish environment, opportunities for water usage from the basin arise. This can especially be important during the more extreme droughts happening nowadays (Cook et al., 2018).

Besides this, the NEED changes the coastal regions via erosion, and therefore coastal management and protection with for example coastal nourishment might need to change. Moreover, the NEED can only become a success if good international collaboration between the involved countries is established. The last point mentioned here is terrorism. It is possible that, one day, the NEED is attacked by terrorists causing for example a breach. However, it would probably take a significant amount of time before a breach somewhere in the dam results in a rise of the water level. This gives inhabitants time to move to safer places. Nonetheless, the dam should be protected to prevent such events from happening.

11 | Discussion

This study focused on the changes in water levels, hydrodynamics, salinity, temperature and sediment within the North Sea basin if it were enclosed by the NEED. This is done by conceptualizing the processes and boundaries in the North Sea basin and analyzing these separately using first order approximations. By doing this, more insight was gained into what processes cause the changes exactly, what processes are dominant, and which are influenced the most.

Based on this research, the conclusion can be drawn that the North Sea basin changes from a tide dominated to a basin which is dominated equally by tides and winds. Moreover, the North Sea becomes a brackish basin instead of the salt water basin it is nowadays. The last main finding is that the NEED has impact on various sectors regarding environment, society and economy.

The pioneering article of Groeskamp & Kjellsson (2020) was the first to come up with quantitative results on the implications of enclosing the North Sea. This research concludes that the construction of the NEED is physically possible and economical feasible. With a numerical ocean model, the study mainly focuses on the impact of the NEED on the ocean circulation around the North Sea basin. However, "an anticlockwise circulation [...] inside the North Sea basin that is driven by wind, baroclinic circulation from freshwater discharge, and very small tidal motions excited within the basin itself" are mentioned as well. This is in accordance with the findings in this research. Also, it is noted that there is "a large impact on the circulation and exchange of nutrients, sediment, and small marine life within the enclosure", which is further investigated in this report: the magnitude of the circulation decreases by 14 and sediment exchange becomes restricted to storm conditions. Concerning the freshening of the basin, the pioneering article is inconclusive. However, the results of this study do not match their statement that it takes approximately 106 years until the salinity is reduced by a factor of 10. Due to the conceptualization of the basin with a two-layer system used in this study, the freshening goes twice as fast. This research is an addition to the already existing research in the sense that the applied methodology and simplifications have not been used before. Moreover, this research takes into account more domains and their changes within the North Sea basin, investigates smaller scale implications and includes a review on the water balance. Although this study gives a good first overview of the major changes in the North Sea basin, the simplifications and assumptions made limit the applicability of the results, as described below.

In the first place, the research is executed on the scale of the entire North Sea basin and complexity in topography and bathymetry is reduced to a two layer bucket system with two depths. It is assumed that parameters are constant over the study area and most spatial variations have been neglected. This allowed for a simplified analysis with first order approximations. However, it should be taken into account that the generic results can vary highly throughout the basin. Especially in estuaries and along coasts, generally locations with many stakeholders involved, spatial and temporal variability occurs.

Secondly, the study looks at the hydrodynamical, freshening, heating and sedimental processes separately. This made it easier to determine the changes in these domains and understand the underlying processes determining the changes. However, the results are different in reality due to the fact that these domains do interact and influence each other. In Chapter 8 a start with the interactions is made, which already results in an additional but minor flow.

Moreover, the English Channel is not taken into account and the Baltic Sea is simplified as a flux into/out of the North Sea basin. Since the characteristics of the English Channel are different from the North Sea basin, the results can not be extrapolated to this region. Therefore, it is not known at this moment what will happen there. The Baltic Sea on the other hand is already an almost enclosed basin. Therefore, it is not expected that the Baltic Sea changes drastically due to the closing and the simplification of a flux seems to be sufficient.

Lastly, this study neglects future developments and assumes that the NEED is built in the current circumstances. However, changes in for example climate, politics, water scarcity and human activity could ask for a different approach. For example, climate change induces a shift in stormy periods and the wind regime of the North Sea. This has implications for wind induced waves and for the temporal distribution of sediment transport. In order to give more accurate recommendations on for example coastal protection, it could be advantageous to take the future developments, on different sectors, into account.

This research mainly presented objective findings, from which it can be concluded that the NEED definitely has strong consequences within the North Sea basin. However, the question if the impact of sea level rise is worse than the effects of the NEED is still open for public debate. Based on this research the opinion of the authors about the NEED is that it has severe negative influences on various sectors, especially concerning the ecology. It is recommended to invest in mitigation strategies against climate change. However, since the impact of these strategies is difficult to predict and it takes a long time to see their effects, possible adaptation strategies should be developed in parallel as well. The NEED can be part of such a strategy and at the same time raise awareness about the kind of solutions needed if nothing is done about climate change now.

12 | Conclusion

In this report, the main research question "How do average water levels, hydrodynamics, salinity, temperature and sediment transport change in space and time within the North Sea basin due to the construction of the NEED and what are the effects?" has been answered. The conclusions will shortly be discussed per subquestion.

After the construction of the NEED, the average water levels inside the North Sea basin stay within a range of 16.2 cm for the current climate and with constant pumping. Applying a RCP8.5 climate scenario for 2100 to the fluxes, gives a range of 37.6 cm. These ranges are an order of magnitude less than the tidal amplitudes prevailing before the construction of the NEED (1 to 4 meters), making a constant pumping rate a feasible option.

Concerning the hydrodynamics, a counterclockwise circulation of 0.035 m/s will be set up in the basin. This circulation consists of three main components: a counterclockwise tidal flow, eastward wind-driven currents and northward barotropic flows, driven by the wind set-up. Since the connection to the oceanic tide is cut off, the basin develops its own astronomical tide, which has a much smaller amplitude. The wave climate will not alter significantly compared to the current situation, because the fetch over the North Sea is large enough for waves to fully develop.

The salinity in the top layer decreases from 35 PSU to 3.5 PSU and will be in a mixed state. The bottom layer in the deep part of the basin stays stratified as there are no large flows. However, when taking into account interactions between these layers, mixing between these layers will be inevitable.

The temperature distribution will change as well, which leads to a cooling of the surface layer with 0.3 °C. This is small compared to the annual amplitude of the temperature. This amplitude also increases due to the NEED which results in higher sea surface temperatures in summer and lower sea surface temperatures in winter compared to the situation without the NEED.

Furthermore, the NEED causes a change in sediment transport and availability. The extreme reduction in current velocity and tides leads to more settlement and consequently a finer layer of seabed material and more clear waters on average. Resuspension and resulting turbidity become wind dominated and erosion will therefore occur only during storms.

The changing hydrodynamics, temperature and salinity interact with each other and give rise to density driven flows. If the North Sea basin changes as predicted, these already small flows, decrease. However, since the changes are obtained for the entire basin, more research should be conducted into this area to better understand the interactions.

All of these changes have impactful implications on the environment, economy and society. Examples of these impacts on the sectors are given, which can be used a starting point for further research.

13 | Recommendations

As this report describes one of the first studies on the NEED, there is still a lot to discover concerning the effects and feasibility of the project. This chapter presents a variety of options for further research. The suggestions will be in the field of study of this research, but of course there is also a lot to discover on aspects that were not looked into.

Firstly, there are three extensions that would improve the accuracy of the results highly: a more integral approach towards the domains, the use of a multiple dimension model, and the inclusion of the English Channel in the study. The first one could focus more on the relation between hydrodynamics, salinity, temperature and sediment and could include feedback processes. This requires an iterative approach and cannot be executed with first order calculations. Chapter 8 can be used as a starting point as it already described the interdependencies by focusing on density. Moreover, setting up a 2- and 3D model is fruitful for better insight in the spatial distribution and variability of the different domains, whereas this study shows the average situation for the entire basin. Including different time scales in the model would be interesting too. For the pioneering study of Groeskamp & Kjellsson (2020), a 3D model was used to analyse the change in hydrodynamics. That model could potentially be extended for research on other domains. Also, small-scale analysis with the use of a model can give valuable knowledge on the exact changes and their impact in vulnerable places, such as coastlines, estuaries, or the Wadden Sea. Besides, inclusion of the English Channel can improve the findings. This study assumed that the processes in the area would differ much from the study area as defined. However, it is important to validate this further and to check what this would imply for the connecting processes that were simplified as fluxes.

Secondly, this study reports briefly on the social, economic and environmental impact of the NEED in Chapter 10. The implications seem to be gigantic in all fields. It would therefore be valuable to look further into this, also on a smaller scale. Although the exact physical effects of the NEED to the North Sea basin will remain uncertain due to its complex character, it is important to prepare all stakeholders on time. This can for example be done by investigating various future scenarios and by taking into account international regulations and legislations. Chapter 10 can be used for inspiration and as a starting point.

Thirdly, as the NEED is a proposal and warning for threats due to climate change, it is important to discuss the results in the light of climate change projections. How can these be compared to the natural changes in the North Sea basin due to climate change? For example, Quante & Colijn (2016) predict sea level rise, ocean acidification, decreased primary production, a rise in temperature, and freshening of the seawater. A comparison to the effects of the NEED on these aspects could be a method to evaluate the impact of the NEED. It is important to note that this study is based on a construction of the dam in current circumstances. However, as (the start of) the realisation of the dam would take multiple decades, future environmental and social conditions that affect the results in its turn should be taken into account.

Next, there are still many uncertainties concerning the design and effects of the pumps in the dam. Chapter 3 described the validity of a constant pumping discharge and the implications on the water level variability. Also, it is found that the pumping stations demand a lot of energy. However, further research could look into the amount of pumping stations, their distribution over the dam and the location over the depth of the dam. For this study it is assumed that the pumps take relatively fresh water from the surface layer of the basin, lengthening the refreshing time. However, other options that influence the process of refreshing can also be considered, e.g. pumping at lower depths or creating a salt water inlet from the Atlantic Ocean. This on the other hand also depends on the assumption concerning the extent of mixing of the water layers of the basin. Finally, the pumps might be a tool to reduce the negative effects of the dam. Think about simulating a stronger general circulation or tides inside the basin by applying an adjusted distribution of pumping stations over the dam.

Lastly, the scope of this research is narrowed down in order to be able to do a more in depth analysis. However, new knowledge can be obtained on many more aspects of the NEED. For example the construction of the dam is an essential field of study. How can this be realized? What phasing is required? What design is optimal? But also, what causes failure and what would be the consequences? Formerly, similar plans to the NEED have been suggested, such as the construction of an open, or half a dam between Scotland and Norway (Wassink, J., 2020). A study on the effects of this design could be done with a similar methodology as used in this report.

References

Accad, Y., & Pekeris, C. (1978). Solution of the Tidal Equations for the M2 and S2 Tides in the World Oceans from a Knowledge of the Tidal Potential Alone. *Philosophical Transactions of the Royal Society of London*, *290*, 235-266.

Becker, G. A. (1981). Beiträge zur hydrographie und wärmebilanz der Nordsee. *Deutsche Hydrografische Zeitschrift*, *34*(5), 167–262.

Beersma, J., Hakvoort, H., Jilderda, R., Overeem, A., & Versteeg, R. (2019). *Neerslagstatistiek en -reeksen voor het waterbeheer 2019* (Research Report). STOWA.

Bergström, S., Andréasson, J., Losjö, K., Stensen, B., & Wern, L. (2011). Hydrologiska och meteorologiska förhållanden i Göta älvdalen. *Swedish Geotechnical Institute, Göta älvutredningen delrapport*, *27*.

Boon, J., van der Kaaij, T., Vos, R., & Gerritsen, H. (1997). *Modelling of suspended matter (SPM) in the North Sea, model set up and first sensitivity analysis* (Research Report). Delft Hydraulics.

Bosboom, J., & Stive, M. (2015). *Coastal Dynamics 1.* Delft, Netherlands: Delft Academic Press.

Brandon, M. (n.d.). *The oceans.* Retrieved from `https://www.open.edu/openlearn/science-maths-technology/the-oceans/content-section-4.4`

Buishand, T. A., Lenderink, G., & Šabalova, M. (2004). *Estimation of future discharges of the river Rhine in the SWURVE project.* KNMI Technical Report, Royal Netherlands Meteorological Institute, De Bilt.

Burchard, H., Flöser, G., Staneva, J. V., Badewien, T. H., & Riethmüller, R. (2008). Impact of density gradients on net sediment transport into the Wadden Sea. *Journal of Physical Oceanography*, *38*(3), 566–587.

CBS. (2019). *Gemiddelde energielevering aardgaswoningen, 2018.* Retrieved 2021-01-28, from `https://www.cbs.nl/nl-nl/maatwerk/2019/38/gemiddelde-energielevering-aardgaswoningen-2018`

Chen, X., Zhang, X., Church, J. A., Watson, C. S., King, M. A., Monselesan, D., ... Harig, C. (2017). The increasing rate of global mean sea-level rise during 1993-2014. *Nature Climate Change*, *7*(7), 492–495.

Church, J. A., & White, N. J. (2006). A 20th century acceleration in global sea-level rise. *Geophysical research letters*, *33*(1).

Common Wadden Sea Secretariat. (2019). *One Wadden Sea. One Global Heritage.* Retrieved 2020-11-30, from `https://www.waddensea-worldheritage.org/one-wadden-sea-one-global-heritage`

Cook, B. I., Mankin, J. S., & Anchukaitis, K. J. (2018). Climate change and drought: From past to future. *Current Climate Change Reports*, *4*(2), 164–179.

Copernicus Climate Change Service (C3S). (2017). *ERA5: Fifth generation of ECMWF atmospheric reanalyses of the global climate. Copernicus Climate Change Service Climate Data Store (CDS).* Retrieved 2020-12-02, from `https://cds.climate.copernicus.eu/cdsapp#!/home`

Cummings, J. A., & Smedstad, O. M. (2013). HYCOM: Hybrid Coordinate Ocean Model, Water Temperature and Salinity. *Data Assimilation for Atmospheric, Oceanic and Hydrologic Applications*, *II*, 303–343.

de Boer, G., Pietrzak, J., & Winterwerp, J. (2006). On the vertical structure of the Rhine region of freshwater influence. *Ocean Dynamics*, *56*, 198–216.

de Boer, G., Pietrzak, J., & Winterwerp, J. (2009). SST observations of upwelling induced by tidal straining in the Rhine ROFI. *Continental Shelf Research*, *29*(1), 263-277. doi: 10.1016/j.csr.2007.06.0

Dobrynin, M., Gayer, G., Pleskachevsky, A., & Günther, H. (2011). Effect of waves and currents on the dynamics and seasonal variations of suspended particulate matter in the North Sea. *Continental Shelf Research*, *31*, 594-610. doi: 10.1016/j.csr.2010.12.014

Earle, S. (2015). *Physical Geology* (2nd Edition ed.). Pressbooks.

Eisma, D., & Irion, G. (1993). Suspended Matter and Sediment Transport. *Pollution of the North Sea*, 20-21. doi: 10.1007/978-3-642-73709-1_2

Elias, E., Stive, M., & Roelvink, J. (2005). Influence of stratification on flow and sediment transports in Texel inlet. In *Proceedings of Coastal Dynamics.*

Elias, E., Van der Spek, A., Wang, Z. B., & De Ronde, J. (2012). Morphodynamic development and sediment budget of the Dutch Wadden Sea over the last century. *Netherlands Journal of Geosciences*, *91*(3), 293–310.

European Environment Agency. (2016). *Indicator Assessment - River Flow.* Retrieved 2021-19-01, from `https://www.eea.europa.eu/data-and-maps/indicators/river-flow-3/assessment`

European Environment Agency. (2017). *Indicator Assessment - Mean Precipitation.* Retrieved 2021-19-01, from `https://www.eea.europa.eu/data-and-maps/indicators/european-precipitation-2/assessment`

Eurosion. (2004). *Living with coastal erosion in Europe: Sediment and Space for Sustainability* (Tech. Rep.).

Frigstad, H., Kaste, Ø., Deininger, A., Kvalsund, K., Christensen, G., Bellerby, R. G., ... King, A. L. (2020). Influence of riverine input on Norwegian coastal systems. *Frontiers in Marine Science*.

Gayer, G., Dick, S., Pleskachevsky, A., & Rosenthal, W. (2006). Numerical modeling of suspended matter transport in the North Sea. *Ocean Dynamics*, *56*, 62-77. doi: 10.1007/s10236-006-0070-5

Gayer, G., & Dobrynin, M. (2020). *Suspended particulate matter distribution in the North Sea.* Retrieved 2020-12-15, from `http://www.coastalwiki.org/wiki/Suspended_particulate_matter_distribution_in_the_North_Sea`

Gerritsen, H., Vos, R. J., Van der Kaaij, T., Lane, A., & Boon, J. (2000). Suspended sediment modelling in a shelf sea (North Sea). *Coastal Engineering*, *41*, 317-352.

Groeskamp, S., & Kjellsson, J. (2020). NEED The Northern European Enclosure Dam for if climate change mitigation fails. *Bulletin of the American Meteorological Society*.

Grunnet, N. M., Ruessink, B., & Walstra, D.-J. R. (2005). The influence of tides, wind and waves on the redistribution of nourished sediment at Terschelling, The Netherlands. *Coastal Engineering*, *52*(7), 617–631.

Gunter, G. (1961). Some relations of estuarine organisms to salinity. *Limnology and Oceanography*, *6*(2), 182–190.

Hendriks, H., van Prooijen, B., Aarninkhof, S., & Winterwerp, J. (2020). How human activities affect the fine sediment distribution in the Dutch Coastal Zone seabed. *Geomorphology*, *367*. doi: 10.1016/j.geomorph.2020.107314

Hickel, W. (1980). The influence of Elbe river water on the Wadden Sea of Sylt (German Bight, North Sea). *Deutsche Hydrografische Zeitschrift*, *33*(2), 43–52.

Hjøllo, S. S., Skogen, M. D., & Svendsen, E. (2009). Exploring currents and heat within the North Sea using a numerical model. *Journal of Marine Systems*, *78*(1), 180–192.

Hofstede, J. L. (2015). Theoretical considerations on how Wadden Sea tidal basins may react to accelerated sea level rise. *Zeitschrift für Geomorphologie*, *59*(3), 377–391.

Holt, J. T., & James, I. D. (1999). Simulation of the southern North Sea in comparison with measurements from the North Sea Project Part 2 Suspended Particulate Matter. *Continental Shelf Research*, *19*, 1617-1642.

Holthuijsen, J. (2007). *Waves in Oceanic and Coastal Waters.* Cambridge University Press.

Huang, R. X. (1993). Real Freshwater Flux as a Natural Boundary Condition for the Salinity Balance and Thermohaline Circulation Forced by Evaporation and Precipitation. *Journal of Physical Oceanography*, *23*(11), 2428 - 2446. doi: 10.1175/1520-0485(1993)023<2428:RFFAAN>2.0.CO;2

Huang, S., Krysanova, V., & Hattermann, F. F. (2013). Projection of low flow conditions in Germany under climate change by combining three RCMs and a regional hydrological model. *Acta Geophysica*, *61*(1), 151–193.

Hughes, R. (2004). Climate change and loss of saltmarshes: consequences for birds. *Ibis*, *146*, 21–28.

Ke, X., Evans, G., & Collins, M. (1996). Hydrodynamics and sediment dynamics of The Wash embayment, eastern England. *Sedimentology*, *43*, 157-174.

Kerner, M. (2007). Effects of deepening the Elbe Estuary on sediment regime and water quality. *Estuarine, coastal and shelf science*, *75*(4), 492–500.

Klijn, F., de Bruijn, K. M., Knoop, J., & Kwadijk, J. (2012). Assessment of the Netherlands' flood risk management policy under global change. *Ambio*, *41*(2), 180–192.

KNMI. (2013). *KNMI Wind Atlas.* Retrieved 2020-12-02, from `http://projects.knmi.nl/knw/Plots/index.php?domain=domain&what=ffmax&height=010&period=1979-2013&domain2=FINO1&what2=rose&height2=010&period2=1979-2013`

KNMI. (2020). *Extreme neerslag.* Retrieved 2021-01-29, from `https://www.knmi.nl/kennis-en-datacentrum/uitleg/extreme-neerslag`

Laîné, A., Nakamura, H., Nishii, K., & Miyasaka, T. (2014). A diagnostic study of future evaporation changes projected in CMIP5 climate models. *Climate dynamics*, *42*(9-10), 2745–2761.

Lane, A. (1989). The heat balance of the North Sea.

Ledden, M., Van den Berg, N., Jong, M., Gelder, P., Heijer, C. K., Vrijling, J., ... Lansen, A. (2014, 01). An idealized meteorological-hydrodynamic model for exploring extreme storm surge statistics in the North Sea. *Coastal Engineering Proceedings*, *1*, 21. doi: 10.9753/icce.v34.management.21

Lee, A. (1980). North Sea: physical oceanography. In *Elsevier oceanography series* (Vol. 24, pp. 467–493). Elsevier.

Leppäranta, M., & Myrberg, K. (2009, 01). Physical Oceanography of the Baltic Sea. doi: 10.1007/978-3-540-79703-6

Madsen, A. T., Murray, A., Andersen, T. J., & Pejrup, M. (2007). Temporal changes of accretion rates on an estuarine salt marsh during the late Holocene — Reflection of local sea level changes - The Wadden Sea, Denmark. *Marine Geology*, *242*(4), 221–233.

Medvedev, I., Rabinovich, A., & Kulikov, A. (2016). Tides in Three Enclosed Basins: The Baltic, Black, and Caspian Seas. *Frontiers in Marine Science*.

Meehl, G. A., Stocker, T. F., Collins, W. D., Friedlingstein, P., Gaye, T., Gregory, J. M., ... others (2007). Global climate projections.

Meyer, E. M., Pohlmann, T., & Weisse, R. (2011). Thermodynamic variability and change in the North Sea (1948–2007) derived from a multidecadal hindcast. *Journal of Marine Systems*, *86*(3-4), 35–44.

Ministerie van Algemene Zaken. (2020). *Offshore wind energy.* Retrieved 2021-01-26, from `https://www.government.nl/topics/renewable-energy/offshore-wind-energy`

Morris, J. T., Sundareshwar, P., Nietch, C. T., Kjerfve, B., & Cahoon, D. R. (2002). Responses of coastal wetlands to rising sea level. *Ecology*, *83*(10), 2869–2877.

Neil, S., & Scourse, J. (2010). Evolution of bed shear stress distribution over the northwest European shelf seas during the last 12,000 years. *Ocean Dynamics*, *60*, 1139-1156. doi: 10.1007/s10236-010-0313-3

Nicholls, R. J., & Cazenave, A. (2010). Sea-level rise and its impact on coastal zones. *science*, *328*(5985), 1517–1520.

NOAH. (2006). *Shear Stress Statistics Year 2006.* Retrieved 2020-12-15, from `https://coastmap.hzg.de/portal/apps/PublicGallery/index.html?appid=175aff24bee04c97bc27a0d63c7dbe66`

Nurser, A. J. G., & Griffies, S. M. (2019). Relating the Diffusive Salt Flux just below the Ocean Surface to Boundary Freshwater and Salt Fluxes. *Journal of Physical Oceanography*, *49*(9), 2365 - 2376. doi: 10.1175/JPO-D-19-0037.1

OSPAR. (2000). *Quality Status Report 2000: Region II: Greater North Sea.* OSPAR Commission for the Protection of the Marine Environment of the North ....

Ottesen, D., Dowdeswell, J., & Bugge, T. (2014). Morphology, sedimentary infill and depositional environments of the Early Quaternary North Sea Basin. *Marine and Petroleum Geology*, *56*, 123-146. doi: http://dx.doi.org/10.1016/j.marpetgeo.2014.04.007

Otto, L., Zimmerman, J., Furnes, G., Mork, M., Saetre, R., & Becker, G. (1990). Review of the physical oceanography of the North Sea. *Netherlands Journal of Sea Research*, *26*(2), 161 - 238. doi: https://doi.org/10.1016/0077-7579(90)90091-T

Pietrzak, J. (2019a). *An Introduction to Oceanography for Civil and Offshore Engineers.* Delft, Netherlands: TU Delft.

Pietrzak, J. (2019b). *An Introduction to Stratified Flows for Civil and Offshore Engineers "From Shelf to Shore".* Delft, Netherlands: TU Delft.

Pietrzak, J., De Boer, G., & Eleveld, M. (2011). Mechanisms controlling the intra-annual mesoscale variability of SST and SPM in the southern North Sea. *Continental Shelf Research*, *31*, 594-610. doi: 10.1016/j.csr.2010.12.014

Piniewski, M., Szcześniak, M., Huang, S., & Kundzewicz, Z. W. (2018). Projections of runoff in the Vistula and the Odra river basins with the help of the SWAT model. *Hydrology Research*, *49*(2), 303–317.

Puls, W., Kuhl, H., Frohse, A., & Konig, P. (1995). Measurements of the Suspended Matter Settling Velocity in the German Bight (North Sea). *Deutsche Hydrografische Zeitschrift*, *47*, 259–276. doi: 10.1007/BF02737787

Puls, W., van Beusekom, J., Brockmann, U., R., D., Hentschke, U., Konig, P., ... Sundermann, J. (1999). SPM concentrations in the German Bight: comparison between a model simulation and measurements. *German Journal of Hydrography*, *51*(2/3), 221-244. doi: 10.1007/BF02764175

Pye, K. (1995). Controls on Long-term Saltmarsh Accretion and Erosion in the Wash, Eastern England. *Journal of Coastal Research*, *11*(2), 337-356.

Quante, M., & Colijn, F. (2016). North Sea Region Climate Change assessment. *Regional Climate Studies*. doi: 10.1007/978-3-319-39745-0

REDstack. (2020). *Continu duurzame energie uit water.* Retrieved 2021-01-26, from `https://deafsluitdijk.nl/nieuws/continu-duurzame-energie-uit-water/`

Reise, K., Baptist, M., Burbridge, P., Dankers, N., Fischer, L., Flemming, B., ... Smit, C. (2010). The Wadden Sea - a universally outstanding tidal wetland. In *The wadden sea 2010. common wadden sea secretariat (cwss); trilateral monitoring and assessment group: Wilhelmshaven.(wadden sea ecosystem; 29/editors, harald marencic and jaap de vlas)* (Vol. 7).

Rijksoverheid. (2020). *Windenergie op zee na 2030.* Retrieved 2021-01-26, from `https://windopzee.nl/onderwerpen-0/wind-zee/2030/`

Rutgersson, A., Omstedt, A., & Räisänen, J. (2002). Net precipitation over the Baltic Sea during present and future climate conditions. *Climate Research*, *22*(1), 27-39.

Saha, S., Moorthi, S., Wu, X., Wang, J., Nadiga, S., Tripp, P., ... Becker, E. (2011). *Ncep climate forecast system version 2 (cfsv2) 6-hourly products.* Boulder CO: Research Data Archive at the National Center for Atmospheric Research, Computational and Information Systems Laboratory. Retrieved from `https://doi.org/10.5065/D61C1TXF`

Sarraf, P. B. a. A. (n.d.). *TEOS-10 method.* Retrieved from `http://www.teos-10.org/`

Schrum, C., & Backhaus, J. O. (1999). Sensitivity of atmosphere - ocean heat exchange and heat content in the North Sea and the Baltic Sea. *Tellus A*, *51*(4), 526–549.

Sharqawy, M. H., Lienhard, J. H., & Zubair, S. M. (2010). Thermophysical properties of seawater: a review of existing correlations and data. *Desalination and water Treatment*, *16*(1-3), 354–380.

Simpson, J., Rippeth, T., & Souza, A. (1993). Periodic stratification in the Rhine ROFI in the North Sea. *Oceanologica Acta*, *16*(1), 23-32.

Sündermann, J., & Pohlmann, T. (2011). A brief analysis of North Sea Physics.

Takahashi, T., Sutherland, S. C., Sweeney, C., Poisson, A., Metzl, N., Tilbrook, B., ... others (2002). Global sea–air co2 flux based on climatological surface ocean pco2, and seasonal biological and temperature effects. *Deep Sea Research Part II: Topical Studies in Oceanography*, *49*(9-10), 1601–1622.

Tentij, M., Van Beusekom, R., Van Gemerden, B., Borch Grell, M., Stampe, T., Hötker, H., ... Van der Eijk, A. (2009). The Wadden Sea - A vision for the conservation of a Natural Heritage.

UNESCO World Heritage Center. (n.d.). *Wadden Sea.* Retrieved 2020-11-24, from `https://whc.unesco.org/en/list/1314`

Van Maren, D., Oost, A., Wang, Z., & Vos, P. (2016). The effect of land reclamations and sediment extraction on the suspended sediment concentration in the Ems Estuary. *Marine Geology*, *376*, 147–157.

Van Wijnen, H., & Bakker, J. (2001). Long-term surface elevation change in salt marshes: a prediction of marsh response to future sea-level rise. *Estuarine, Coastal and Shelf Science*, *52*(3), 381–390.

Vermeersen, B. L., Slangen, A. B., Gerkema, T., Baart, F., Cohen, K. M., Dangendorf, S., ... others (2018). Sea-level change in the Dutch Wadden Sea. *Netherlands Journal of Geosciences*, *97*(3), 79–127.

Wang, Z. B., Elias, E. P., van der Spek, A. J., & Lodder, Q. J. (2018). Sediment budget and morphological development of the Dutch Wadden Sea: impact of accelerated sea-level rise and subsidence until 2100. *Netherlands Journal of Geosciences*, *97*(3), 183–214.

Wang, Z. B., Hoekstra, P., Burchard, H., Ridderinkhof, H., De Swart, H., & Stive, M. (2012). Morphodynamics of the Wadden Sea and its barrier island system. *Ocean & coastal management*, *68*, 39–57.

Wassink, J. (2020). *Damming the North Sea. Is that a good idea?* Retrieved 2021-01-29, from `https://www.delta.tudelft.nl/article/damming-north-sea-good-idea`

Waypoint Amsterdam. (2020). *Tidal Streams North Sea South referred to HW Hoek van Holland.* Retrieved 2021-12-01, from `https://www.waypointamsterdam.com/Handy_stuf/Tidal_streams_North_sea_south/Noordzee_zuid1.html`

Windfinder. (2020). *Windfinder, average values North Sea.* Retrieved 2020-12-02, from `https://www.windfinder.com/windstatistics/forties_north_sea_platform`

Winkler, M., Bassin, J., Kleerebezem, R., van der Lans, R., & van Loosdrecht, M. (2012). Temperature and salt effects on settling velocity in granular sludge technology. *Water Research*, *46*, 3897-3902. doi: 10.1016/j.watres.2012.04.

Winter, N., & Johannessen, J. (2005). North Sea Circulation: Atlantic Inflow and its Destination.

Winton, M. (2006). Surface albedo feedback estimates for the ar4 climate models. *Journal of Climate*, *19*(3), 359–365.

Ylöstalo, P., Seppälä, J., Kaitala, S., Maunula, P., & Simis, S. (2016). Loadings of dissolved organic matter and nutrients from the Neva River into the Gulf of Finland - Biogeochemical composition and spatial distribution within the salinity gradient. *Marine Chemistry*, *186*, 58–71.

Zitman, T. (2019). *Lecture Slides course 'Inleiding Waterbouwkunde, CTB2410.* TU Delft.

A | Conceptualisation

This appendix gives the relevant figure and calculations that were used in setting up the conceptual model.

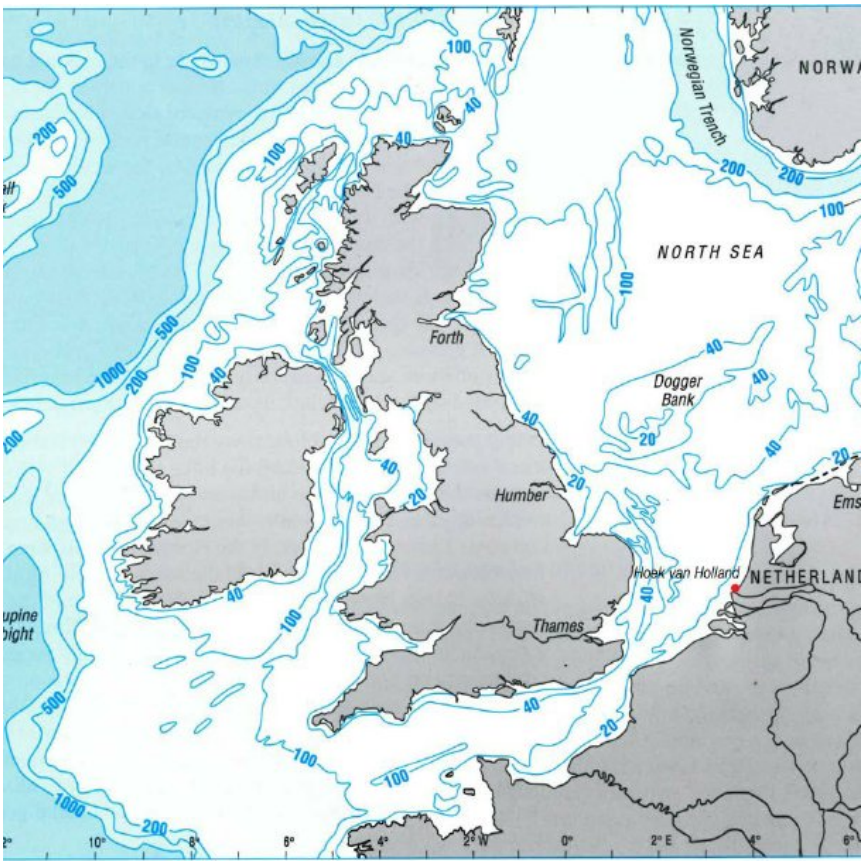

Figure A.1: North Sea basin with contour lines of depths below MSL. (Ledden et al., 2014)

A.1 Momentum Equation

The horizontal momentum equation is given by

$$\frac{du}{dt} + \frac{du^2}{dx} + \frac{duv}{dy} + \frac{duw}{dz} - fv + \frac{1}{\rho}\frac{dp}{dy} - F_x - \frac{d}{dz}\left(\nu_t \frac{dv}{dz}\right) = 0 \tag{A.1}$$

B | Water level variations

This appendix gives an overview of the monthly water fluxes that have been used to set up the water balances in Chapter 3. Figure B.1 shows the river discharges that have been used, Figure B.2 gives an overview of the monthly fluxes and the resulting water level variations (computed with equation 3.3), and Figure B.3 shows the monthly inflow from the Baltic Sea into the North Sea basin.

	Source		Jan	Feb	March	April	May	June	July	August	Sept	Okt	Nov	Dec	Average
Rhine (at Lobith)	1	m3/s	2900	2550	2700	2500	2300	2250	2250	1950	1700	1700	1950	2450	2267
Meuse (at Borgharen)	1	m3/s	490	450	370	290	180	120	95	90	90	125	260	400	247
Elbe	2	m3/s	850	925	1030	1100	800	620	560	510	475	490	600	710	723
Glomma	3	m3/s	579	455	373	598	1512	1119	560	859	829	821	714	560	748
Gota Alv	4	m3/s	600	500	450	750	1000	400	250	250	400	650	850	700	567
Weser	2	m3/s	500	500	510	450	275	230	200	175	175	190	250	380	320
Rivers SubTotal		m3/s	***5919***	***5380***	***5433***	***5688***	***6067***	***4739***	***3915***	***3834***	***3669***	***3976***	***4624***	***5200***	***4870***
			122%	110%	112%	117%	125%	97%	80%	79%	75%	82%	95%	107%	100%
Other Rivers		m3/s	4046	3677	3714	3888	4147	3239	2676	2620	2508	2718	3160	3554	3329
TOTAL RIVERS		m3/s	**9964**	**9057**	**9147**	**9576**	**10214**	**7978**	**6591**	**6454**	**6178**	**6694**	**7784**	**8754**	**8200**

Figure B.1: River discharges used for the water balance of the North Sea basin. The discharge from the IJssel is included in the Rhine discharge, as the Rhine discharge is considered more upstream at Lobith. Sources: 1. Klijn et al. (2012); 2. S. Huang et al. (2013); 3. Frigstad et al. (2020); 4. Bergström et al. (2011).

	Unit	Jan	Feb	March	April	May	June	July	August	Sept	Okt	Nov	Dec	Average
Evaporation	m3/s	-4723	-5600	-8667	-13701	-17333	-18398	-20129	-18866	-14937	-10120	-6272	-5253	-12000
Precipitation	m3/s	22018	17791	13216	10006	10698	12638	14175	19798	20317	22502	23188	23653	17500
Baltic Sea	m3/s	12308	10616	17770	21430	22056	22845	18380	14316	12739	12170	11164	10209	15500
Rivers	m3/s	9964	9057	9147	9576	10214	7978	6591	6454	6178	6694	7784	8754	8200
Sum (= required monthly pumping)	m3/s	**39567**	**31864**	**31466**	**27311**	**25636**	**25062**	**19017**	**21703**	**24296**	**31246**	**35864**	**37364**	**29200**
Yearly averaged pumping	m3/s	29200	29200	29200	29200	29200	29200	29200	29200	29200	29200	29200	29200	
Pumping difference yearly vs monthly	m3/s	10367	2664	2267	-1889	-3564	-4137	-10183	-7497	-4904	2047	6665	8164	0
Area	m2	5.16E+11												
Depth Change (no pumps)	cm/month	19.89	16.02	15.82	13.73	12.89	12.60	9.56	10.91	12.21	15.71	18.03	18.78	
Depth change (P_year)	cm/month	5.21	1.34	1.14	-0.95	-1.79	-2.08	-5.12	-3.77	-2.47	1.03	3.35	4.10	
WATER LEVEL VARIATON		5.21	6.55	7.69	6.74	4.95	2.87	-2.25	-6.02	-8.48	-7.45	-4.10	0.00	

Figure B.2: Overview of monthly fluxes and resulting water level variation in the North Sea basin. The colours in the left column correspond with the colours as used in Figure 3.1. The colour scale in the data indicates the variation over the months.

	Source		Jan	Feb	March	April	May	June	July	August	Sept	Okt	Nov	Dec	Average
P-E Baltic Sea	1	mm/month	13	0	21	19	29	34	15	0	-3	-3	-5	-3	10
P-E Baltic Sea		**m3/s**	**2502.7**	**25.6**	**4042.8**	**3779.7**	**5582.9**	**6763.6**	**2887.7**	**0.0**	**-596.8**	**-577.5**	**-994.6**	**-577.5**	**1900**
Neva	2	m3/s	1700	1700	1900	2650	2900	2900	2800	2750	2650	2550	2450	2000	2412.5
Vistula	3	m3/s	800	1000	1600	1850	1300	1200	1150	900	750	700	650	750	1054
Sum biggest rivers		m3/s	2500	2700	3500	4500	4200	4100	3950	3650	3400	3250	3100	2750	3467
			72%	78%	101%	130%	121%	118%	114%	105%	98%	94%	89%	79%	
Rivers Baltic Sea		m3/s	**9806**	**10590**	**13728**	**17650**	**16473**	**16081**	**15493**	**14316**	**13336**	**12747**	**12159**	**10786**	**13600**
SUM BALTIC SEA		m3/s	**12308**	**10616**	**17770**	**21430**	**22056**	**22845**	**18380**	**14316**	**12739**	**12170**	**11164**	**10209**	**15500**

Figure B.3: Overview of monthly fluxes and resulting Baltic Sea flow into the North Sea. Sources: 1. Groeskamp & Kjellsson (2020), Google Earth Engine; 2. Ylöstalo et al. (2016); 3. Piniewski et al. (2018).

C | Hydrodynamics

This appendix gives an elaboration on the computations that have been done for the hydrodynamics, concerning discharge-driven currents, wind-driven currents, the tide and the sensitivity analysis.

C.1 Discharge-driven currents

To define the area, the total length of the dam is 637 km, of which the Northern dam is 476 km and the Southern dam is 161 km long. This means that $476/637 \cdot 100\% = 74.7\%$ of the total discharge is pumped out through the Northern dam.

This gives a discharge of $29200 \cdot 0.747 = 21812$ m^3/s through the Northern dam and a discharge of $29200 \cdot 0.253 = 7388$ m^3/s through the Southern dam (the total discharge follows from the water balance, see Figure 2.2). Moreover, the flow is concentrated in the upper 10 m.

The total area over which the flow is computed is thus:

$$A = b \cdot d = 476000 \cdot 10 = 4760000 \text{ m}^2$$

This gives a flow velocity of:

$$u = \frac{Q}{A} = \frac{21812}{4760000} = 4.6 \cdot 10^{-3} \text{ m/s}$$

C.2 Wind-driven currents

The shear stress on the water surface due to wind is computed using equation 4.11. This wind shear is caused by a wind from the Southwest and thus has an angle of 45° to the true North. The shear stress in y-direction is computed by splitting the shear stress vector into x- and y-components.

$$\tau_s = 1.4 \cdot 10^{-3} \rho_{air} W^2 = 1.4 \cdot 10^{-3} \cdot 1.24 \cdot 8^2 = 0.11 \text{ N/m}^2$$
$$\tau_{s,y} = \tau_s \cdot \sin(45°) = 0.079 \text{ N/m}^2$$

The density of air is 1.24 kg/m^3 (as computed using equation 6.9). The average wind speed at 10 m height (W) is 8 m/s and the year-round dominating direction is Southwest (Appendix D, (KNMI, 2013)).

The wind-driven velocity at the surface, which is directed 45° to the right of the wind direction, is thus:

$$V_0 = \frac{\tau_{s,y}}{\rho_0 \sqrt{\nu_t f}} = \frac{0.079}{1025\sqrt{10^{-1} \cdot 1.15 \cdot 10^{-4}}} = 0.023 \text{ m/s}$$

For the vertical eddy viscosity, $\nu_t = 10^{-1}$ m^{2}s^{-1} is taken (Pietrzak, 2019a). f is the coriolis parameter (Section 2.3). Figure C.1 shows the decrease in velocity over depth, combined with the spiralling motion described by the velocity vector over depth, as computed using equation 5.2.

C.3 Tide

C.3.a Resonance

It is computed whether resonance can occur for the four major tidal constituents (M_2, S_2, O_1 and K_1) in the North Sea basin by comparing the wavelengths of the different tidal constituents to the length of the basin.

Table C.1 shows the respective periods of the four major tidal constituents.

The wave propagation speed in shallow water with an average depth is given by:

$$c = \sqrt{9.81 \cdot 80} = 28 \text{ m/s}$$

The wavelengths of the major tidal constituents are computed using $L = cT$ and shown in Table C.2

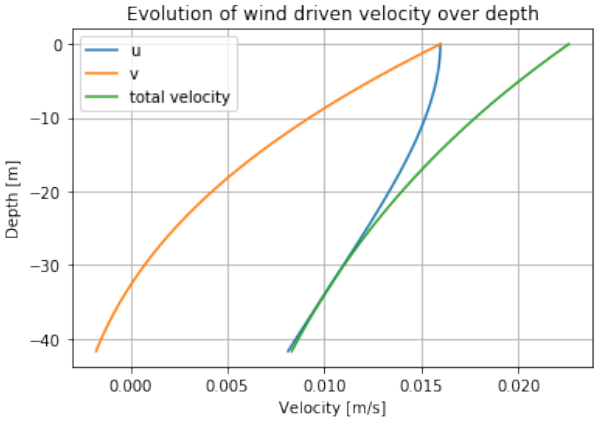

Figure C.1: A plot of the u- and v-components of the velocity and the total velocity. The velocity decreases downward while describing a spiralling motion.

Table C.1: The periods of the four major tidal constituents: K_1, O_1, M_2 and S_2, retrieved from (Bosboom & Stive, 2015).

Tidal component	Period [hr]	Period [s]
K_1	23.93	86148
O_1	25.82	92952
M_2	12.42	44712
S_2	12.00	43200

Table C.2: The wavelengths of the four major tidal constituents (K_1, O_1, M_2 and S_2) in km, computed using $L = cT$ and $c = 28$ m/s.

Tidal component	Wavelength [km]
K_1	2413
O_1	2604
M_2	1253
S_2	1210

C.3.b Tidal velocity

The amplitude of the tidal velocity for the M_2-constituent can be computed using equation 4.7 in Section 4.3.

ω is computed using the period of M_2 from Table C.1:

$$\omega = \frac{2\pi}{T} = \frac{2\pi}{44712} = 1.405 \cdot 10^{-4} \text{rad}^{-1}$$

The wave number k is computed using the wavelength of M_2 from Table C.2:

$$k = \frac{2\pi}{L} = \frac{2\pi}{1253 \cdot 10^3} = 5.015 \cdot 10^{-6} \text{m}^{-1}$$

The tidal amplitude a is half the tidal height. For the found tidal height of 0.2 m, the tidal amplitude is thus 0.1 m. This gives a maximum tidal velocity of:

$$\hat{u} = \frac{g \cdot a \cdot k}{\omega} = \frac{9.81 \cdot 0.1 \cdot 5.015 \cdot 10^{-6}}{1.405 \cdot 10^{-4}} = 0.035 \text{ m/s}$$

To check whether the used equation is realistic, the result is compared to the tidal velocity it gives for current tidal amplitudes. A tidal amplitude of 2 m results in a velocity of 0.7 m/s, which is realistic for tidal velocities without the NEED. This suggests that the used equation gives realistic results.

C.4 Sensitivity analysis

Table C.3 shows the results of varying the input parameters within certain bounds. This Appendix explains why exactly these ranges were taken.

- $W_{extreme}$: Based on wind speed statistics (KNMI, 2013)
- $W_{average}$: Based on wind speed statistics (KNMI, 2013)
- ρ_{air}: The air density varies on a yearly basis between 1.22 kg/m^3 and 1.26 kg/m^3.
- ρ: The density for salty seawater has been used for the computations. Over the years, the density will decrease due to freshening of the basin. Therefore, as a lower bound for the density, the density of freshwater, 1000 kg/m^3, has been used.
- Coriolis parameter f: An average coriolis parameter at the latitude of 52 °N has been used for all computations. In reality however, the North Sea stretches from 51°N to 60°N. This variation is accounted for in the range of the Coriolis parameter.
- Pumping discharge Q: Q can be estimated rather accurately, based on extensive datasets on the water balance in the North Sea basin. The upper bound for Q is the discharge for the climate change RCP8.5 scenario in 2100 as computed in Chapter 3.
- Cross-sectional area discharge current A: The width of the cross-sectional area is fixed to the width of the dam. The depth however, is uncertain and based on estimations until what depth the discharge-driven flows reach. Therefore, a range of depths from 5 m to 20 m has been applied here to find A.
- Tidal range: The tidal range estimated based on a comparison with similar (semi)-closed off seas. This is a very rough estimate and could vary by a factor 2 or even more.

Table C.3: Sensitivity of computed wave heights, set-up and velocities by their input parameters

Varied parameter			Impacted parameter		
Parameter	Lower bound	Upper bound	Parameter	Lower bound	Upper bound
$W_{extreme}$	30 m/s	40 m/s	H_{m0}	15.3 m	21.6 m
			Set-up	2.9 m	5.18 m
$W_{average}$	7 m/s	9 m/s	H_{m0}	1.2 m	2.0 m
			u_{wind}	1.7 cm/s	2.7 cm/s
			$u_{barotropic}$	1.4 cm/s	2.3 cm/s
ρ_{air}	1.22 kg/m^3	1.26 kg/m^3	u_{wind}	2.2 cm/s	2.3 cm/s
ρ	1000 kg/m^3	1025 kg/m^3	u_{wind}	2.3 cm/s	2.2 cm/s
f	$1.13 \cdot 10^{-4}$	$1.26 \cdot 10^{-4}$	$u_{barotropic}$	2.0 cm/s	1.8 cm/s
			u_{wind}	0.23 cm/s	0.21 cm/s
Q	29200 m^3/s	30747 m^3/s	$u_{discharge}$	0.5 cm/s	0.6 cm/s
A	2380000 m^2	9520000 m^2	$u_{discharge}$	0.96 cm/s	0.24 cm/s
Tidal range	5 cm	40 cm	u_{tide}	0.88 cm/s	7.0 cm/s

D | Wind data

Figure D.1 in this appendix shows the wind data that has been used for the computations concerning wind driven currents, wind setup and wave heights in Chapter 4.

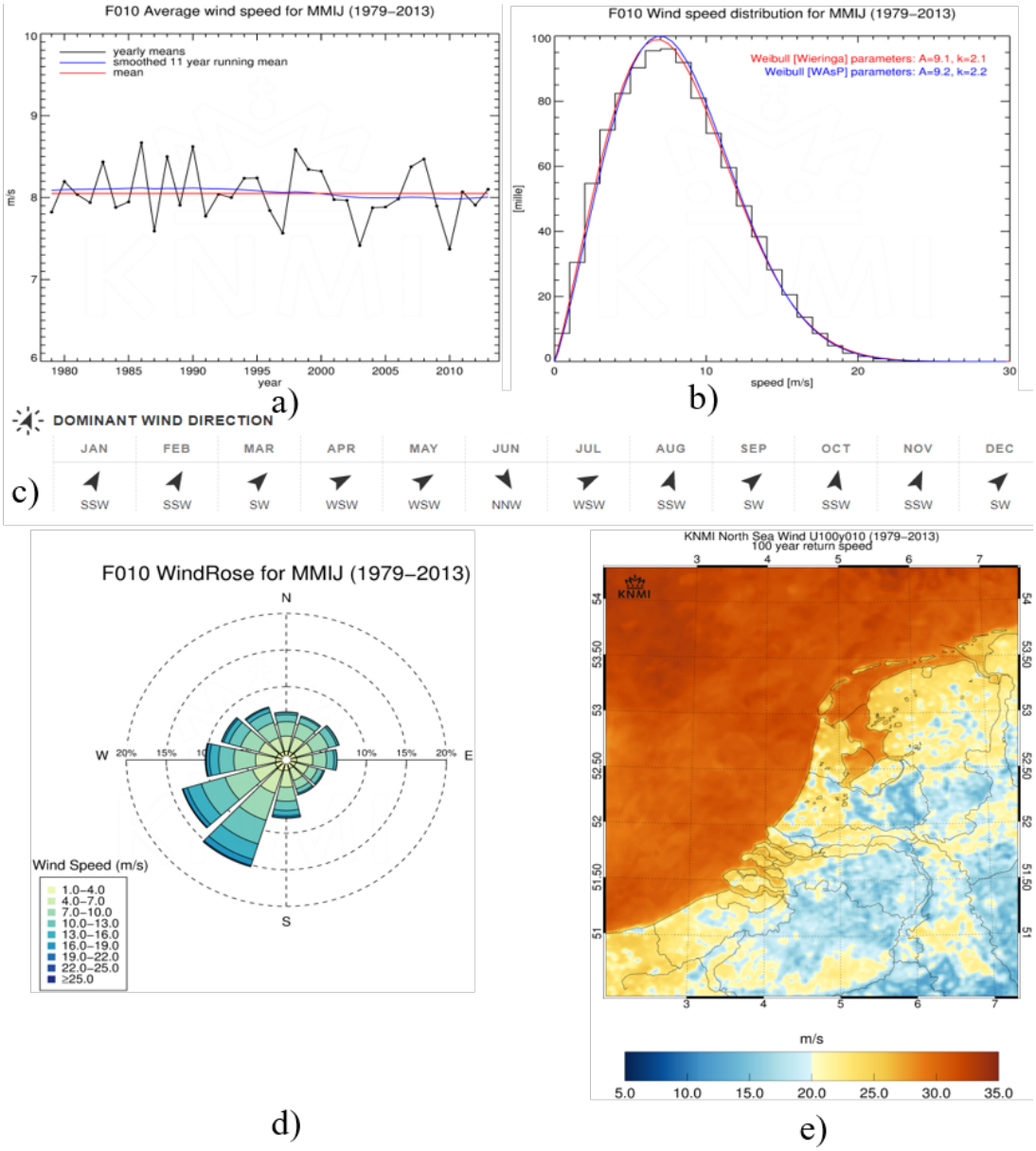

Figure D.1: a) The average mean yearly wind speed at Meteomast IJmuiden (ca 75km offshore west of IJmuiden) (KNMI, 2013). b) Weibull distribution of wind speed at Meteomast IJmuiden KNMI (2013). Both of these images show that 8 m/s is the average wind speed. c) Distribution of the wind directions over the year Windfinder (2020). This distribution clearly shows that southwest/west is the dominating wind direction year-round. d) Wind rose at Meteomast IJmuiden (KNMI, 2013). Again, southwest is the dominating wind direction. e) Extreme wind speeds with a 100 year return period above the North Sea: extreme wind speeds go up to 35 m/s (12 Beaufort) (KNMI, 2013).

E | Salinity

This appendix shows the salinity and temperature distribution for the Baltic Sea. Furthermore, the equations from subsection 5.2.b are calculated.

E.1 Baltic Sea

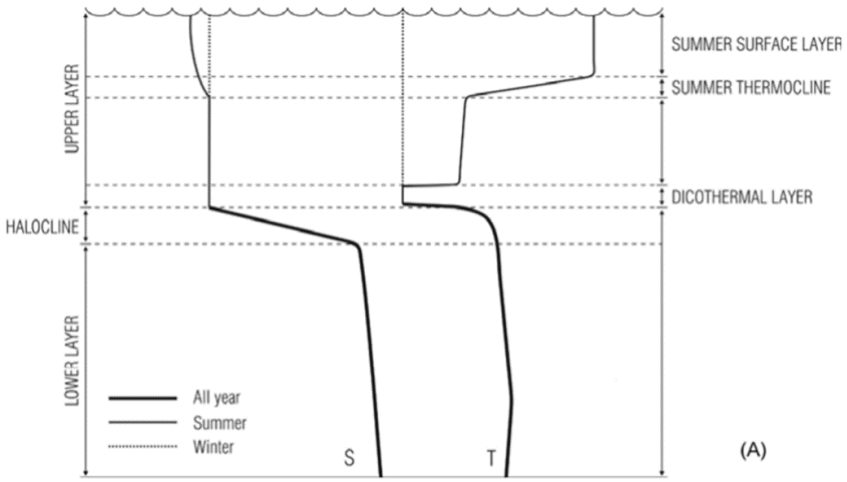

Figure E.1: A schematic diagram of vertical stratification of Baltic Sea water masses (Leppäranta & Myrberg, 2009), where S is the salinity and T is temperature.

E.2 Formulas from effects and interactions

The discharge D that needs to be pumped out of the basin is equal to $D = 29200$ m^3/s, see subsection 2.2. The volume V of the basin that needs to be pumped out is $625000 \cdot 825000 \cdot 40 = 2.06 \cdot 10^{13}$ m^3. The salinity is reduced from 35 PSU to 3.5 PSU, therefore:

$$\Delta t = \frac{2.06 \cdot 10^{13}}{29200} \cdot \log \frac{3.5}{35} \approx 50 \text{ years}$$

At the Ekman depth, a velocity of $0.04 \cdot V_0$ is directed opposite to the wind direction. The flow V_0 is derived in equation C.2 and equal to $V_0 = 0.023$ m/s, the resulting flow at the Ekman depth is 1 mm/s with a wind velocity of $W = 8$ m/s. The length over which this flow velocity works is equal to the basin width: $L = 625000$ m. Therefore the renewal time at the deep part of the basin will be:

$$T = \frac{L}{U} = \frac{625000}{0.001} \approx 20 \text{ years}$$

The external and internal Rossby raidi are:

$$R_d = \frac{\sqrt{gH}}{f} = \frac{\sqrt{9.81 \cdot 40}}{1.15 \cdot 10^{-4}} = 172.3 \text{ km}$$

$$g' = \frac{\rho_2 - \rho_1}{\rho_s} g = \frac{1028 - 1003}{1025} \cdot 9.81 = 0.24 \text{ m/s}^2$$

$$R_i = \frac{\sqrt{g'H}}{f} = \frac{\sqrt{0.24 \cdot (100 - 40)}}{1.15 \cdot 10^{-4}} = 33 \text{ km}$$

The effect of the wind-induced set-up found in Subsection 4.6 is used to assess the effect on the internal slope. With the average densities of:

$$\rho_1 = 1003 \text{ kg/m}^3 \qquad \rho_2 = 1027 \text{ kg/m}^3$$

Now equation 5.7 for the internal slope can be calculated respectively for an average wind and a large storm:

$$\frac{\partial h_2}{\partial x} = -\frac{1003}{1027 - 1003} \cdot \frac{0.071 \cdot 2}{625000} = -9.16 \cdot 10^{-6}$$
$$\frac{\partial h_2}{\partial x} = -\frac{1003}{1027 - 1003} \cdot \frac{1.73 \cdot 2}{625000} = -1.75 \cdot 10^{-4}$$

This yields a depth difference of the internal slope during an average wind of: $\partial h_2 = 5.8$ m
The depth difference of the internal slope during a large storm is: $\partial h_2 = 110$ m

F | Sediment

This appendix shows more background information about the sediment dynamics in the North Sea, that is used for the analysis on the changing sediment transport due to the NEED.

F.1 Sediment Budget

Table F.1 gives an overview of the sediment fluxes that are considered to set up the sediment budget. The budget is given for both the current situation and the situation with NEED, together with the references for the values in the current situation. Figure 7.1 in Chapter 7 visualises the information from the table.

Table F.1: Average annual in- and outgoing fluxes (in Mtons/yr) of the sediment budget in the North Sea Basin in the current situation and in the situation with NEED.

	Current situation (no NEED) (Mtons/year)	**Situation with NEED (Mtons/year)**	**Comment**	**Reference**
The Atlantic Ocean	+11, -14	0	Inflow along the English coast. Outflow along the Norwegian coast.	Eisma & Irion (1993)
The Channel	22-30	0		Eisma & Irion (1993)
Rivers	23	23	Only river basins with a drainage area exceeding 10,000 km^2 have been considered	Eurosion (2004)
Baltic	0.5	0.5		Eisma & Irion (1993)
Coastal Erosion	9	9	Mainly cliff erosion, thus dominated by waves and storms, not by tides	Gerritsen et al. (2000)
Bed Erosion	9-13.5	<9		Eisma & Irion (1993)
Dumping	14	14	Due to dredging activities in harbors and river mouths	Boon et al. (1997)
Dumping on land	-3 to -2	-3 to -2	Due to beach nourishment	Eisma & Irion (1993)
Primary production	1	1		Eisma & Irion (1993)
Atmospheric deposition	1	1		Eisma & Irion (1993)
Deposition	-45	>-45		Gerritsen et al. (2000)
Min net flux	28.5	<10.5		
Max net flux	42	10.5		
Range of influx	61-142.6			Combination of the references above
Range of outflux	45-62			Combination of the references above

F.2 Sediment distribution

Figure F.1 shows the average fine sediment distribution at the sea bottom and Figure F.2 shows the average SPM concentrations annually, in March and in August. It shows clearly that there is a big difference between calm and stormy periods (respectively August and March).

F.3 Bed shear stress

Background information on the bedshear stresses in the North Sea basin are given by the figures in this subsection. Figure F.3 shows the relation between flow velocity, particle size and settlement. If the NEED reduces the flow velocity in the basin from 50 to 3.5 cm/s, it becomes clear from the graph that no sand can be in suspension. Figure F.4 shows maps of NOAH (2006), indicating the bottom shear stress by tides and winds separately.

F.4 Case studies for sediment transport

This section shows the sediment transport changes at specific locations in the enclosed North Sea. The locations are shown in Figure F.5a. Figures F.5b and F.6 show the topography and morphology of The

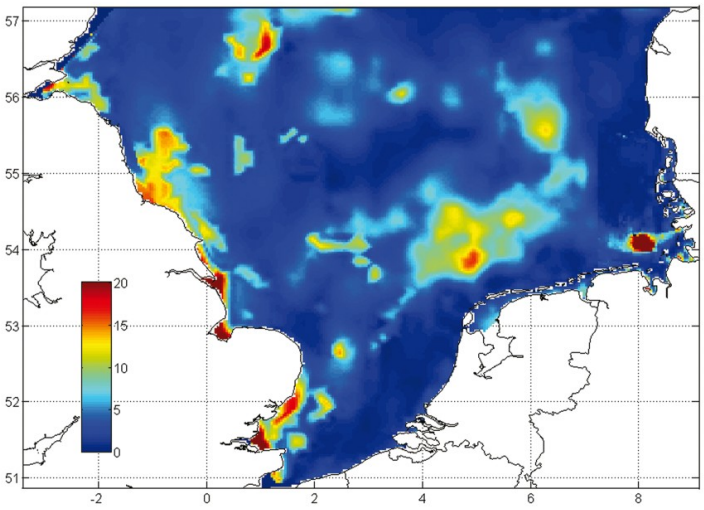

Figure F.1: Map of the distribution of fine sediment content (smaller than 20 μm) in the upper 20 cm of the bottom (in %) (Gayer & Dobrynin, 2020).

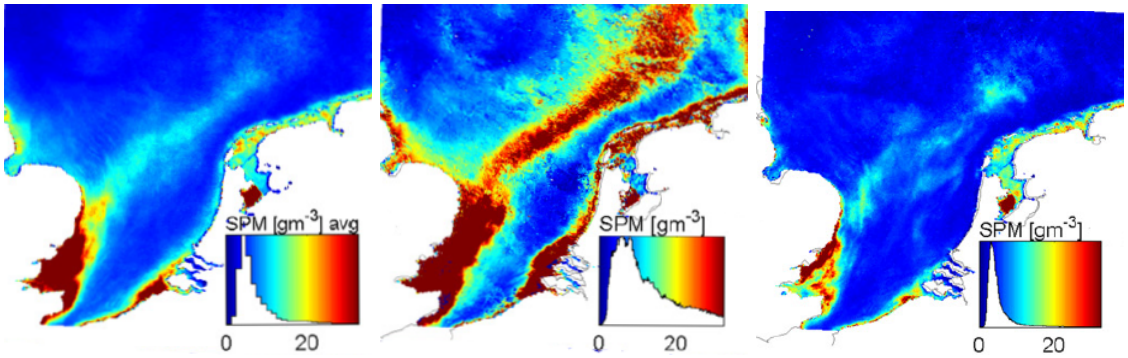

Figure F.2: Distribution of suspended sediment in g/m^3. From left to right: average during a year, during March and during August (Pietrzak et al., 2011).

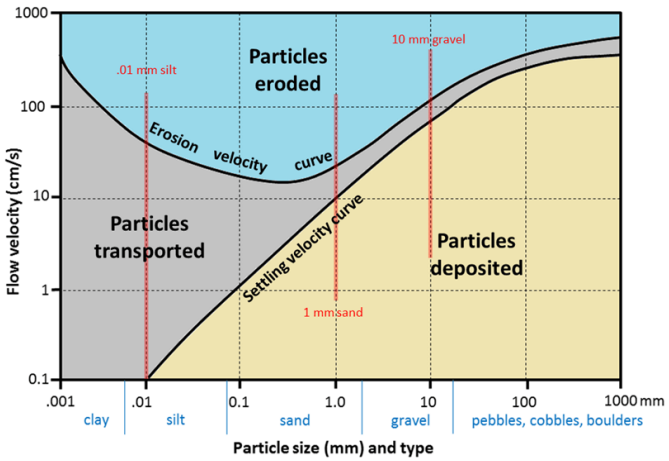

Figure F.3: The Hjulstrom curve (Earle, 2015)

Wash and Southern Bight respectively. Table F.2 shows the changes in the bed shear stress, deposition rate and erosion rate due to the dam. τ_{mean} is computed by using equation 7.2 from Section 7.3. The τ_{cur} with NEED is computed by dividing the current τ_{cur} by 200. The current shear stresses are derived from Hendriks et al. (2020). The bed concentration c_{bot} is derived from Dobrynin et al. (2011).

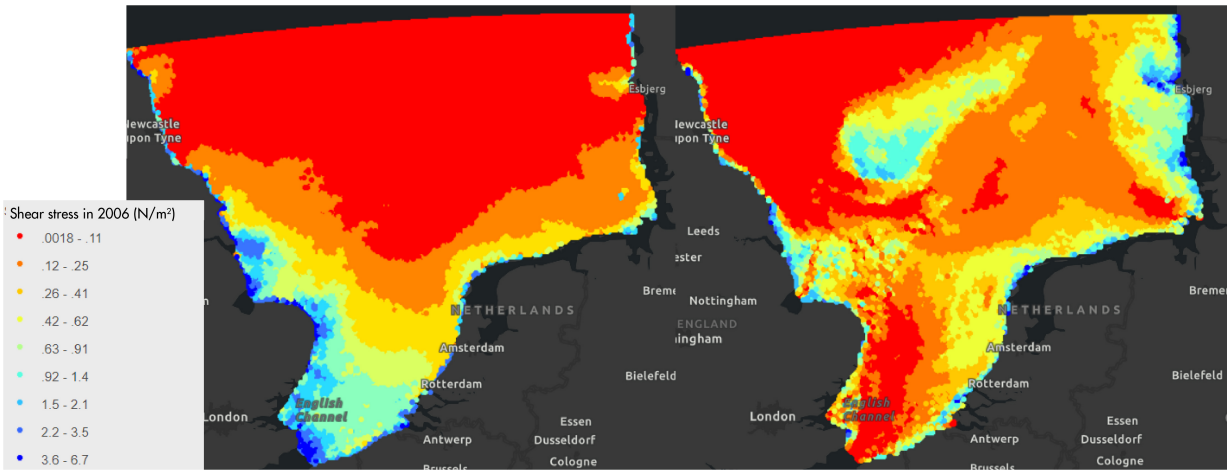

Figure F.4: Mean bed shear stress induced by currents (left) and waves (right) (NOAH, 2006).

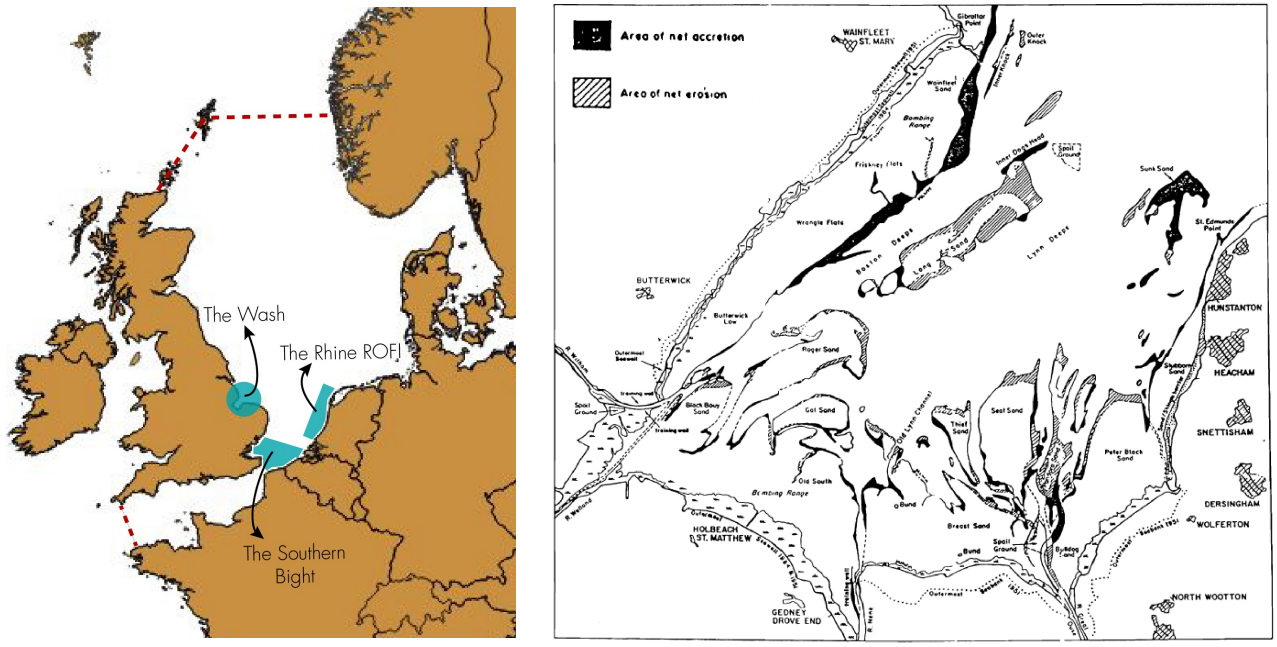

(a) (b)

Figure F.5: a) Locations of the regions that are investigated more extensively in Section 7.4 concerning sediment transport. b) Map of the Wash area, indicating the complex pattern of accretion and erosion (Pye, 1995).

Table F.2: Deposition and erosion rates in the Rhine ROFI before and after the construction of the NEED, close to the coast (at 7 m depth) and further offshore (20 m depth).

	Off shore (d = 20 m)		**Close shore (d = 7 m)**	
	Current situation	**With NEED**	**Current situation**	**With NEED**
w_s (m/s)		0.001		
E_0 (kg/m^2/s)		0.10		
$\tau_{dep,cr}$ (N/m^2)		0.20		
$\tau_{ero,cr}$ (N/m^2)		0.40		
τ_{mean} (N/m^2)	0.93	0.02	0.73	0.01
τ_{cur} (N/m^2)	0.70	0.00	0.50	0.00
τ_{wave} (N/m^2)	0.50	0.50	0.70	0.70
c_{bot} (kg/m^2)	8.00	8.00	10.00	10.00
M_{dep} (kg/m/s)	0	0.007	0	0.010
M_{ero} (kg/m^2/s)	0.13	0.00	0.08	0.00

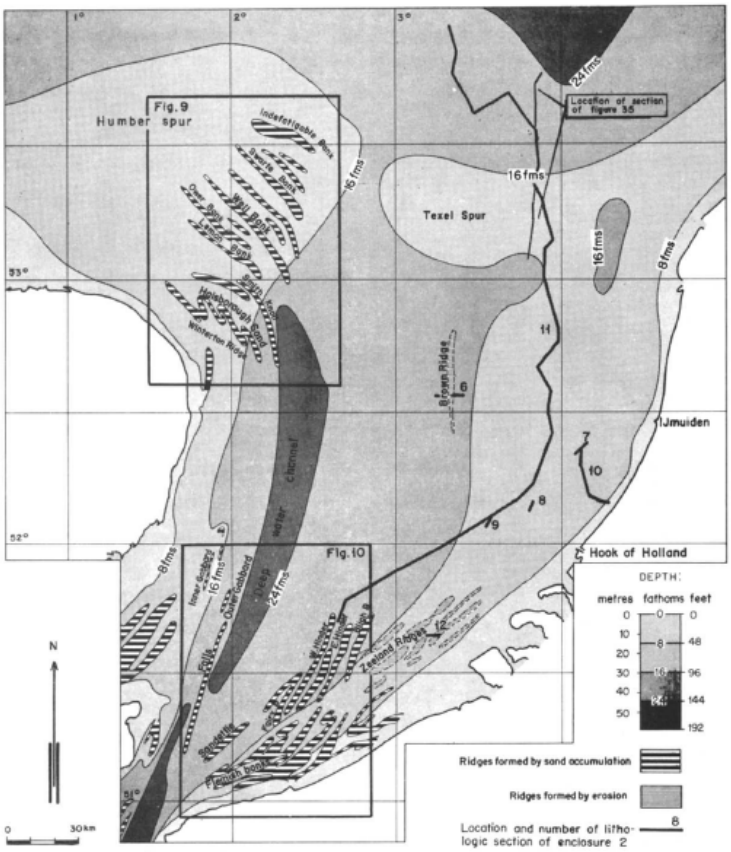

Figure F.6: Map of the Southern Bight, including the bathymetry and the locations of the sand ridges (Otto et al., 1990).

G | Drowning of the Wadden Sea

This appendix presents the two tables with sea-level rise rates related to Chapter 9, regarding the changes due to the NEED in the Wadden Sea UNESCO World Heritage.

Table G.1: Critical sea level rise rates in mm/year for the six tidal basins of the Dutch Wadden Sea (West to East) as found by Wang et al. (2018).

Basin	**Texel**	**Eierland**	**Vlie**	**Ameland**	**Pinkegat**	**Zoutkamp**
Critical rate of SLR	7.0	18.0	6.3	10.4	32.7	17.1
30% uncertainty range	5.5-8.1	14.2-20.9	5.0-7.3	8.2-12.1	25.8-37.9	13.5-19.8

Table G.2: Rates of total relative sea level rise in mm/year for the six tidal basins of the Dutch Wadden Sea (West to East) for the years 2030, 2050 and 2100 for three different emission scenarios as found by Wang et al. (2018). Numbers in **bold** indicate rates that exceel the critical rate as given in Table G.1.

Scenario		**Texel**	**Eierland**	**Vlie**	**Ameland**	**Pinkegat**	**Zoutkamp**
RCP2.6	2030	4.9	4.9	5.9	4.9	6.5	5.8
	2050	5.2	5.2	5.7	5.2	6.2	5.5
	2100	5.0	5.0	5.0	5.0	5.0	5.0
RCP4.5	2030	5.8	5.8	**6.8**	5.8	7.4	6.7
	2050	6.3	6.3	**6.8**	6.3	7.3	6.6
	2100	6.6	6.6	**6.6**	6.6	6.6	6.6
RCP8.5	2030	6.8	6.8	**7.8**	6.8	8.4	7.7
	2050	**8.9**	8.9	**9.4**	8.9	9.9	9.2
	2100	**11.9**	11.9	**11.9**	**11.9**	11.9	11.9